# Three-dimensional ultrasound study of fetal craniofacial anatomy

N.M. Roelfsema

The work presented in this thesis was financially supported by the Netherlands Organization for Scientific Research, grand no: 902-37-116. It was conducted at the department of Obstetrics and Gynecology and in collaberation with the department of Plastic and Reconstructive Surgery, Erasmus MC, Rotterdam, The Netherlands

J.E. Jurriaanse Stichting and GE Healthcare financially supported the printing of this thesis

The following parts of this publication have been published previously and have been reproduced with permission from the publishers: Elsevier Ltd.(Roelfsema et al. Three-dimensional sonographic measurement of normal fetal brain volume during the second half of pregnancy. Am J Obstet Gynecol 2004;190:275-80) and the International Society of Ultrasound in Obstetrics and Gynecology (Roelfsema et al. Three-dimensional ultrasonography of prenatal skull base development. Ultrasound Obstet Gynecol 2007:29:372-7; Roelfsema et al. Craniofacial variability index determined by three-dimensional ultrasound in isolated versus syndromal cleft lip/palate. Ultrasound Obstet Gynecol 2007;29:265-70; Roelfsema et al. Craniofacial variability index in utero; a three-dimensional ultrasound study. Ultrasound Obstet Gynecol 2007;29:258-64; Roelfsema et al. Three-dimensional sonographic determination of normal fetal mandibular and maxillary development during the second half of pregnancy. Ultrasound Obstet Gynecol 2006;28:950-7; Dikkeboom et al. The role of three-dimensional ultrasound in visualizing the fetal cranial sutures and fontanels during the second half of pregnancy. Ultrasound Obstet Gynecol 2004;24:412-6).

Front cover: © N.M. Roelfsema

# Three-Dimensional Ultrasound Study of Fetal Craniofacial Anatomy

## Drie-dimensionaal ultrageluidsonderzoek van de foetale craniofaciale anatomie

**PROEFSCHRIFT**

TER VERKRIJGING VAN DE GRAAD VAN DOCTOR
AAN DE ERASMUS UNIVERSITEIT ROTTERDAM
OP GEZAG VAN DE RECTOR MAGNIFICUS
PROF.DR. S.W.J. LAMBERTS
EN VOLGENS BESLUIT VAN HET COLLEGE VOOR PROMOTIES
DE OPENBARE VERDEDIGING ZAL PLAATSVINDEN OP
WOENSDAG 31 OKTOBER 2007 OM 15.45 UUR

DOOR

**Nanette Marianne Roelfsema**
GEBOREN TE NORG

**PROMOTIECOMMISSIE:**

| | |
|---|---|
| Promotoren: | Prof.jhr.dr. J.W. Wladimiroff |
| | Prof.dr. S.E.R. Hovius |
| Overige leden: | Prof.dr.ir. N. Bom |
| | Prof.dr. E.A.P. Steegers |
| | Prof.dr. M.H. Breuning |
| Copromotor: | Dr. L.N.A. van Adrichem |

*Voor Mam*

# Contents

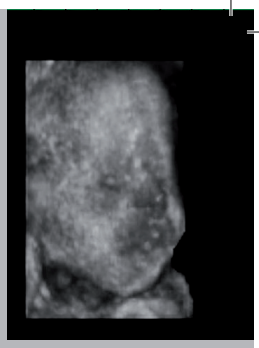

Chapter 1

# Literature overview and research objectives

## 1.1 LITERATURE OVERVIEW

### 1.1.1 Three-dimensional ultrasound in general

Ultrasound has placed itself in a strong position as an imaging technique in day to day obstetric care. This is the result of many advantages over techniques such as MRI (magnetic resonance imaging) and CT (computer tomography), in particular the flexibility of the technique, the moderate costs, the possibility of real-time imaging and the use of non-ionizing radiation.[1] In the Netherlands, ultrasound is used on a regular basis in all obstetric units and by most regional midwifery services. During the last decades the image quality has strongly improved, partially due to the development of new ultrasound techniques.

When using the technique of conventional two-dimensional ultrasound (2DUS) the ultrasonographer tries to form a mental three-dimensional (3D) picture of the fetal anatomy from two-dimensional (2D) planes. This process tends to become more difficult and time-consuming when the structure itself and the circumstances are more complicated, thus enhancing the risk of misinterpretation.[2] This shortcoming of conventional ultrasound techniques opened up the way for three-dimensional ultrasound (3DUS) in fetal imaging at the beginning of the 90s.[3-5]

### 1.1.2 Three-dimensional ultrasound in prenatal diagnosis

Different methods in obtaining a three-dimensional ultrasound image have been developed: the defocusing lens method, free hand scanning with or without electromagnetic sensing, and mechanical devices to move the transducer. These devices may be external or integrated within the probe along with a position sensor (automatic volume scanning).[6,7]

In commonly used (2D) ultrasound probes an acoustic lens is used converging the ultrasonic beam in the direction of the slice width. The ultrasonic beam is best kept small to optimize the resolution of the 2D image. In the defocusing lens (3D) method, however, a lens is used which diverges the beam and produces a thick slice width. From the returning echoes a volume image is displayed. This allows real-time volume scanning, but as a result of the thick slice width the resolution is poor.[6] Moreover, the size of the displayed volume image is restricted to the thickness of the ultrasonic beam. This technique is therefore not commonly used in prenatal diagnosis.

The other techniques use computer processing for 3D reconstruction. With movement of the ultrasound probe (free hand or mechanically) a consecutive set of 2D planes is acquired and constructed into a 3D data set by a computer. By using a position sensor or electromagnetic sensing device the position of every pixel of the 2D images within the volume is determined and a 3D reconstruction can be built.

The 3D-ultrasound machine used in the present study (Voluson 530D; Kretztechnik AG, Zipf, Austria), is equipped with an automatic volume scanning method. The ultrasound probe has a built-in mechanical device to move the transducer along with a position sensor. The

patient setting of a 3DUS examination is identical to that of a conventional two-dimensional (2D) ultrasound examination. Before 3D acquisition can take place, orientation with real-time 2DUS and optimization of the B-mode image (the normal 2DUS mode) is necessary. The abdominal as well as the vaginal 3DUS probe offers a mechanical fan-like rotating device, which can obtain a large number of adjoining section planes. Acquisition takes place automatically after the examiner defines a region of interest ('volume-box'). The digitized information of every section plane is loaded into a computer along with the information regarding its position. The incorporation of scaling data permits measurement. The 3D-data set is thus composed of a set of voxels, each with a certain grey value and brightness. These values are interpolated to the voxels in-between two section planes.[1,6,8]

After acquisition, three orthogonal planes in the direction of the three orthogonal axes (*x,y,z*) are displayed on the monitor (multiplanar view) (Figure 1). These planes can be moved and rotated freely with an automatic update of the perpendicular planes. 3D-image reconstruction takes place after a box is set around the region of interest within the volume thus extracting unwanted parts. A similar mechanism is used when using 'Cartesian storing', storing the part of interest of the volume in a box-like configuration. The reconstructed image can be further optimized with the help of an 'electronic scalpel device' removing obscuring structures and adjusting the threshold control suppressing small echo signals. 3D appearance of the image is realized by shading, which is achieved by depth cueing. The distance to the imaginary 'look-in window' determines the grey value of a pixel in the image. The shorter the distance, the brighter the pixel in the reconstructed 3D image.[3,6,8] The 3D-volume or part of it (Cartesian storing) can be stored for later analysis. Cartesian storing enables further processing on a computer.

Different modes can be used to display the 3D-reconstruction image. Surface-modes enable visualization of the surface of the rendered structure surrounded by hypo-echoic structures (fluid), whereas transparent modes can accentuate the for instance hyper- or hypo-echoic

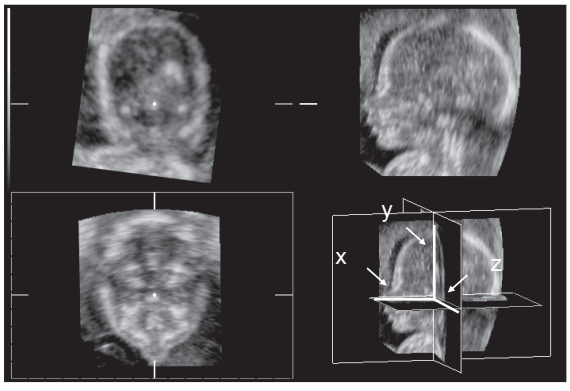


**Figure 1.** Multiplanar view, three orthogonal planes in the direction of the three orthogonal axis (*x,y,z*) are displayed on the monitor.

structures and therefore visualize bony or cystic structures within the volume. For optimal 3D effect the rendered image can be rotated and displayed from various angles.[8]

Three-dimensional ultrasound is essentially based on processing of the returned 2DUS information, and therefore tissue exposition in 3DUS is equal to that in 2DUS. But if, as a result of the computer processing in 3DUS, less time is spent to the actual scanning of the fetus and more to post-processing of ultrasound information, fetal tissues are exposed to even a lesser amount of ultrasound and therefore possible bioeffect.[9]

A number of advantages of 3DUS over conventional 2DUS has been described:[10-13]

i. A possible reduction of patient examination time;
ii. The data can be permanently stored, transported and reviewed retrospectively. This allows re-analysis of the stored volume and consultation at tertiary facilities;
iii. Simultaneous display of three perpendicular planes providing more accurate assessment of anatomic details and exact identification of biometry planes. Rotation of the volume allows assessment of planes often not available with conventional 2D ultrasound;
iv. Direct volume measurement;
v. Rendering and rotation of the reconstruction image allows evaluation of the spatial relationship of different structures within the volume;
vi. Improved recognition of reconstruction images by parents or colleagues who have limited knowledge of ultrasound imaging. This provides a better understanding of fetal abnormalities or reassurance in case of normality for parents who have a previous child with anomalies.

Because the 3DUS volume is derived from 2DUS planes, some of the factors known to limit 2DUS imaging (i.e. maternal obesity, reduced amount of amniotic fluid, fetal position and shadowing of overlying structures) also limit 3D sonography. Several specific 3DUS limitations have been noted:[10-13]

i. Time is required to learn 3D ultrasound scanning;[14]
ii. Motion artifacts can appear during data acquisition;
iii. Limited size of the volume box leads to limitation in size of the collected volume data;
iv. Volume storage requires a high storage capacity;
v. After recollection of a stored volume it can be difficult to achieve orientation. Furthermore, the recognition of an artifact can be hampered when the cause of the artifact has not been stored in the volume.
vi. For good image quality in reconstruction rendering, some contrast between the boundaries is necessary. Surface reconstruction, for instance, is difficult without some amount of amniotic fluid in front of the structure that is to be displayed;
vii. Structural abnormalities in a rendered image can be mimicked with the electronic scalpel option, when the threshold is set too high or as a result of shadowing of overlying

structures. Especially if these overlying structures are not visible in the stored volume (Cartesian storing).

Several studies have been conducted in order to compare 3DUS with conventional 2DUS. However none of these studies were randomized controlled trials and many of the study populations are biased.[15] Furthermore, comparison of these studies is complicated by the use of different 3DUS machines, with different resolution and application possibilities.

In the study of Merz et al (1995), Platt et al (1998), Dyson et al (2000) and Xu et al (2002), 3DUS showed to be superior to 2DUS in the general detection of fetal malformations (Table I).[11,14,16,17] Merz et al (1995) found 3DUS to be disadvantageous in only 2%, which were fetuses with cardiac malformations.[11] Dyson et al (2000) performed 3DUS when a potential advantage was suspected, which might explain the high diagnostic advantage. However, 3DUS had an impact on clinical management in only 3 pregnancies.[16] In the study of Platt et al (1998) 3DUS

**Table I:** Overview of literature comparing 2D- and 3D ultrasound in the detection of fetal anomalies.

| | *Methods* | *GA* | *N* | *2D and 3D equipment* | *3D + (%)* | *3D - (%)* | *2D/ 3D = (%)* | *Remarks* |
|---|---|---|---|---|---|---|---|---|
| Merz et al (1995)[11] | Additional 3DUS after malformation detected with 2D | 13- 40 wks | 204* | Combison 330 and 530 (Kretz) | 127/ 204 (60) | 4/ 204 (2) | 73/ 204 (36) | |
| Platt et al (1998)[14] | Additional 3DUS for all high risk patients | ±12- 35 wks | 32*¶ | Combison 530 | 3/ 32 (9) | 0 | 29/ 32 (91) | Obstetrical and gynaeco- logical anomalies |
| Dyson et al (2000)[16] | Additional 3DUS after malformation detected with 2D | 12- 38 wks | 103# | Combison 530 | 53/ 103 (51) | 4/ 103 (4) | 46/ 103 (45) | 103 anomalies in 63 fetuses |
| Scharf et al (2001)[26] | Additional 3DUS for low and high risk patients | 7- 41 wks | 40* | Dyna view SSD- 1700 (Aloka), Voluson 530D | 1/ 40 (2.5) | 12/ 40 (30) | 27/ 40 (67.5) | |
| Xu et al (2002)[17] | Additional 3DUS for all high risk patients | 16- 42 wks | 58# | Voluson 530D (Kretz) | 35/58 (60) | 0 | 23/58 (40) | 58 anomalies in 40 fetuses |

GA; gestational age, N; number, +/ -/ =; number and (percentage) of cases/ abnormalities in which 3D ultrasound proved to be advantageous/ disadvantageous/ or was equal to 2D.*Number of pregnancies with a fetal anomaly, #Number of anomalies seen in the fetuses ¶Only the abdominal scans are taken into account

improved or changed the diagnosis in only 9%. The authors explain the relative infrequency of improved diagnosis on the basis of their inexperience with 3DUS.[14]

3D sonography can be especially helpful in the evaluation of complex abnormalities, for instance skeletal dysplasia.[13,18-20] In 3 out of 7 fetuses with skeletal dysplasias studied by Hull et al (2000), 3DUS showed additional information about the face and scapula. This improved confidence in prenatal diagnosis.[21] Also Krakow et al found that 3D improved diagnostic accuracy in five cases of skeletal dysplasia.[22] Ruano et al (2004) concluded that both three-dimensional helical computer tomography (3D-HCT) and 3DUS perform better than 2DUS in the diagnosis of skeletal abnormalities. 3D-HCT identified even more abnormalities than 3DUS, but with both modalities it was possible to make the correct diagnosis in all six cases.[23] In a case of diastrophic dysplasia*, Sepulveda et al (2004) were able to show the facial dysmorpism and hitch hiker thumbs that are associated with the condition, both could have easily been missed on 2DUS.[24] Also Seow et al (2004) stress the usefulness of 3D ultrasound in increasing the accuracy in diagnosing a complex malformation, such as camptomelic dyplasia*.[20]

The study of Nelson et al (2001) shows comparable results for both methods in the evaluation of normal anatomy. The reviewers of 3D volume data were unaware of the results of the 2DUS studies. They evaluated parameters such as measurement, completeness of organ visualization, abnormalities that were identified and image quality. In quality of diagnosis, sonographic measurements (difference < 5%), as well as organ visualization no real differences were found.[25]

Scharf et al (2001) showed comparable or worse outcome of visualization of different structures and organs of the normal fetus with 3DUS. Advantages were only seen in one case of neural tube anomaly. The authors found the benefit of 3DUS not to lie in the visualization of normal fetal morphology, but more in presenting complex malformations (Table I).[26]

Latest developments in the line of 3DUS have been 'real-time 3DUS' or 4D ultrasound. The fourth, temporal dimension, allows 3D imaging of the moving fetus.[27] By using temporal tracking (gating) techniques, also regularly moving objects such as the heart can be rendered and evaluated in 3 dimensions.[28] Especially, the possibility of magnification of a region of interest after acquisition of the volume and the visualization of the different phases of the cardiac cycle, image-by-image facilitates analysis of the structures.[29]

### 1.1.3 Prenatal diagnosis of craniofacial abnormalities

Craniofacial defects are among the most common of congenital anomalies.[30] For instance the incidence of facial clefting in the Netherlands is estimated to be as high as 1.75 in 1000 live births.[31] Furthermore, many congenital and inherited anomalies can affect the fetal face.[30] In over 150 syndromes with clinical implications, craniofacial involvement is described.[32]The

* Syndromes/sequences are identified at p 179-180.

diagnosis of minor craniofacial anomalies can be very useful in the diagnosis of specific syndromes and can aid in predicting the prognosis.[33]

*Two-dimensional ultrasound*

In prenatal diagnosis, especially in a low-risk population, the detection rate of isolated craniofacial anomalies and minor malformations may vary from 14 to 58% (Table II).[34-37] The sensitivity of ultrasound screening depends on the skill and experience of the ultrasonographer, the equipment status, the gestational age at which the sonography is performed, the definition of abnormality and the degree at which abnormalities are ascertained postnatally.[38] This will largely explain the variability in detection rate of fetal face abnormalities.

In a high-risk population, Pilu et al (1986) reported a sensitivity for ultrasound diagnosis of craniofacial anomalies as high as 78% (14 out of 18) in 223 pregnancies and specificity of 100%. Two fetuses with micrognathia were not diagnosed as a result of unfavorable fetal position.[39] Turner and Twining (1993) found 24 fetal facial abnormalities in 3200 examinations, mostly micrognathia and clefting, which was isolated in only 3 fetuses. False-negative rates are not reported by the authors.[40] In a retrospective study, Ghi et al (2002) found complete correlation of the prenatal diagnosis of 43 craniofacial anomalies and postnatal follow-up. However, no attempt was made to define the degree of extension of clefting into the palate. False-negative diagnosis was also not determined. In 11 out of 12 patients 3DUS was successful, but it did not provide any further diagnostic information.[41]

Craniofacial anomalies are often identified after associated abnormalities in other organs and structures are found.[41,42] Detection of isolated fetal craniofacial abnormalities, for instance

**Table II:** Detection rates of isolated craniofacial malformations in low-risk populations.

| *Authors* | *Methods* | *N* | *Sensitivity (%)* | *Specificity (%)* | *Remarks* |
|---|---|---|---|---|---|
| Crane et al (1994)[34] | Randomized clinical trial on the detection rate of routine ultrasonography in the USA (RADIUS-trial) | 15281 fetuses (7685 screened, 7596 not screened) | 30 (14% in the non-screened group) | 100 | 3 out of 10 cleft lip/ palate detected, examination of the fetal face was not part of the study protocol |
| Hafner et al (1997)[35] | Targeted ultrasonography of the fetal face | 5407 pregnancies | 50 | 99.8 | |
| Clementi et al (2000)[36] | Retrospective analysis for detection of cleft lip/ palate in 12 European countries | 709027 births | 14 (CL/P=18; CP=7) | Not known | Large regional variation of sensitivity: range: 0- 86% |
| Cash et al (2001)[37] | Retrospective analysis of routine ultrasound for detection of cleft lip/ palate in specialized hospital | 23577 pregnancies | 58 (CL/P=82; CL=67; CP=0) | 100 | Distracted from Table 1 (p 434)[37]; only isolated cases are taken into account |

CL/P= cleft lip/ palate, CL= cleft lip, CP= cleft palate

craniosynostosis, is less common.[43] Determining the extent of an anomaly, for example facial clefting into lip and palate, can also be difficult. This is represented in the low detection rate of cleft palate, which is caused by the loss of ultrasound signal due to the maxillary bone or by shadowing of the tongue.[40,41] Micrognathia can also be difficult to diagnose antenatally. Merz et al noted that only in 70% of cases the true fetal profile, used for evaluation of the mandible, was shown on 2DUS. This could lead to an underestimation of the growth of the fetal mandible.[44] Furthermore, fetal mandibular development lags behind on maxillary development, which may also lead to an overestimation of micrognathia on ultrasound prenatally.[42] On the other hand in a case-report of Pilu et al (1986), micrognathia was not diagnosed in a targeted evaluation of the mandible in the second trimester, but only in the third trimester when polyhydramnios had developed.[45]

Dysmorphic features in the fetus are often subtle and can easily been missed, even in a post-mortem examination.[46] Some syndrome-specific craniofacial features only develop later in pregnancy, as proven by a case of achondroplasia* described by Ghi et al (2002) as well as by Turner and Twining (1993), in which the stigmata of the disease developed after 20 weeks of gestation.[40,41] Measurement may be more objective in the assessment of craniofacial dysmorphism and more subtle abnormalities (e.g. in micrognathia).[47,48] This stresses the necessity of developing normal centile charts for craniofacial dimensions to facilitate prenatal diagnosis of craniofacial abnormalities.

*Three-dimensional ultrasound*

Because of the curvilinear structure of the face, the advantages of 3DUS are especially applicable in the detection of fetal craniofacial malformations.[49,50] 3DUS can facilitate diagnosis of complex syndromes with specific, often subtle, facial abnormalities. This allowed the prenatal diagnosis of Fryns syndrome*[51], Pfeiffer syndrome*[52], Treacher Collins syndrome*[53,54], congenital ichthyosis*[55,56], hypohidrotic ectodermal dysplasia*[57], Brachmann-de Lange syndrome*[58], Larsen syndrome*[59], Goldenhar syndrome*[60], Cat-eye syndrome*[61] and oculoauriculofrontonasal syndrome*[62]. Furthermore, 3DUS can be especially helpful in determining the extent of malformations such as cleft lip/ palate[44,63,64], otocephaly*[65], holoprocencephaly*[66,67], frontonasal malformation*[68] and in the diagnosis of craniofacial tumours [69-73].

Two-dimensional ultrasound and three-dimensional ultrasound have been compared in detecting craniofacial malformations more excessively in several studies.[44,74-76]

Additional information on the fetal face was found in 20- 71% of cases, whereas, 3DUS was found to be disadvantageous in only 2-9% (Table III). Most of these cases are false positives and could have been caused through lack of experience. In other cases no explanation is given. Mangione et al (2003) studied the practicability of 3DUS in diagnosing craniofacial dysmorphology. 3DUS was performed after suggestive findings presented at 2DUS examination.

* Syndromes/sequences are identified at p 179-180.

All 3D records were recorded and reviewed by a pediatrician-geneticist specialized in dysmorphology. The authors do not describe if this specialist also evaluated the 2DUS records. The 3D examination was satisfactory in 61% (25 of 41 cases). However, in none of the cases 3DUS proved to be the decision-making factor (Table III).[76]

**Table III:** Overview of literature comparing 2D- and 3D ultrasound in the detection of fetal craniofacial anomalies.

| *Authors* | *Methods* | *GA (wks)* | *N* | *2D and 3D equipment* | *3D + (%)* | *3D - (%)* | *2D/ 3D = (%)* | *Remarks* |
|---|---|---|---|---|---|---|---|---|
| Merz et al (1997)[44] | Additional 3DUS, all high risk patients | 9- 37 | 25 | Combison 530 (Kretz) | 5/ 25 (20) | 0 | 20/ 25 (80) | |
| Chen et al (2001)[74] | Retrospective analysis, additional 3DUS after malformation detected with 2D | 20- 34 | 21 | Aloka SSD-680 (2D), Combison 530 and Voluson 530D (3D) | 15/ 21 (71) | 0 | 6/ 21 (29) | Only cleft lip/ palate |
| Chmait et al (2002)[75] | Additional 3DUS after malformation detected with 2D | 15- 35 | 53 | 128 XP (Acuson), HDI (ATL), Elegra (Siemens), Combison 530 and Voluson 530D (3D) | 22/ 53 (42) | 1/ 53 (2) | 30/ 53 (56) | Only cleft lip/ palate |
| Mangione et al (2003)[76] | Additional 3DUS after malformation detected with 2D | 22- 36 | 41* | Voluson 530D | 20/ 34 (59) | 3/ 34 (9) | 11/ 34 (32) | Only craniofacial dysmorphology |

GA; gestational age, N; number, +/ -/ =; number and (percentage) of cases/ abnormalities in which 3D ultrasound proved to be advantageous/ disadvantageous/ or was equal to 2D. *Seven cases are not included because 3DUS was not possible

### 1.1.4 Assessment of craniofacial development

Different methods have been developed for objective evaluation of craniofacial development after birth to improve syndrome diagnosis. Anthropometry is a simple, non-invasive method based on surface dimensions, measured with for instance a measuring tape or marking gauge. In the radiographic cephalometric method, bony landmarks are assessed by use of X-ray. Other techniques to aid evaluation and measurement of craniofacial anatomy are photogrammetry (measurements are made with the use of a camera), 3D photogrammetry (the object is viewed from more than one photo-station simultaneously)[77], laser scanning and three-dimensional

craniofacial surface imaging from CT-scans and MRI.[33] Quantitative analysis can also be performed with the last two methods by extracting facial landmarks from the images.[78]

Multivariate analysis of these data allows patron profile analysis in order to evaluate the relationship of different parts of the head and to follow development in time. Samples of individuals are compared to normal population and expressed in Z-scores to illustrate the deviation of 'normality'. This also allows comparison of patients with for instance parents and groups with known diagnosis.[77] Application of the anthropometric and cephalometric methods in infants and adults has been described in Down Syndrome[79], various cleft palate syndromes and Pierre Robin sequence*[80,81], chondrodysplasia*[82] and fetal alcohol syndrome*[83].

A detailed prenatal ultrasound scan contains different routinely performed craniofacial measurements, such as biparietal diameter and head circumference. Other measurements are mostly carried out when indicated, i.e. intra-ocular and extra-ocular distance. Some craniofacial measurements carried out after birth, are difficult to obtain with the help of 2D ultrasound or have simply not been applied antenatally.

The anthropometric and cephalometric methods described above have been applied in one study using ultrasound in prenatal diagnosis. Escobar et al (1988, 1990) used conventional 2DUS for obtaining normal values for different cephalometric distances.[84,85] The authors also used Z-scores and pattern variability indexes in order to detect specific craniofacial abnormalities (fetal alcohol syndrome*, Crouzon syndrome* and thanatophoric dysplasia*). The authors found that Z-scores as well as pattern profile analysis might have an additional value in the diagnosis of fetuses with mild abnormalities or abnormality patterns, for instance in fetal alcohol syndrome*.[86] Note that with ultrasound both anthropometric and cepalometric measurements can be determined, as both soft-tissue as bony landmarks can be made visible by the technique.

Other authors have described the value of specific craniofacial measurement in the second half of pregnancy as possible tools in the detection of fetal malformation (Table IV).[47,87-104] Especially the length of the nasal bone has recently been of public interest as an additional tool in the screening of Down syndrome.[105] So far, different craniofacial structures have been studied with 3DUS. The application possibilities of both quantitative and qualitative evaluation are listed in Table V. Especially on the subject of cleft lip and palate several studies have been conducted. Ulm et al (1999)[106] and Lee et al (2000)[107] describe methods to evaluate the lip and or the alveolus. Whereas, Rotten and Levaillant (2004)[63] and Campbell et al[108] explain how to visualize the hard palate.

In conclusion, the 3-dimensional ultrasound technique offers potential advantages over 2DUS, especially in the evaluation of complex anatomy. These advantages seem to be especially applicable to the fetal head and face. Isolated craniofacial anomalies and minor malformations can be very difficult to determine *in utero* with conventional (2D) ultrasound.

* Syndromes/sequences are identified at p 141-143.

**Table IV:** Overview of literature on 2D ultrasound measurements of fetal craniofacial structures.

| *Structure* | *Measurement* | *Authors* | *N* | *GA (week)* |
|---|---|---|---|---|
| Skull base | Length and width of sphenoid ridge, otic cartilage and angles of cranial fossa | Degani et al (2002)[87] | 386 | 14- 40 |
| Palpebral fissure | Palpebral fissure slant (angle between palpebral fissure and frontal midline) | Mielke et al (1997)[88] | 70 | 14- 36 |
| Ear | Ear length | Birnholz et al (1988)[89] | 180 | 15- 40 |
| | Ear length and width | Shimizu et al (1992)[90] | 124 | 18- 42 |
| | Ear length | Lettieri et al (1993)[91] | 424 | 14- 25 |
| | Ear length | Chitkara et al (2000)[92] | 4240 | 15- 40 |
| | Ear length | Yeo et al (2003)[93] | 447 | 14- 41 |
| Nose | Nasal width and nostril distance | Goldstein et al (1997)[94] | 302 | 14- 40 |
| | Nasal width | Pinette et al (1997)[95] | 782 | 14- 40 |
| | Nasal width | Ben Ami et al (1998)[96] | 229 | 15- 42 |
| | Nasal bone length | Guis et al (1995)[97] | 376 | 14- 34 |
| | Nasal bone length | Bunduki et al (2003)[98] | 1923 | 16- 24 |
| | Nasal bone length | Sonek et al (2003)[99] | 3537 | 11- 38 |
| | Nasal bone length | Gámez et al (2004)[100] | 2035 | 19- 22 |
| Palate | Alveolar ridge width | Goldstein et al (1999)[101] | 302 | 14- 40 |
| | Palate length, width and area | Sherer et al (2004)[102] | 602 | 15- 41 |
| Mandible | Mandibular length | Otto and Platt (1991)[103] | 134 | 14- 39 |
| | Mandibular length | Chitty et al (1993)[47] | 184 | 12- 27 |
| | Anteroposterior and laterolateral diameters | Paladini et al (1999)[104] | 262 | 12- 37 |

GA; gestational age, N; number

Anthropometric and cephalometric measurement and the analysis of z-scores and profile patterns might be helpful in the diagnosis of these anomalies. Combining the advantages of 3DUS with objective assessment could aid in the evaluation of normal and abnormal craniofacial development.

## 1.2 RESEARCH OBJECTIVES

In view of the above, we formulated the following objectives for this study:

1. To develop a 3D sonographic method of establishing fetal craniofacial biometry. Measurements will be distracted from literature on postnatal anthropometric and cephalometric methods which have proven useful in the assessment of (ab)normal craniofacial development;
2. To develop reproducibility and normal data relative to gestational age for these measurements and analyze variability;

**Table V:** Overview of literature of 3D assessment of fetal craniofacial structures.

| *Assessment of:* | | *Authors* | *N* | *GA (week)* |
|---|---|---|---|---|
| Cranial sutures and fontanels | | Pretorius and Nelson (1994)[109] | 8 | 16- 39 |
| Fetal frontal bones and metopic suture | | Faro et al (2005)[110] | 16 | 9-34 |
| Forehead length, height and area | | Sivan et al (1997)[111] | 130 | 16- 38 |
| Brain volume | | Endres and Cohen (2001)[112] | 85 | 16- 40 |
| | | Chang et al (2003)[113] | 203 | 20- 40 |
| Lips and palate | | Lee et al (2000)[107] | 7 | ? |
| | | Campbell et al (2005) [108] | 8 | 20- 31 |
| | | Rotten and Levaillant (2004)[63] | 96 | 22- 39 |
| Tooth buds | | Ulm et al (1999)[106] | 17 | 18- 31 |
| Ear | Morphology, lying axis, orientation and cranial location | Shih et al (1998)[114] | 125 | 19- 38 |
| | Length, width, area and shape | Chang et al (2000)[115] | 122 (+ 7 trisomies) | 17- 41 |
| Maxilla, Mandible | Maxillary and mandibular width, inferior facial angle | Rotten et al (2002)[116] | 245/ 371 (+38 anomalies) | 18- 28 |
| | Diagnostic approaches for evaluation | Lee et al (2002)[117] | 9 cases of micrognа-thia | 16- 36 |
| | Mandibular body length | Tsai et al (2004)[118] | 183 cross sectional+ 40 serial cases | 14- 39 |

GA; gestational age, N; number

3. To apply this 3D sonographic method to prenatal diagnosis of craniofacial malformations, such as cleft lip/ palate.

## 1.3 References


1. Nelson TR, Pretorius DH. Three-dimensional ultrasound imaging. *Ultrasound Med Biol* 1998; 24: 1243-1270.
2. Steiner H, Staudach A, Spitzer D, Schaffer H. 3-Dimensional Ultrasound in Obstetrics and Gynecology - Technique, Possibilities and Limitations. *Hum Reprod* 1994; 9: 1773-1778.
3. Baba K, Satoh K, Sakamoto S, Okai T, Ishii S. Development of An Ultrasonic System for 3-Dimensional Reconstruction of the Fetus. *J Perinat Med* 1989; 17: 19-24.
4. Kuo HC, Chang FM, Wu CH, Yao BL, Liu CH. The primary application of three-dimensional ultrasonography in obstetrics. *Am J Obstet Gynecol* 1992; 166: 880-886.
5. Nelson TR, Pretorius DH. 3-Dimensional Ultrasound of Fetal Surface-Features. *Ultrasound Obstet Gynecol* 1992; 2: 166-174.
6. Baba K. Development of Three-Dimensional Ultrasound in Obstetrics and Gynecology: Technical Aspects and Possibilities. In *3-D Ultrasound in Obstetrics and Gynecology*, Merz E. Lippincott Williams and Wilkins: Philadelphia, 1998
7. Nelson TR. Three-dimensional imaging. *Ultrasound Med Biol* 2000; 26 Suppl 1: 35-38.

8. Gritzky A, Brandl H. The VoluSon (Kretz) Technique. In *3-D Ultrasound in Obstetrics and Gynecology*, Merz E. Lippincott Williams and Wilkins: Philadelphia, 1998; 9-15.

9. Abramowicz JS, Kossoff G, Marsal K, Ter Haar G. Literature review by the ISUOG Bioeffects and Safety Committee. *Ultrasound Obstet Gynecol* 2002; 19: 318-319.

10. Merz E, Bahlmann F, Weber G, Macchiella D. Three-dimensional ultrasonography in prenatal diagnosis. *J Perinat Med* 1995; 23: 213-222.

11. Merz E, Bahlmann F, Weber G. Volume scanning in the evaluation of fetal malformations: a new dimension in prenatal diagnosis. *Ultrasound Obstet Gynecol* 1995; 5: 222-227.

12. Lee A, Deutinger J, Bernaschek G. "Voluvision": three-dimensional ultrasonography of fetal malformations. *Am J Obstet Gynecol* 1994; 170: 1312-1314.

13. Steiner H, Spitzer D, Weiss-Wichert PH, Graf AH, Staudach A. Three-dimensional ultrasound in prenatal diagnosis of skeletal dysplasia. *Prenat Diagn* 1995; 15: 373-377.

14. Platt LD, Santulli T, Carlson DE, Greene N, Walla CA. Three-dimensional ultrasonography in obstetrics and gynecology: Preliminary experience. *Am J Obstet Gynecol* 1998; 178: 1199-1204.

15. Platt LD. Three-dimensional ultrasound, 2000. *Ultrasound Obstet Gynecol* 2000; 16: 295-298.

16. Dyson RL, Pretorius DH, Budorick NE, Johnson DD, Sklansky MS, Cantrell CJ, Lai S, Nelson TR. Three-dimensional ultrasound in the evaluation of fetal anomalies. *Ultrasound Obstet Gynecol* 2000; 16: 321-328.

17. Xu HX, Zhang QP, Lu MD, Xiao XT. Comparison of two-dimensional and three-dimensional sonography in evaluating fetal malformations. *J Clin Ultrasound* 2002; 30: 515-525.

18. Moeglin D, Benoit B. Three-dimensional sonographic aspects in the antenatal diagnosis of achondroplasia. *Ultrasound Obstet Gynecol* 2001; 18: 81-83.

19. Viora E, Sciarrone V, Bastonero S, Errante G, Botta G, Campogrande M. Three-dimensional ultrasound evaluation of short-rib polydactyly syndrome type II in the second trimester: a case report. *Ultrasound Obstet Gynecol* 2002; 19: 88-91.

20. Seow KM, Huang LW, Lin YH, Pan HS, Tsai YL, Hwang JL. Prenatal three-dimensional ultrasound diagnosis of a camptomelic dysplasia. *Arch Gynecol Obstet* 2004; 269: 142-144.

21. Hull AD, Pretorius DH, Lev-Toaff A, Budorick NE, Salerno CC, Johnson MM, James G, Nelson TR. Artifacts and the visualization of fetal distal extremities using three- dimensional ultrasound. *Ultrasound Obstet Gynecol* 2000; 16: 341-344.

22. Krakow D, Williams J, Poehl M, Rimoin DL, Platt LD. Use of three-dimensional ultrasound imaging in the diagnosis of prenatal-onset skeletal dysplasias. *Ultrasound Obstet Gynecol* 2003; 21: 467-472.

23. Ruano R, Molho M, Roume J, Ville Y. Prenatal diagnosis of fetal skeletal dysplasias by combining two-dimensional and three-dimensional ultrasound and intrauterine three-dimensional helical computer tomography. *Ultrasound Obstet Gynecol* 2004; 24: 134-140.

24. Sepulveda W, Sepulveda-Swatson E, Sanchez J. Diastrophic dysplasia: prenatal three-dimensional ultrasound findings. *Ultrasound Obstet Gynecol* 2004; 23: 312-314.

25. Nelson TR, Pretorius DH, Lev-Toaff A, Bega G, Budorick NE, Hollenbach KA, Needleman L. Feasibility of performing a virtual patient examination using three- dimensional ultrasonographic data acquired at remote locations. *J Ultrasound Med* 2001; 20: 941-952.

26. Scharf A, Ghazwiny MF, Steinborn A, Baier P, Sohn C. Evaluation of two-dimensional versus three-dimensional ultrasound in obstetric diagnostics: a prospective study. *Fetal Diagn Ther* 2001; 16: 333-341.
27. Campbell S. 4D, or not 4D: that is the question. *Ultrasound Obstet Gynecol* 2002; 19: 1-4.
28. Deng J. Terminology of three-dimensional and four-dimensional ultrasound imaging of the fetal heart and other moving body parts. *Ultrasound Obstet Gynecol* 2003; 22: 336-344.
29. Viñals F, Poblete P, Giuliano A. Spatio-temporal image correlation (STIC): a new tool for the prenatal screening of congenital heart defects. *Ultrasound Obstet Gynecol* 2003; 22: 388-394.
30. de Elejalde MM, Elejalde BR. Visualization of the fetal face by ultrasound. *J Craniofac Genet Dev Biol* 1984; 4: 251-257.
31. Spauwen PH. [Fifty years of plastic surgery in the Netherlands. IV. Treatment of children with cleft lip and palate]. *Ned Tijdschr Geneeskd* 2000; 144: 973-980.
32. Gorlin RJ, Cohen MM, Levin IS. Syndromes of the Head and the Neck. Oxford University Press, 1990.
33. Cohen MM, Jr. Syndromology: an updated conceptual overview. IX. Facial dysmorphology. *Int J Oral Maxillofac Surg* 1990; 19: 81-88.
34. Crane JP, LeFevre ML, Winborn RC, Evans JK, Ewigman BG, Bain RP, Frigoletto FD, McNellis D. A randomized trial of prenatal ultrasonographic screening: impact on the detection, management, and outcome of anomalous fetuses. The RADIUS Study Group. *Am J Obstet Gynecol* 1994; 171: 392-399.
35. Hafner E, Sterniste W, Scholler J, Schuchter K, Philipp K. Prenatal diagnosis of facial malformations. *Prenat Diagn* 1997; 17: 51-58.
36. Clementi M, Tenconi R, Bianchi F, Stoll C. Evaluation of prenatal diagnosis of cleft lip with or without cleft palate and cleft palate by ultrasound: experience from 20 European registries. EUROSCAN study group. *Prenat Diagn* 2000; 20: 870-875.
37. Cash C, Set P, Coleman N. The accuracy of antenatal ultrasound in the detection of facial clefts in a low-risk screening population. *Ultrasound Obstet Gynecol* 2001; 18: 432-436.
38. Chitty LS. Ultrasound screening for fetal abnormalities. *Prenat Diagn* 1995; 15: 1241-1257.
39. Pilu G, Reece EA, Romero R, Bovicelli L, Hobbins JC. Prenatal diagnosis of craniofacial malformations with ultrasonography. *Am J Obstet Gynecol* 1986; 155: 45-50.
40. Turner GM, Twining P. The Facial Profile in the Diagnosis of Fetal Abnormalities. *Clin Radiol* 1993; 47: 389-395.
41. Ghi T, Perolo A, Banzi C, Contratti G, Valeri B, Savelli L, Morselli GP, Bovicelli L, Pilu G. Two-dimensional ultrasound is accurate in the diagnosis of fetal craniofacial malformation. *Ultrasound Obstet Gynecol* 2002; 19: 543-551.
42. Wong GB, Mulliken JB, Benacerraf BR. Prenatal sonographic diagnosis of major craniofacial anomalies. *Plast Reconstr Surg* 2001; 108: 1316-1333.
43. van der Ham LI, Cohen-Overbeek TE, Paz y Geuze HD, Vermeij-Keers C. The ultrasonic detection of an isolated craniosynostosis. *Prenat Diagn* 1995; 15: 1189-1192.
44. Merz E, Weber G, Bahlmann F, Miric-Tesanic D. Application of transvaginal and abdominal three-dimensional ultrasound for the detection or exclusion of malformations of the fetal face. *Ultrasound Obstet Gynecol* 1997; 9: 237-243.

45. Pilu G, Romero R, Reece EA, Jeanty P, Hobbins JC. The prenatal diagnosis of Robin anomalad. *Am J Obstet Gynecol* 1986; 154: 630-632.

46. Chambers HM, Knowles S, Staples A, Tamblyn M, Haan EA. Anthropometric measurements in the second trimester fetus. *Early Hum Dev* 1993; 33: 45-59.

47. Chitty LS, Campbell S, Altman DG. Measurement of the fetal mandible--feasibility and construction of a centile chart. *Prenat Diagn* 1993; 13: 749-756.

48. Nicolaides KH, Salvesen DR, Snijders RJ, Gosden CM. Fetal facial defects: associated malformations and chromosomal abnormalities. *Fetal Diagn Ther* 1993; 8: 1-9.

49. Lee A, Deutinger J, Bernaschek G. Three dimensional ultrasound: abnormalities of the fetal face in surface and volume rendering mode. *Br J Obstet Gynaecol* 1995; 102: 302-306.

50. Pretorius DH, Nelson TR. Fetal face visualization using three-dimensional ultrasonography. *J Ultrasound Med* 1995; 14: 349-356.

51. Van Wymersch D, Favre R, Gasser B. Use of three-dimensional ultrasound to establish the prenatal diagnosis of Fryns syndrome. *Fetal Diagn Ther* 1996; 11: 335-340.

52. Benacerraf BR, Spiro R, Mitchell AG. Using three-dimensional ultrasound to detect craniosynostosis in a fetus with Pfeiffer syndrome. *Ultrasound Obstet Gynecol* 2000; 16: 391-394.

53. Hsu TY, Hsu JJ, Chang SY, Chang MS. Prenatal three-dimensional sonographic images associated with Treacher Collins syndrome. *Ultrasound Obstet Gynecol* 2002; 19: 413-422.

54. Tanaka Y, Kanenishi K, Tanaka H, Yanagihara T, Hata T. Antenatal three-dimensional sonographic features of Treacher Collins syndrome. *Ultrasound Obstet Gynecol* 2002; 19: 414-415.

55. Bongain A, Benoit B, Ejnes L, Lambert JC, Gillet JY. Harlequin fetus: three-dimensional sonographic findings and new diagnostic approach. *Ultrasound Obstet Gynecol* 2002; 20: 82-85.

56. Vohra N, Rochelson B, Smith-Levitin M. Three-dimensional sonographic findings in congenital (harlequin) ichthyosis. *J Ultrasound Med* 2003; 22: 737-739.

57. Sepulveda W, Sandoval R, Carstens E, Gutierrez J, Vasquez P. Hypohidrotic ectodermal dysplasia - Prenatal diagnosis by three-dimensional ultrasonography. *J Ultrasound Med* 2003; 22: 731-735.

58. Le Vaillant C, Quere MP, David A, Berlivet M, Boog G. Prenatal diagnosis of a 'minor' form of Brachmann-de Lange syndrome by three-dimensional sonography and three-dimensional computed tomography. *Fetal Diagn Ther* 2004; 19: 155-159.

59. Shih JC, Peng SS, Hsiao SM, Wang JH, Shyu MK, Lee CN, Hsieh FJ. Three-dimensional ultrasound diagnosis of Larsen syndrome with further characterization of neurological sequelae. *Ultrasound Obstet Gynecol* 2004; 24: 89-93.

60. Volpe P, Gentile M. Three-dimensional diagnosis of Goldenhar syndrome. *Ultrasound Obstet Gynecol* 2004; 24: 797-804.

61. Volpe P, Buonadonna AL, Campobasso G, Di Carlo A, Stanziano A, Gentile M. Cat-eye syndrome in a fetus with increased nuchal translucency: three-dimensional ultrasound and echocardiographic evaluation of the fetal phenotype. *Ultrasound Obstet Gynecol* 2004; 24: 485-487.

62. Johnson JM, Benoit B, Pierre-Louis J, Keating S, Chitayat D. Early prenatal diagnosis of oculoauriculofrontonasal syndrome by three-dimensional ultrasound. *Ultrasound Obstet Gynecol* 2005; 25: 184-186.

63. Rotten D, Levaillant JM. Two- and three-dimensional sonographic assessment of the fetal face. 2. Analysis of cleft lip, alveolus and palate. *Ultrasound Obstet Gynecol* 2004; 24: 402-411.

64. Pilu G, Visentin A, Ambrosini G, D'Antona D, Andrisani A. Three-dimensional sonography of unilateral Tessier number 7 celft in a mid-trimester fetus. *Ultrasound Obstet Gynecol* 2005; 26: 97-100.

65. Lin HH, Liang RI, Chang FM, Chang CH, Yu CH, Yang HB. Prenatal diagnosis of otocephaly using two-dimensional and three- dimensional ultrasonography. *Ultrasound Obstet Gynecol* 1998; 11: 361-363.

66. Manabe A, Hata T, Aoki S, Matsumoto M, Yanagihara T, Yamada Y, Irikoma S, Miyazaki K. Three-dimensional sonographic visualization of fetal facial anomaly. *Acta Obstet Gynecol Scand* 1999; 78: 917-918.

67. Lai TH, Chang CH, Yu CH, Kuo PL, Chang FM. Prenatal diagnosis of alobar holoprosencephaly by two-dimensional and three-dimensional ultrasound. *Prenat Diagn* 2000; 20: 400-403.

68. Shipp TD, Mulliken JB, Bromley B, Benacerraf B. Three-dimensional prenatal diagnosis of frontonasal malformation and unilateral cleft lip/palate. *Ultrasound Obstet Gynecol* 2002; 20: 290-293.

69. Sepulveda W, Muhlhausen G, Flores X, Gutierrez J, Avila R. Giant hemangiopericytoma of the fetal neck - Prenatal two- and three-dimensional sonographic findings. *J Ultrasound Med* 2003; 22: 831-835.

70. Merhi ZO, Haberman S, Roberts JL, Sobol-Benin G. Prenatal Diagnosis of Palatal Teratoma by 3-Dimensional Sonography and Color Doppler Imaging. *J Ultrasound Med* 2005; 24: 1317-1320.

71. Paladini D, Vassallo M, Sglavo G, Lapadula C, Longo M, Nappi C. Cavernous lymphangioma of the face and neck: prenatal diagnosis by three-dimensional ultrasound. *Ultrasound Obstet Gynecol* 2005; 26: 300-302.

72. Petrikovsky BM, Kaplan GP. Fetal dacryocystocele: comparing 2D and 3D imaging. *Pedriatr Radiol* 2003; 33: 582-583.

73. Sepulveda W, Wojakowski AB, Elias D, Otano L, Gutierrez J. Congenital dacryocystocele: prenatal 2- and 3-dimensional sonographic findings. *J Ultrasound Med* 2005; 24: 225-230.

74. Chen ML, Chang CH, Yu CH, Cheng YC, Chang FM. Prenatal diagnosis of cleft palate by three-dimensional ultrasound. *Ultrasound Med Biol* 2001; 27: 1017-1023.

75. Chmait R, Pretorius D, Jones M, Hull A, James G, Nelson T, Moore T. Prenatal evaluation of facial clefts with two-dimensional and adjunctive three-dimensional ultrasonography: a prospective trial. *Am J Obstet Gynecol* 2002; 187: 946-949.

76. Mangione R, Lacombe D, Carles D, Guyon F, Saura R, Horovitz J. Craniofacial dysmorphology and three-dimensional ultrasound: a prospective study on practicability for prenatal diagnosis. *Prenat Diagn* 2003; 23: 810-818.

77. Allanson JE. Objective techniques for craniofacial assessment: what are the choices? *Am J Med Genet* 1997; 70: 1-5.

78. Zonneveld FW, Fukuta K. A decade of clinical three-dimensional imaging: a review. Part 2: Clinical applications. *Invest Radiol* 1994; 29: 574-589.

79. Allanson JE, O'Hara P, Farkas LG, Nair RC. Anthropometric craniofacial pattern profiles in Down syndrome. *Am J Med Genet* 1993; 47: 748-752.

80. Garn SM, Lavelle M, Smith BH. Quantification of dysmorphogenesis: pattern variability index, sigma z. *AJR Am J Roentgenol* 1985; 144: 365-369.

81. Garn SM, Smith BH, Lavelle M. Applications of pattern profile analysis to malformations of the head and face. *Radiology* 1984; 150: 683-690.

82. Hunter AG. Craniofacial anthropometric analysis in several types of chondrodysplasia. *Am J Med Genet* 1996; 65: 5-12.

83. Frias JL, King GJ, Williams CA. Cephalometric assessment of selected malformation syndromes. *Birth Defects Orig Artic Ser* 1982; 18: 139-150.

84. Escobar LF, Bixler D, Padilla LM, Weaver DD, Williams CJ. A morphometric analysis of the fetal craniofacies by ultrasound: fetal cephalometry. *J Craniofac Genet Dev Biol* 1990; 10: 19-27.

85. Escobar LF, Bixler D, Padilla LM, Weaver DD. Fetal craniofacial morphometrics: in utero evaluation at 16 weeks' gestation. *Obstet Gynecol* 1988; 72: 674-679.

86. Escobar LF, Bixler D, Padilla LM. Quantitation of craniofacial anomalies in utero: fetal alcohol and Crouzon syndromes and thanatophoric dysplasia. *Am J Med Genet* 1993; 45: 25-29.

87. Degani S, Leibovitz Z, Shapiro I, Gonen R, Ohel G. Ultrasound evaluation of the fetal skull base throughout pregnancy. *Ultrasound Obstet Gynecol* 2002; 19: 461-466.

88. Mielke G, Dietz K, Franz H, Reiss I, Gembruch U. Sonographic assessment of the fetal palpebral fissure slant--an additional tool in the prenatal diagnosis of syndromes. *Prenat Diagn* 1997; 17: 323-326.

89. Birnholz JC, Farrell EE. Fetal Ear Length. *Pediatrics* 1988; 81: 555-558.

90. Shimizu T, Salvador L, Allanson J, Hughes-Benzie R, Nimrod C. Ultrasonographic measurements of fetal ear. *Obstet Gynecol* 1992; 80: 381-384.

91. Lettieri L, Rodis JF, Vintzileos AM, Feeney L, Ciarleglio L, Craffey A. Ear Length in 2Nd-Trimester Aneuploid Fetuses. *Obstet Gynecol* 1993; 81: 57-60.

92. Chitkara U, Lee L, El-Sayed YY, Holbrook RH, Jr., Bloch DA, Oehlert JW, Druzin ML. Ultrasonographic ear length measurement in normal second- and third- trimester fetuses. *Am J Obstet Gynecol* 2000; 183: 230-234.

93. Yeo L, Guzman ER, Ananth CV, Walters C, Day-Salvatore D, Vintzileos AM. Fetal aneuploidy by sonographic ear length. *J Ultrasound Med* 2003; 22: 565-576.

94. Goldstein I, Tamir A, Itskovitz-Eldor J, Zimmer EZ. Growth of the fetal nose width and nostril distance in normal pregnancies. *Ultrasound Obstet Gynecol* 1997; 9: 35-38.

95. Pinette MG, Blackstone J, Pan YQ, Pinette SG. Measurement of fetal nasal width by ultrasonography. *Am J Obstet Gynecol* 1997; 177: 842-845.

96. Ben Ami M, Weiner E, Perlitz Y, Shalev E. Ultrasound evaluation of the width of the fetal nose. *Prenat Diagn* 1998; 18: 1010-1013.

97. Guis F, Ville Y, Vincent Y, Doumerc S, Pons JC, Frydman R. Ultrasound evaluation of the length of the fetal nasal bones throughout gestation. *Ultrasound Obstet Gynecol* 1995; 5: 304-307.

98. Bunduki V, Ruano R, Miguelez J, Yoshizaki CT, Kahhale S, Zugaib M. Fetal nasal bone length: reference range and clinical application in ultrasound screening for trisomy 21. *Ultrasound Obstet Gynecol* 2003; 21: 156-160.

99. Sonek JD, McKenna D, Webb D, Croom C, Nicolaides K. Nasal bone length throughout gestation: normal ranges based on 3537 fetal ultrasound measurements. *Ultrasound Obstet Gynecol* 2003; 21: 152-155.

100. Gamez F, Ferreiro P, Salmean JM. Ultrasonographic measurement of fetal nasal bone in a low-risk population at 19-22 gestational weeks. *Ultrasound Obstet Gynecol* 2004; 23: 152-153.

101. Goldstein I, Jakobi P, Tamir A, Goldstick O. Nomogram of the fetal alveolar ridge: a possible screening tool for the detection of primary cleft palate. *Ultrasound Obstet Gynecol* 1999; 14: 333-337.

102. Sherer DM, Sokolovski M, Santoso PG, Dalloul M, Abulafia O. Nomograms of sonographic measurements throughout gestation of the fetal hard palate width, length and area. *Ultrasound Obstet Gynecol* 2004; 24: 35-41.

103. Otto C, Platt LD. The Fetal Mandible Measurement - An Objective Determination of Fetal Jaw Size. *Ultrasound Obstet Gynecol* 1991; 1: 12-17.

104. Paladini D, Morra T, Teodoro A, Lamberti A, Tremolaterra F, Martinelli P. Objective diagnosis of micrognathia in the fetus: the jaw index. *Obstet Gynecol* 1999; 93: 382-386.

105. Cicero S, Sonek JD, McKenna DS, Croom CS, Johnson L, Nicolaides KH. Nasal bone hypoplasia in trisomy 21 at 15-22 weeks' gestation. *Ultrasound Obstet Gynecol* 2003; 21: 15-18.

106. Ulm MR, Kratochwil A, Ulm B, Lee A, Bettelheim D, Bernaschek G. Three-dimensional ultrasonographic imaging of fetal tooth buds for characterization of facial clefts. *Early Hum Dev* 1999; 55: 67-75.

107. Lee W, Kirk JS, Shaheen KW, Romero R, Hodges AN, Comstock CH. Fetal cleft lip and palate detection by three-dimensional ultrasonography. *Ultrasound Obstet Gynecol* 2000; 16: 314-320.

108. Campbell S, Lees C, Moscoso G, Hall P. Ultrasound antenatal diagnosis of cleft palate by a new technique: the 3D 'reverse face' view. *Ultrasound Obstet Gynecol* 2005; 25: 12-18.

109. Pretorius DH, Nelson TR. Prenatal visualization of cranial sutures and fontanelles with three- dimensional ultrasonography. *J Ultrasound Med* 1994; 13: 871-876.

110. Faro C, Benoit B, Wegrzyn P, Chaoui R, Nicolaides KH. Three-dimensional sonographic description of the fetal frontal bones and metopic suture. *Ultrasound Obstet Gynecol* 2005; 26: 618-621.

111. Sivan E, Chan L, Uerpairojkit B, Chu GP, Reece EA. Growth of the fetal forehead and normative dimensions developed by three-dimensional ultrasonographic technology. *J Ultrasound Med* 1997; 16: 401-405.

112. Endres LK, Cohen L. Reliability and validity of three-dimensional fetal brain volumes. *J Ultrasound Med* 2001; 20: 1265-1269.

113. Chang CH, Yu CH, Chang FM, Ko HC, Chen HY. The assessment of normal fetal brain volume by 3-D ultrasound. *Ultrasound Med Biol* 2003; 29: 1267-1272.

114. Shih JC, Shyu MK, Lee CN, Wu CH, Lin GJ, Hsieh FJ. Antenatal depiction of the fetal ear with three-dimensional ultrasonography. *Obstet Gynecol* 1998; 91: 500-505.

115. Chang CH, Chang FM, Yu CH, Liang RI, Ko HC, Chen HY. Fetal ear assessment and prenatal detection of aneuploidy by the quantitative three-dimensional ultrasonography. *Ultrasound Med Biol* 2000; 26: 743-749.

116. Rotten D, Levaillant JM, Martinez H, Ducou le Pointe H, Vicaut E. The fetal mandible: a 2D and 3D sonographic approach to the diagnosis of retrognathia and micrognathia. *Ultrasound Obstet Gynecol* 2002; 19: 122-130.

117. Lee W, McNie B, Chaiworapongsa T, Conoscenti G, Kalache KD, Vettraino IM, Romero R, Comstock CH. Three-dimensional ultrasonographic presentation of micrognathia. *J Ultrasound Med* 2002; 21: 775-781.

118. Tsai MY, Lan KC, Ou CY, Chen JH, Chang SY, Hsu TY. Assessment of the facial features and chin development of fetuses with use of serial three-dimensional sonography and the mandibular size monogram in a Chinese population. *Am J Obstet Gynecol* 2004; 190: 541-546.

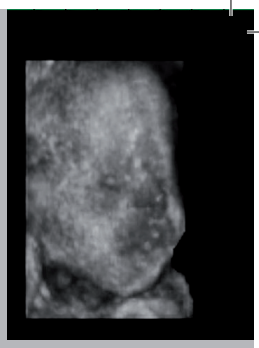

Chapter 2

# Methodology for 2D and 3D fetal craniofacial biometry assessment

## 2.1 METHODOLOGY

### 2.1.1 Study subjects

In a longitudinal study design a total of 126 women with a normal singleton pregnancy consented to participate in the study, which was approved by the Hospital Ethics Review Board. Another six women with a fetal anomaly known or suspected to affect craniofacial anatomy and 15 women with a pregnancy that was complicated by fetal cleft lip/ palate consented to participate. Pregnancy duration was determined from the last reliable menstrual period, or in case of uncertainty, adjusted by ultrasound in the first trimester of gestation.

*Population of normal pregnancies*

Women were recruited from the antenatal outpatient's and regional midwifery services. Included were only women without maternal disease known to affect fetal growth, i.e. pre-existent hypertension, diabetes mellitus and pregnancies that were not at risk for craniofacial abnormality. A total of 126 women remained in the study after three (2%) women were excluded retrospectively from the analysis. The reasons for exclusion were a prenatally detected fetal malformation (n=1; spina bifida), a congenital malformation or disease recognised after birth (n=1; mildly hydropic child, cause unknown) or no follow-up available (n=1). These criteria for exclusion were based on literature for assessment of normal biometry by Altman and Chitty.[1]

Pregnancy duration varied between 18 and 34 weeks (median 26 weeks). Maternal age ranged between 19 and 40 years (median 30 years). 95% of the birth weights were situated between the 5$^{th}$ and the 95$^{th}$ percentile, adjusted for maternal parity and fetal sex, according to the Kloosterman tables.[2] Sixty-five (52%) infants were male and 61 (48%) were female.

In each pregnancy, three-dimensional (3D) sonographic examinations were performed four times at 3- 5 week intervals. The third or last examination could not be performed in five pregnancies and five records were not, or only partly, available for analysis, resulting in a total of 494 complete recordings.

Standard craniofacial biometry (biparietal diameter, frontal occipital diameter, head circumference, intra-ocular diameter and outer-ocular diameter) was also measured by two-dimensional ultrasound for comparison with three-dimensional ultrasound.

Intraobserver variability was determined in 22 normal singleton pregnancies, six of which also participating in the serial study. Pregnancy duration was equally distributed over the same gestational period.

*Population with a fetal anomaly*

All 21 women were recruited from the Division of Obstetrics and Prenatal Medicine. Pregnancy duration varied between 19 and 34 weeks (median 25 weeks). Maternal age ranged between 20 and 40 years (median 29 years). 3D ultrasound examinations were performed only once

after a fetal abnormality was suspected on a detailed two-dimensional (2D) ultrasound scan. The researcher knew the outcome of the 2D ultrasound examination at the time of the 3D examination.

### 2.1.2 Recording technique

Three-dimensional sonographic assessment of the fetal head and face was performed using a standard Voluson 530 D (Kretztechnik AG, Zipf, Austria) with a 3- 5 MHz transducer (VAW 3-5). An internal mechanism in the transducer sliced through the images and recorded a truncated pyramidal volume. Depth, longitudinal and transverse dimensions were adjustable. An opening angle of 50 to 70 degrees and a sampling angle of 30 to 85 degrees was used, resulting in a maximum volume of 3.2 litre. The depth range for the region of interest was set at 6-13 cm. 'Normal' frequency range (mid resolution/ mid penetration) was used in most patients, but was adjusted to 'penetration' (lower resolution/ high penetration) in case of obesity. Frequency range 'resolution' was used in case of thin women and/or superficial position of the fetus. Scanning time for one recorded volume ranged between 4 and 8 seconds, depending on fetal movement and size of the recorded volume.

The region of interest was defined containing the complete fetal head. Three different types of acquisition of the fetal face and head were made. A sagittal scan (frontal view of the face composed of sagittal planes); a coronal scan (side of the head composed of coronal planes); and a transverse scan (side of the head composed of transverse planes). Acquisition of the sagittal scan of the face started at the mid-sagittal plane with the fetus facing the transducer. A coronal scan was made starting acquisition just in front of the ear. A transverse scan was made by using the regular plane for measurement of the biparietal diameter[3] starting the acquisition. Multiple volume recordings were made of each fetus (normal group: range 2-11, median 5; group with fetal abnormalities: range 4- 9, median 7) to obtain one good volume for every type of acquisition. The best volume data were then collected on a transportable magnetic disk for later analysis (Iomega Corp., Roy, UT, USA). Total time for the 3DUS-examination was 15- 60 minutes (median 30) for the normal group, which included normal growth assessment with 2DUS, and 15- 50 (median 20) for the group with fetal anomalies.

A total set of 41 craniofacial measurements, proven useful in the assessment of postnatal (ab)normal craniofacial development, were extracted from literature on anthropometric and cephalometric measurements.[4-11] These measurements were selected on the basis of applicability with 3D ultrasound and covering the various aspects of fetal facial anatomy.

Measurements were made using the 3D view program (Kretztechnik AG, version 4.0) on a personal computer with an Iomega Jaz Drive. This took 20- 30 minutes. The methodology of these measurements is described hereafter (chapter 2.1.3).

One observer (NR) performed all 3D ultrasound examinations and measurements.

The reproducibility study consisted of recording two volume data sets from the same fetus at a time interval of approximately 20 minutes. The first recorded data set was analyzed twice

with a minimal time interval of one week. This second analysis was done while being blinded for the first analysis.

Sixteen out of the 41 original craniofacial measurements were used for pattern profile analysis and calculation of a craniofacial variability index. These measurements were selected on the basis of reproducibility and relevance (covering best the facial height, width and depth)



### 2.1.3 Craniofacial measurements

These measurements are based on postnatal cephalometric and anthropometric techniques, using bony and soft-tissue landmarks, respectively. The landmarks in this study are mostly the landmarks used in the original studies[4-11], however if bony landmarks were better visible on 3DUS than the original soft-tissue landmarks, bony landmarks were used.

*Measurements derived from the sagittal scan mode of 3D acquisition.*

**Measurement 1– 7 (soft-tissue landmarks are used unless mentioned otherwise):**[4-6]

Landmarks: *Vertex (a)*: the highest point of the head, *nasion (c)*: the deepest part of the nasal root, *pronasale (d)*: the tip of the nose, *subnasion (e)*: the deepest point of concavity at the base of the nose, *gnathion (f)*: lowest median landmark on the lower border of the mandible, o*pisthion (g)*: lowest posterior point of the skull (inner border; bony landmark). (Figure1; a-g)

Position of the fetal head: "upright position" (approximately Frankfurter horizontal[#]): the horizontal axis connects the middle of the anterior rim of the maxilla with the 'opisthion' (lowest posterior point of the skull). (Figure 2)

Measurement plane: midsagittal plane.

1. Skull height (forehead height): nasion- vertex†. (Figure 3)
2. Total facial height: nasion – gnathion†. (Figure 3)
3. Upper facial height (nasal length): nasion- subnasion†. (Figure 3)
4. Lower facial height: subnasion- gnathion†. (Figure 3)
5. Length of the back of the nose: nasion- pronasale. (Figure 4)
6. Nasal protrusion: pronasale- subnasion. (Figure 4)
7. Philtrum length: subnasion- superior aspect of the vermilion border of the upper lip. (Figure 4)

---

* The Frankfurter horizontal is the standard orientation of the head for craniofacial measurement in anthropology. In this position the lowest point on the lower margin of the bony orbit can be connected to the upper margin of the cutaneous external auditory meatus by a horizontal line.

† measure parallel to the vertical axis.

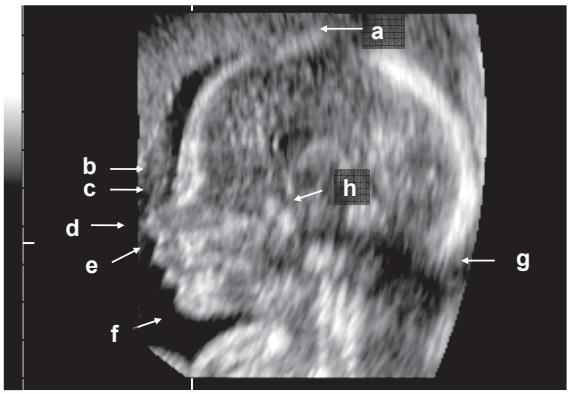


**Figure 1.** Landmarks used for measurements in the mid-sagittal plane: a= vertex; b= glabella; c= nasion; d= pronasale; e= subnasion; f= gnathion; g= opisthion; h= sella turcica.

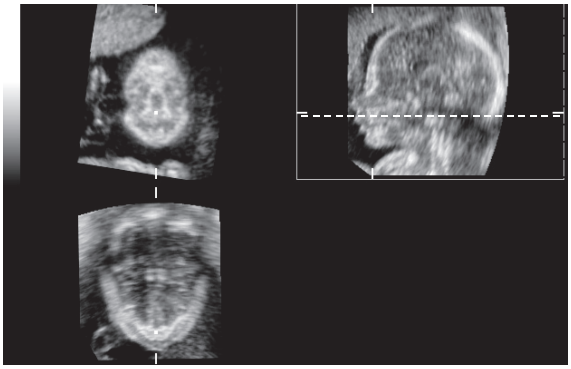

**Figure 2.** 'Upright' position of the fetal head: the horizontal axis (line) connects the middle of the anterior rim of the maxilla with the opisthion.

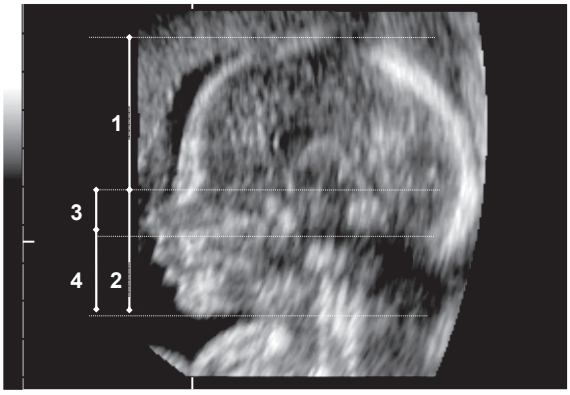


**Figure 3.** Measurements 1- 4: 1= skull height; 2= total facial height; 3= upper facial height; 4= lower facial height.

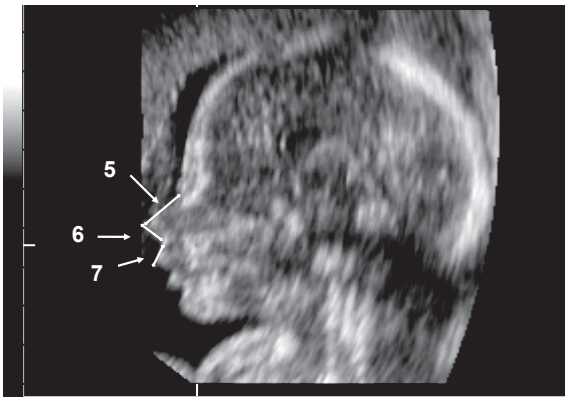


**Figure 4.** Measurements 5- 7: 5= length of the back of the nose; 6= nasal protrusion; 7= philtrum length.

**Measurements 8- 16 (bony landmarks are used):**[6-10]

Landmarks: *glabella (b)*: prominence on the frontal bone above the root of the nose at the level of the superior orbital ridges, *sella turcica (h)*: transverse view: middle of cross formed by sphenoid ridge and the otic cartilage. (Figure 1 and 5)

Position of the head and measurement plane are identical to measurements 1-7. The sella turcica, which is best traced in the transverse plane, is marked by a dot (=cursor), the point of intersection of the three perpendicular planes (Figure 5).

8. Palatal length: anterior- posterior maxillary bone. (Figure 6)
9. Anterior skull base length: glabella- sella turcica. (Figure 7)
10. Posterior cranial fossa length: sella- opisthion. (Figure 7)[#]
11. Sella-nasion (bony landmark). (Figure 6)
12. Degree of maxillary protrusion: angle between sella- nasion and nasion- anterior rim of the maxilla. (Figure 8)
13. Degree of mandibular protrusion: angle between sella- nasion and nasion- anterior rim of the mandibula. (Figure 8)
14. Anterior cranial base/ palatal plane angle: angle between sella- nasion and middle of the anterior rim- the posterior rim of the maxilla. (Figure 9)
15. Anterior cranial base/ mandibular plane angle: angle between sella- nasion and middle of the anterior rim- the posterior rim of the mandibula. (Figure 9)
16. Skull base angle: angle between sella- nasion and sella- frontal bony border of the foramen magnum. (Figure 10)

# In Garn et al (1984)[8] this measurement is termed 'posterior skull base length'. In Jeffery (2002)[10] this is more correctly named the posterior cranial fossa length. The actual posterior part of the skull base (the distance between the sella turcica and the basion) can not be measured prenatally with 3D ultrasound due to shadowing which is caused by the position of the basion behind the maxilla/ mandibula.

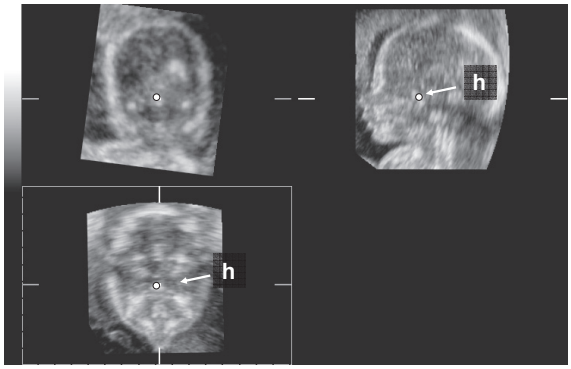


**Figure 5.** Sella turcica (h) in sagittal and transversal view.

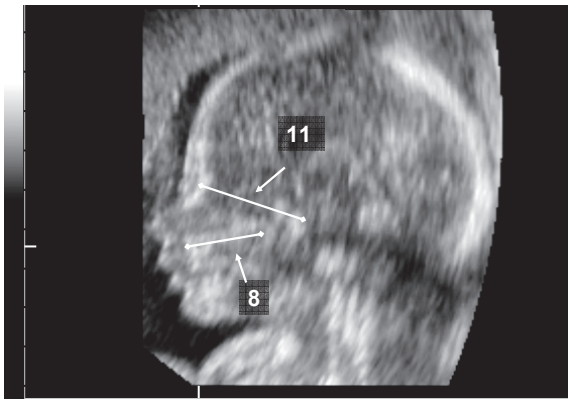


**Figure 6.** Measurements 8; palatal length, and 11; sella- nasion.

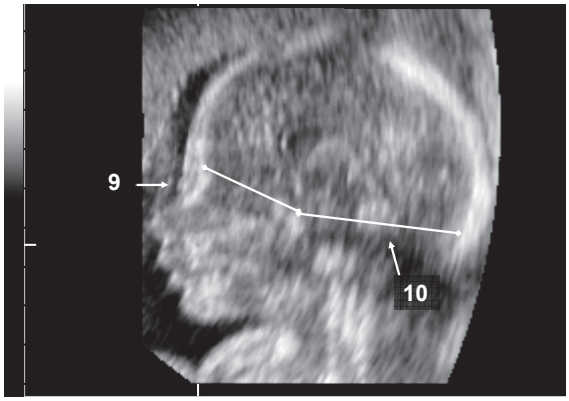


**Figure 7.** Measurement 9; anterior skull base length and 10; posterior cranial fossa length.

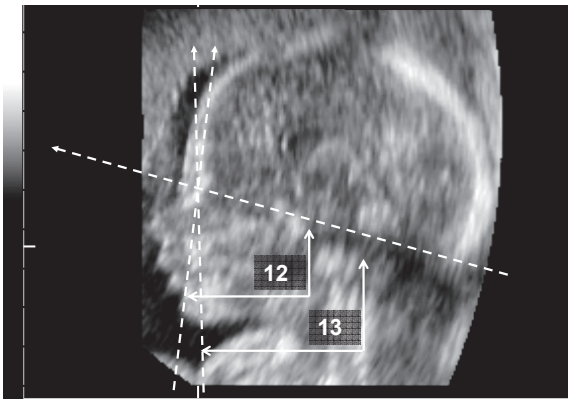


**Figure 8.** Measurements 12; degree of maxillary protrusion, and 13; degree of mandibular protrusion.

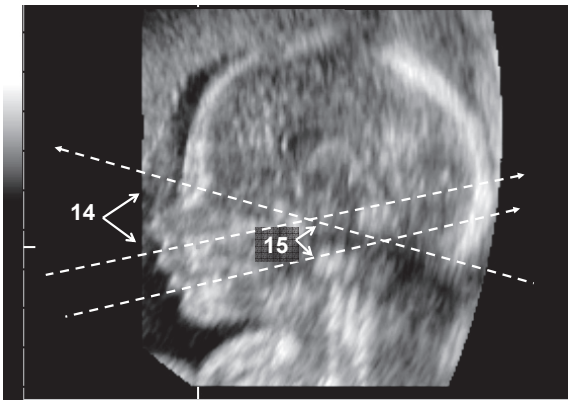


**Figure 9.** Measurements 14; anterior cranial base/ palatal plane angle, and 15; anterior cranial base/ mandibular plane angle.

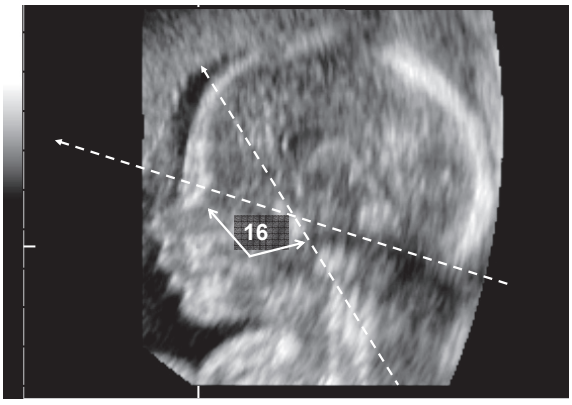


**Figure 10.** Measurement 16; skull base angle.

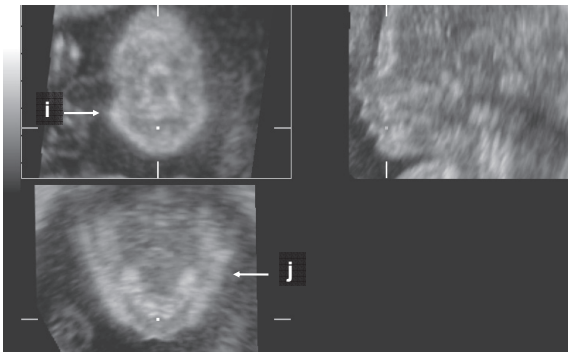


**Figure 11.** Landmarks used for measurements 17- 23: i= zygoma; j= gonion.

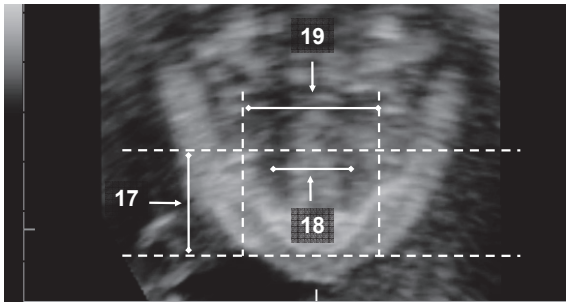


**Figure 12.** Measurement 17-19: 17 = maxillary corpus length; 18 = inner palate width; 19 = outer palate width.

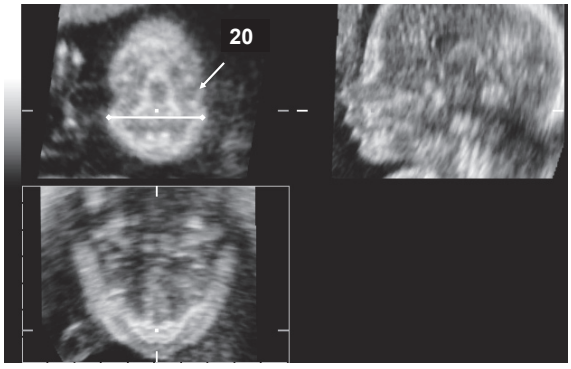


**Figure 13.** Measurement 20; bizygomatic breadth.

**Measurements 17 - 23 (bony landmarks are used):**[5,6,8]

Landmarks: *Zygoma (i)*: the most lateral point of the zygomatic arch (in coronal plane: just under the orbital rim), *gonion (j)*: the most lateral aspect of the mandible. (Figure 11)

Position of the head: identical to measurements 1-16.

**17-19:**

Measurement plane: transverse. Cursor marks the middle of the anterior rim of the maxilla in the sagittal plane.

17. Maxillary corpus length: anterior- posterior border of the maxilla*. (Figure 12)
18. Inner palate width: inner borders of the maxilla, halfway the length of the maxilla†. (Figure 12)
19. Outer palate width: outer borders of the maxilla*. (Figure 12)

**20:**

Measurement plane: coronal plane in the same multiplanar view as 17-19.

20. Bizygomatic breadth (facial width): left zygoma- right zygoma. (Figure 13)

**21-22:**

Measurement plane: transverse. Cursor marks the middle of the anterior rim of the mandibula in the sagittal plane.

21. Mandibular corpus length: frontal rim of the mandibula- gonion*. (Figure 14)
22. Bigonial breadth (mandible width): left- right gonion†. (Figure 14)

**23:**

Measurement plane: midsagittal plane

23. Gonion-sella: Move cursor in the transverse plane of the multiplanar view from the gonion to the midline. Measure in the midsagittal plane: cursor- sella†. (Figure 15)

**Measurement 24, 25 (soft tissue landmarks):**[5,6]

Landmarks: *Cheilion (k)*: corner of the mouth. (Figure 16)

Position of the head: identical to measurements 1-23.

**24:**

Measurement plane: coronal, cursor marks subnasion in midsagittal plane.

24. Nasal width: outer borders of the alae nasi. (Figure 17)

* Measure parallel to the vertical axis.

† Measure parallel to the horizontal axis.

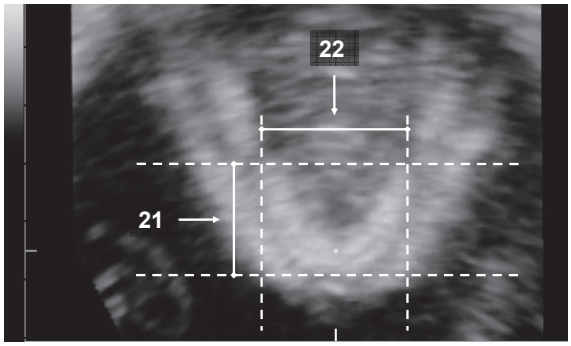


**Figure 14.** Measurement 21; mandibular corpus length, and 22; bigonial breadth.

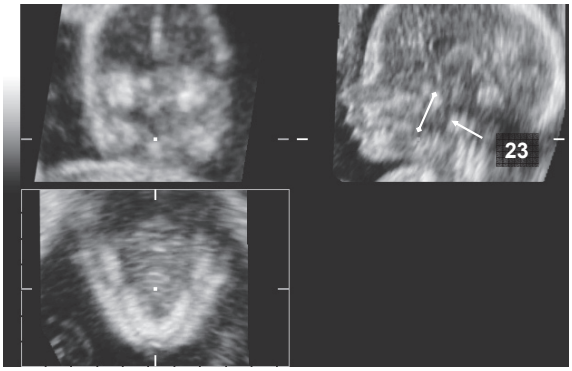


**Figure 15.** Measurement 23; gonion- sella turcica.

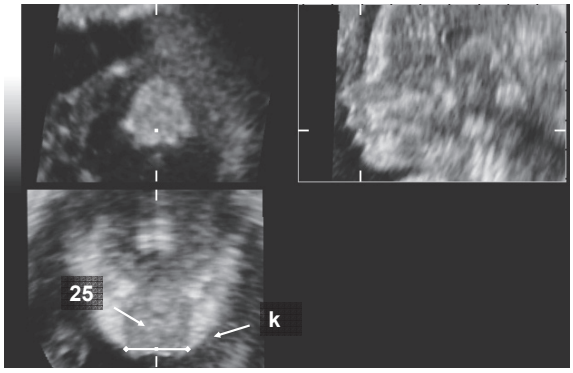


**Figure 16.** Landmark cheilion (k) and measurement 25; mouth width.

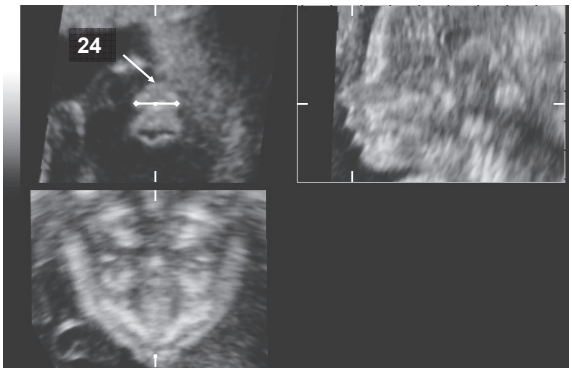


**Figure 17.** Measurement 24; nasal width.



**25:**

Measurement plane: transverse, cursor marks the mouth in midsagittal plane.

25. Mouth width: left- right cheilion. (Figure 16)

**Measurement 26 (bony landmarks):**[11]

Position of the head: rotate 'skull base' (defined as the line between glabella and opisthion) parallel to the horizontal axis. Measurement with VOCAL-mode (method for measuring volume).

26. Brain volume: the internal borders of the skull are traced manually with stepwise rotation of 30 degrees, taking the skull base as the lower border. (Figure 18)

*Measurements derived from the transverse scan mode of 3D acquisition.*

**Measurements 27 – 31 (bony landmarks):**[3,12]

Position of the fetal head: transverse planes are parallel to the plane used for head circumference measurement[3]. In the multiplanar mode the sagittal view shows the mid-sagittal plane. (Figure 19)

**27-29:**

Measurement plane: plane described first by Campbell (1977).[3]

27. Biparietal distance: maximal diameter of the skull perpendicular to midline (outer borders). (Figure 20)
28. Fronto-occipital distance: maximal diameter frontal- posterior skull border parallel to midline (outer borders). (Figure 20)
29. Head circumference: circumference traced manually around the skull. (Figure 20)

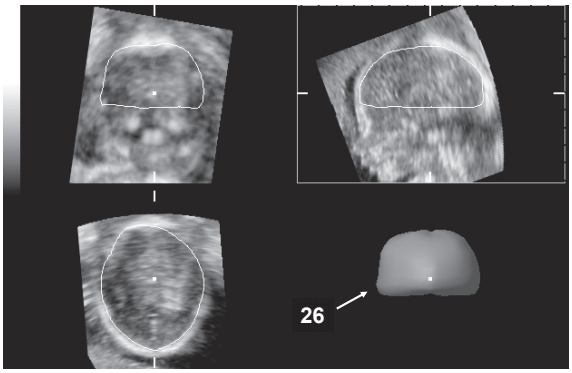


Figure 18. Measurement 26; fetal brain volume.

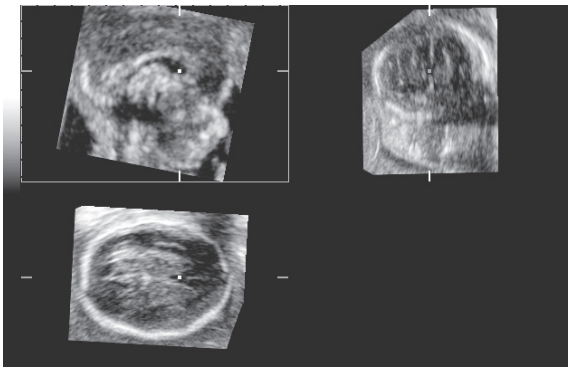

**Figure 19.** Position of the fetal head used for measurement 27-31.

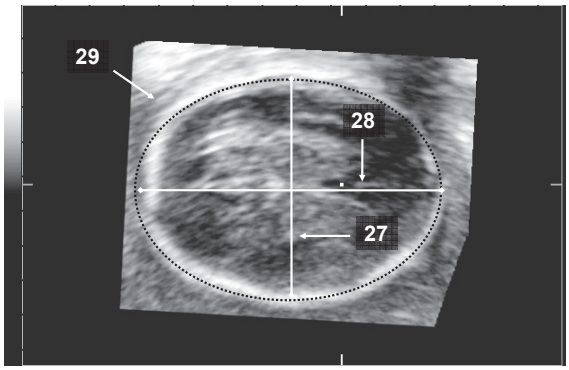


**Figure 20.** Measurement 27-29: 27 = biparietal distance; 28 = frontal occipital distance; 29 = head circumference.

**30-31:**

Measurement plane: transverse: maximal visible width between orbita.

30. Inter ocular distance: inner borders of the orbits. (Figure 21)
31. Outer ocular distance: outer borders of the orbits. (Figure 21)

*Measurements derived from the coronal scan mode of 3D acquisition.*

**Measurement 32 - 41 (soft tissue landmarks)**:[5,6]

Landmarks: *Tragus (l)*: the middle and most anterior aspect of the ear. (Figure 22)

**32-35:**

Position of the fetal head : identical to measurement 1-25

**32- 34:**

Measurement plane: first move cursor in transverse plane until the most superior aspect of the ear is visible in the sagittal plane. Mark this point by using a 'distance' measurement. Move the cursor back in the transverse plane until the tragus is visible in the coronal plane. Measure in the sagittal plane.

32. Ear length: superior - inferior aspect of the ear. (Figure 22)
33. Ear width: tragus- posterior part of the helix, perpendicular to ear length measurement. (Figure 22)
34. Ear rotation: Angle between line connecting superior and inferior aspect of the ear and the vertical axis (Figure 23)

**35:**

Measurement plane: Move cursor in transverse plane, parallel to vertical axis from tragus to midline. Measurement in mid-sagittal plane.

35. Ear position: cursor (tragus)- nasion*. (Figure 24)

**36-37:**

Position of the head: rotation over *z-axis* (for explanation see the three orthogonal axes (*x,y,z*) in Chapter 1, Figure 1) in the mid-sagittal plane, until nasion and the tragus are both in the transverse plane.

Measurement plane: transverse plane.

36. Bitragal breadth: tragus to midline, multiplied by 2.* (Figure 25)
37. Upper facial depth: tragus (calliper)- nasion.† (Figure 25)

* Measure parallel to the vertical axis.

† Measure parallel to the horizontal axis

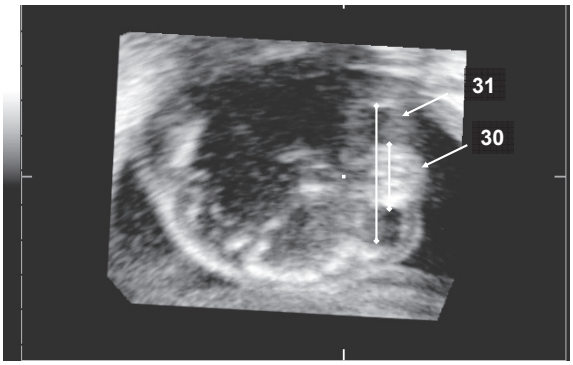


**Figure 21.** Measurement 30; inter ocular distance, and 31; outer ocular distance.

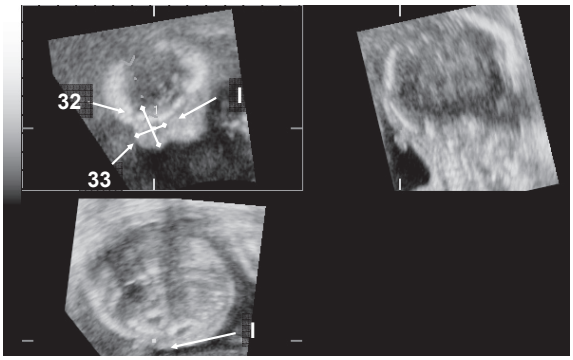


**Figure 22.** Landmark l; tragus, measurement 32; ear length, and 33 ear width.

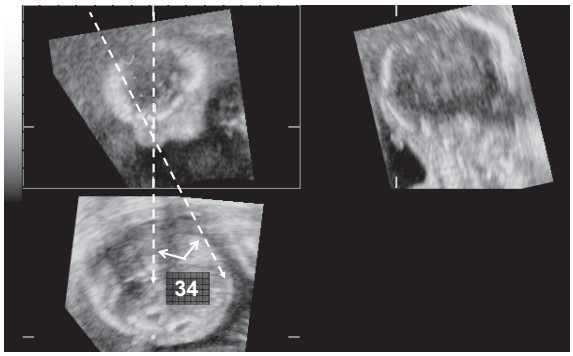


**Figure 23.** Measurement 34; ear rotation.

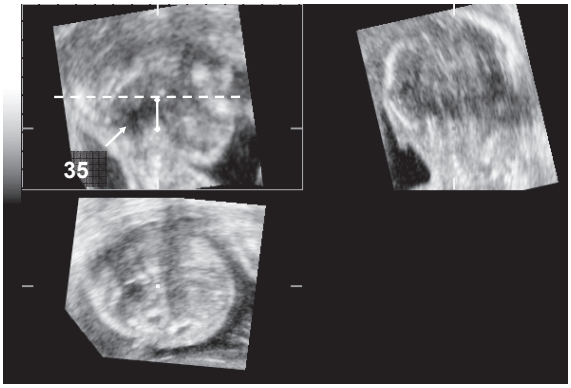


**Figure 24.** Measurement 35; ear position.

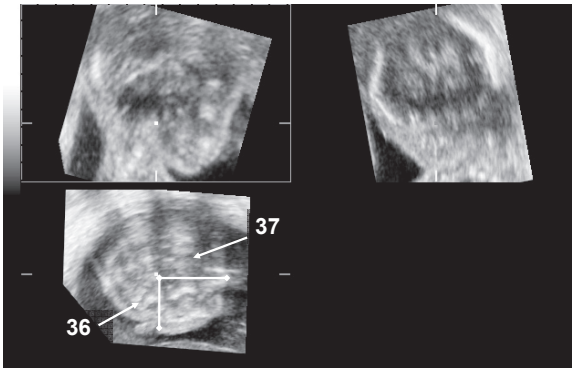


**Figure 25.** Measurement 36; bitragal breadth, and 37; upper facial depth.

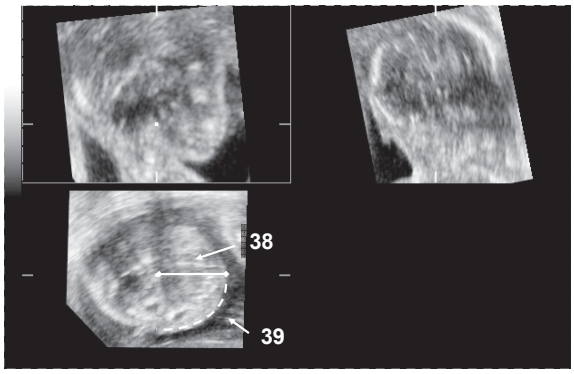


**Figure 26.** Measurement 38; mid facial depth, and 39; maxillary curvature.

**38-39:**

Position of the head: rotation over Z-axis in the mid-sagittal plane, until maxilla and the tragus are both in the transverse plane.

Measurement plane: transverse plane.

38. Midfacial depth: tragus- anterior rim of the maxilla.* (Figure 26)
39. Maxillary curvature: curvature from tragus- anterior rim of the maxilla and multiplied by 2. (Figure 26)

**40- 41:**

Position of the head: rotation over Z-axis in the mid-sagittal plane, until gnathion and the tragus are both in the transverse plane.

Measurement plane: transverse plane.

40. Lower facial depth: tragus- gnathion.† (Figure 27)
41. Mandibular curvature: curvature from tragus- gnathion, multiplied by 2. (Figure 27)

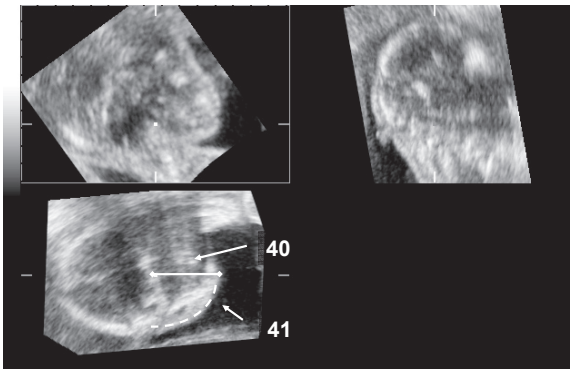


**Figure 27.** Measurement 40; lower facial depth, and 41; mandibular curvature.

* Measure parallel to the horizontal axis.

† Measure parallel to the horizontal axis

## 2.2 STATISTICAL ANALYSIS

Statistical analysis was performed on a personal computer with the SPSS version 10.1 (SPSS Corp, Chicago, Ill). Analysis of the reproducibility study consisted of nested analysis of variance to separate the within subjects variation in components due to differences between repeated tests within subjects and repeated analyses of the same recorded volume. A total variation of less than 10-11% was considered acceptable.

For the 41 measurements in the normal subjects the relationship of the measurement versus gestational age was analyzed with regression analysis for repeated measurements (random coefficients model) using SAS PROC MIXED (SAS Institute, Cary, NC). Data were centered by using the halfway point of gestational age (GA) (20 weeks), and calculations were done using x=GA- 20 as the time axis. For various parameters it was required to add a quadratic component of gestational age. Weight-specific reference-intervals were calculated according to this model. The random coefficients model was also used for determination of the relationship between ratios of different measurements versus gestational age as well as for the 95-percent confidence limits of the mean values. For some parameters a log transformation was required to get a proper fit.

The agreement between biparietal diameter, frontal occipital diameter, head circumference, inter and outer ocular diameter measured by both 2D- and 3D ultrasound was determined by calculation of the intraclass correlation coefficient (ICC). Systematic differences between these 3D- and 2D ultrasound measurements were calculated by means of the paired Student-t test.

Sixteen craniofacial measurements were selected on the basis of literature[13-15], relevance and reproducibility for craniofacial pattern profile analysis. The gestational age-related fitted mean and standard deviation (SD) were used for calculation of individual Z-scores for every measurement at each point in time according to the equation: (measured value minus fitted mean value)/SD. A craniofacial pattern profile can be made after calculation of the Z-scores for every measurement. A craniofacial pattern profile is a way of illustrating, classifying and/or comparing Z-scores of different individuals. A Z-score smaller than –2 or greater than +2 is considered abnormal.

The craniofacial variability index (CVI) for each individual at each point in time quantifies the differences between the 16 resulting Z-scores and is defined as the standard deviation of these. To determine normal values relative to gestational age, regression analysis for repeated measurements (random coefficients model) of the calculated CVI-values using SAS PROC MIXED was carried out again and gestational age-specific reference intervals were calculated according to this model. An index above the 95th percentile was classified as abnormal.

Z-scores and the craniofacial variability index were calculated for the abnormal fetuses using the derived equations.

Comparison of individual CVI data between different groups within the population with fetal cleft lip/ palate was done with the T-test. The Mann-Whitney U test was used to compare the number of abnormal Z-scores (among the 16) between the groups.

A p value of less than 0.05 was considered significant.

## 2.3 References


1. Altman DG, Chitty LS. Charts of fetal size: 1. Methodology. *Br J Obstet Gynaecol* 1994; 101: 29-34.
2. Kloosterman G. On intrauterine growth. *Int J Obstet Gynaecol* 1970; 8: 895-912.
3. Campbell S, Thoms A. Ultrasound measurement of the fetal head to abdomen circumference ratio in the assessment of growth retardation. *Br J Obstet Gynaecol* 1977; 84: 165-174.
4. Stengel-Rutkowski S, Schimanek P, Wernheimer A. Anthropometric definitions of dysmorphic facial signs. *Hum Genet* 1984; 67: 272-295.
5. Ward RE, Jamison PL, Farkas LG. Craniofacial variability index: a simple measure of normal and abnormal variation in the head and face. *Am J Med Genet* 1998; 80: 232-240.
6. Hall JG, Froster-Iskenius UG, Allanson JE. Handbook of Normal Physical Measurements. Oxford University Press Inc.: New York, 1995.
7. Goodman RM, Gorlin RJ. Head and facial measurements. In *Atlas of the face in genetic disorders.*, Goodman RM, Gorlin RJ. The C.V. Mosby Company: Saint Louis, 1977; 48-63.
8. Garn SM, Smith BH, Lavelle M. Applications of pattern profile analysis to malformations of the head and face. *Radiology* 1984; 150: 683-690.
9. Gorlin RJ, Cohen MM, Levin IS. Syndromes of the Head and the Neck. Oxford University Press, 1990.
10. Jeffery N. A high-resolution MRI study of linear growth of the human fetal skull base. *Neuroradiology* 2002; 44: 358-366.
11. Gordon IRS. Measurement of cranial capacity in children. *Br J Radiol* 1966; 39: 377-381.
12. Jeanty P, Cousaert E, Hobbins JC, Tack B, Bracken M, Cantraine F. A longitudinal study of fetal head biometry. *Am J Perinatol* 1984; 1: 118-128.
13. Allanson JE. Objective techniques for craniofacial assessment: what are the choices? *Am J Med Genet* 1997; 70: 1-5.
14. Garn SM, Lavelle M, Smith BH. Quantification of dysmorphogenesis: pattern variability index, sigma z. *AJR Am J Roentgenol* 1985; 144: 365-369.
15. Escobar LF, Bixler D, Padilla LM, Weaver DD. Fetal craniofacial morphometrics: in utero evaluation at 16 weeks' gestation. *Obstet Gynecol* 1988; 72: 674-679.

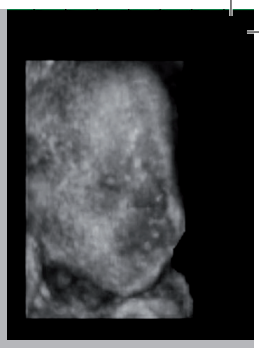

Chapter 3

# Normal fetal craniofacial development

In this Chapter, first the results of the 3D craniofacial measurements are presented (sub-Chapter 3.1). Particular attention will be given to: (i) normal fetal brain volume (sub-Chapter 3.2); (ii) development of the fetal skull base (sub-Chapter 3.3); (iii) development of the fetal maxilla and mandible (sub-Chapter 3.4) and (iv) comparison of pre- and postnatal development (sub-Chapter 3.5).

## 3.1 NORMAL FETAL CRANIOFACIAL BIOMETRY

A complete set of four 3D volume measurements was collected in 116 out of 126 women. A recording from the last scan was not performed in five women. The last scan was not available in one and partially unavailable in four women. This resulted in 495 and 494 recordings for measurements derived from the sagittal and coronal scan, respectively. A total of 498 recordings was available for measurements derived from the transverse scan.

In general it was not possible to retrieve reliable measurements when fetal movement complicated the 3D ultrasound recording. Another limitation was the difficulty in recording the entire fetal head with advancing gestational age as a result of the limited 3D transducer sector size.

Measurements derived from the sagittal scan were technically successful in 88- 97% of recordings (Table I). When the fetus was situated deep in the pelvic region and/ or the fetal face was constantly directed towards the maternal sacrum it was not possible to perform a sagittal scan. Furthermore, soft-tissue measurements obtained from the sagittal scan are difficult to assess when structures are in front of the fetal face. If the ultrasound beam is filtered or reflected by these obscuring structures, this may also complicate bony measurements.

Measurements in the transverse scan were derived from 91- 99% of the recordings (Table II). The transverse and coronal scan are often easier to retrieve. Only when the fetus was in cephalic position looking up to the symphysis or down to the sacrum of the mother during the entire examination, it was not possible to obtain the transverse nor the coronal scan. This occurred more often in late pregnancy when the head is situated deep in the pelvis.

Coronal scan derived measurements were successful in 94- 99% of 3D recordings (Table I). When the fetus is larger, in cephalic position and situated deep in the pelvic region, the mandible may be especially difficult to retrieve. With advancing gestational age the fetus is more often in cephalic position with the chin on the chest which complicates measurement of the mandible. Also in the presence of a reduced amount of amniotic fluid, the limbs or umbilical cord are more often situated in front of the mouth and chin. These restrictions also apply to the visualization of the mandible in the sagittal scan. Fetal limbs, uterine wall or placenta may obscure the fetal ear, which makes visualizing the ear more difficult.

Related measurements are discussed together. This in contrast to Chapter 2, where measurements are described in a logical order with respect to 3D-measurement methodology.

**Table I:** Sagittal and coronal measurements. Number of successful measurements (total number out of 495 and 494 recordings for sagittal and coronal measurements, respectively), scanning mode and results of reproducibility study in the sub study of 22 pregnancies. (A total coefficient of variation larger than 11% is underlined.)

| | Scan mode | Number of successful measurement (%) | $CV_I$ (%) | $CV_{II}$ (%) | $CV_{total}$ (%) |
|---|---|---|---|---|---|
| Skull height | Sagittal | 451 (91) | 4.5 | 3.4 | 5.6 |
| Total facial height | Sagittal | 466 (94) | 3.9 | 5.8 | 7.0 |
| Upper facial height | Sagittal | 474 (96) | 4.8 | 7.9 | 9.2 |
| Lower facial height | Sagittal | 464 (94) | 6.7 | 7.4 | 10.0 |
| Bizygomatic breadth | Sagittal | 481 (97) | 6.0 | 5.7 | 8.3 |
| Length of back of nose | Sagittal | 463 (94) | 8.2 | 9.3 | 12.4 |
| Nasal protrusion | Sagittal | 457 (92) | 13.7 | 17.0 | 21.8 |
| Philtrum length | Sagittal | 448 (91) | 14.6 | 5.3 | 15.5 |
| Nasal width | Sagittal | 467 (94) | 6.7 | 3.7 | 7.7 |
| Mouth width | Sagittal | 436 (88) | 9.7 | 6.0 | 11.4 |
| Palatal length | Sagittal | 459 (93) | 8.5 | 5.3 | 10.0 |
| Inner palate width | Sagittal | 470 (95) | 10.2 | 10.7 | 14.8 |
| Outer palate width | Sagittal | 471 (95) | 5.3 | 9.5 | 10.9 |
| Bigonial breadth | Sagittal | 466 (94) | 8.6 | 2.8 | 9.0 |
| Ant cranial base/ palatal plane angle | Sagittal | 460 (93) | 3.6 | 2.4 | 4.3 |
| Ant cranial base/ mandibular plane angle | Sagittal | 440 (89) | 3.3 | 1.9 | 3.8 |
| Sella-nasion | Sagittal | 464 (94) | 5.4 | 5.5 | 7.7 |
| Gonion- sella | Sagittal | 445 (90) | 7.4 | 10.3 | 12.7 |
| Bitragal breadth | Coronal | 488 (99) | 4.2 | 0.3 | 4.2 |
| Upper facial depth | Coronal | 471 (95) | 4.5 | 5.6 | 7.2 |
| Ear length | Coronal | 465 (94) | 6.5 | 8.5 | 10.7 |
| Ear width | Coronal | 465 (94) | 10.3 | 7.5 | 12.7 |
| Ear rotation | Coronal | 462 (94) | 24.5 | 20.9 | 32.2 |
| Ear position | Coronal | 467 (95) | 14.5 | 12.0 | 18.8 |

$CV_I$: Coefficient of Variation for differences between repeated tests within women; $CV_{II}$ : Coefficient of Variation for differences between repeated analyses of the same recorded volume; $CV_{Total}$: Total Coefficient of Variation.

**Table II:** Transverse measurements. Number of successful measurements (total number out of 498 recordings) and results of reproducibility study in the sub study of 22 pregnancies. Comparison between 2DUS and 3DUS.

| | Number of successful measurement (%) | $CV_I$ (%) | $CV_{II}$ (%) | $CV_{total}$ (%) | ICC | Mean difference 2DUS and 3DUS (mm) | p-value |
|---|---|---|---|---|---|---|---|
| BPD | 494 (99) | 1.5 | 0.6 | 1.6 | 0.99 | 0.9 | <0.001 |
| FOD | 494 (99) | 2.1 | 0.0 | 2.1 | 0.98 | 0.4 | 0.014 |
| HC | 494 (99) | 1.9 | 0.7 | 2.0 | 0.99 | 5.4 | <0.001 |
| IOD | 451 (91) | 4.4 | 2.2 | 4.9 | 0.89 | 0.1 | 0.084 |
| OOD | 451 (91) | 2.4 | 2.1 | 3.2 | 0.98 | 0.3 | <0.001 |

$CV_I$: Coefficient of Variation for differences between repeated tests within women; $CV_{II}$ : Coefficient of Variation for differences between repeated analyses of the same recorded volume; $CV_{Total}$: Total Coefficient of Variation; ICC: Intra class Correlation Coefficient; BPD: biparietal distance; FOD: fronto-occipital distance; HC: head circumference; IOD: intra ocular distance; OOD: outer ocular distance.



### 3.1.1 Skull height, total facial height, upper facial height, lower facial height and bizygomatic breadth (facial width)

*Results*

The reproducibility study showed a coefficient of variation (CV) for differences between repeated tests within women of 3.9- 6.7%. The CV for differences between repeated analyses of the same recorded volume was 3.4- 7.9%. The total coefficient of variation was within 11% for all five measurements (Table I). Intra-observer variability was therefore considered acceptable.

Regression analysis demonstrated a statistically significant quadratic fitted curve for skull height, total facial height, upper facial height as well as lower facial height data relative to gestational age (Figures A1-A4; Appendix p181-182). Bizygomatic breadth data showed a statistically significant linear increase relative to gestational age (Figure A5; Appendix p182)

When comparing skull height (SH) and total facial height (TFH), a relatively higher increment of total facial height is found, resulting in a statistically significant gestational age- related linear decrease of the SH/ TFH- ratio (Figure 1 and 2). At 18 weeks of gestation, skull height is found to be larger than total facial height, but depicts a 1:1 relation at 34 weeks of gestation. The upper-to-lower-facial-height-ratio remains fairly constant during the second trimester and first part of the third trimester (Figure 3). The facial width shows a steeper increase than the facial height, resulting in a statistically significant linear decrease in facial index relative to gestational age (Figure 4 and 5).

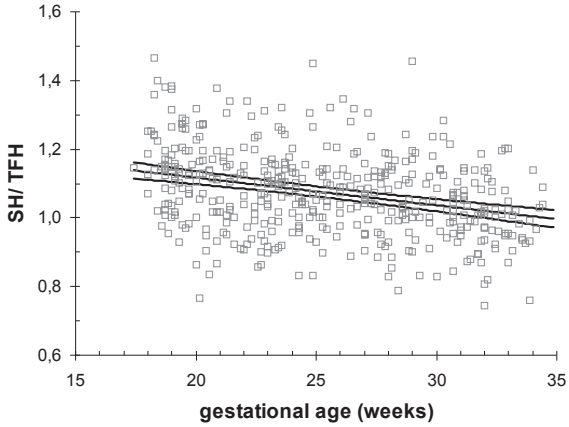


**Figure 1:** Skull height (SH)\ total facial height (TFH)-ratio relative to gestational age (weeks). Curves represent fitted mean values with 95% confidence limits.

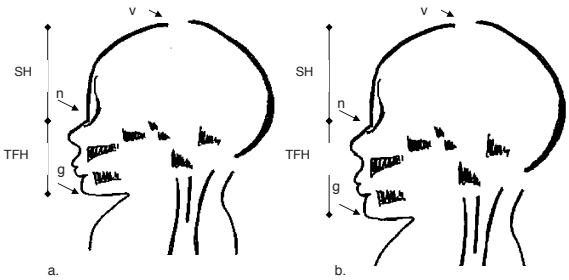


**Figure 2:** Schematic drawing of the sagittal section of a fetus at 18 weeks (a) and the effect of a higher increment of total facial height (TFH) relative to skull height (SH) at 34 weeks (b) of gestation (v: vertex, n: nasion, g: gnathion).

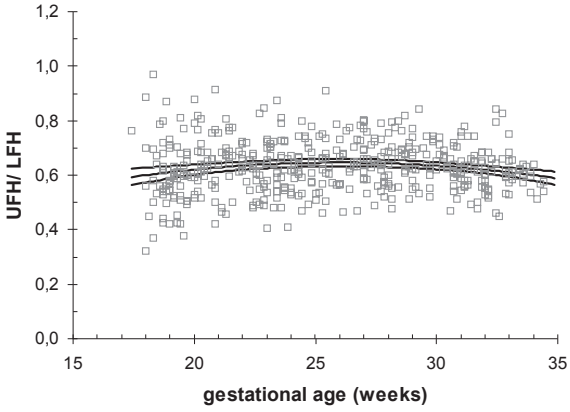


**Figure 3:** Upper facial height (UFH)\ lower facial height (LFH)-ratio relative to gestational age (weeks). Curves represent fitted mean values with 95% confidence limits.

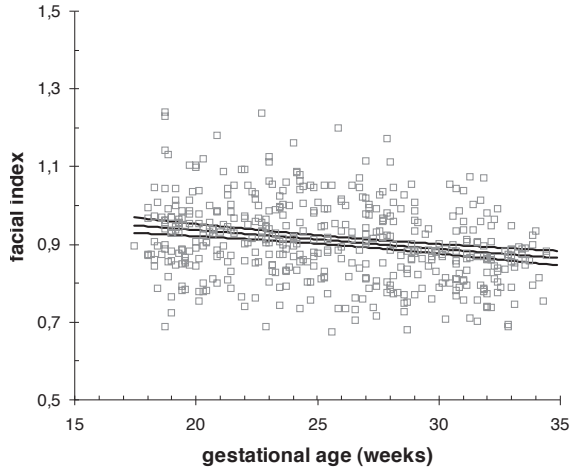


**Figure 4**: Facial index (total facial height/ bizygomatic breadth) relative to gestational age (weeks). Curves represent fitted mean values with 95% confidence limits.



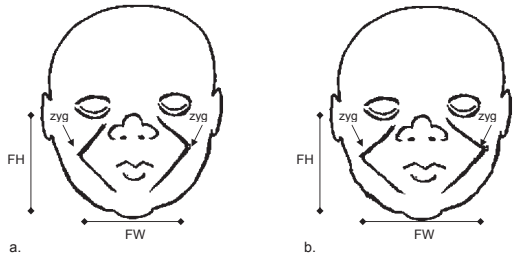


**Figure 5:** Schematic drawing of a coronal view of a fetus at 18 weeks (a) and the effect of a higher increment of bizygomatic breadth (FW) relative to total facial height (FH) at 34 weeks (b) of gestation (zyg: zygoma).

*Comment*

Earlier fetal ultrasound biometry data are available for skull height, total facial height and bizygomatic breadth. Escobar et al (1990) obtained values for these distances by means of two-dimensional ultrasound at 16, 26 and 36 weeks of gestation, respectively.[1] Skull height and total facial height were not depicted perpendicular to the horizontal axis (see Chapter 2, p 4) which may explain the difference between their values at 26$^{th}$ week of gestation and ours. Bizygomatic breadth seems to be measured in a more posteriorly oriented plane than ours, which may explain the somewhat higher values found in their study (Table III).

Abramowitz et al (1992) described a method of cheek-to-cheek diameter measurement in a coronal plane at the level of the nostrils and lips, which is rotated more posteriorly compared to our method.[2] They assessed this diameter cross-sectionally at 20 to 41 weeks of gestation. The mean values correspond well to ours (Table III).

**Table III:** Comparison of data on mean bizygomatic breadth, derived from the literature and current study.

| | | Study period (weeks) | Number of subjects | Bizygomatic breadth (mm) | | |
|---|---|---|---|---|---|---|
| | | | | 20w | 26w | 34w |
| 3D | Current study<br>(95% confidence limits) | 18- 34 | 126 | 30.3<br>(29.8-30.8) | 43.1<br>(42.7-43.6) | 60.3<br>(59.5-61.1) |
| 2D | Escobar et al (1990)[1] | 16, 26, 36 | 89 | | 45.0 | |
| | Abramowitz et al (1991)[2] | 20- 41 | 243 | 30 | 42 | 57 |

3D: 3D ultrasound, 2D: 2D ultrasound, w: weeks of gestation.

Other data are collected from post-mortem studies. Chambers et al (1993) established figures for 19 anthropometric measurements in 260 autopsies at 13- 26 weeks of gestation. Two of these measurements represent the distance between chin and nasion (total facial height) and the distance between chin and vertex (total facial height and skull height together).[3] Total facial height values in the current study are somewhat higher than the data derived from autopsies. Our figures on skull height, however, appear to be considerably below their obtained results. This could point to a difference in landmark positioning (nasion) between the skull height and total facial height. However, the difficulty of determining the upper edge of the skull (vertex) due to the position of the head against the uterus wall, could induce a small underestimation of skull height in our study.

In the post-mortem study of Eriksen et al (1995) mid-sagittal tissue blocks of 47 fetuses at 13- 22 weeks gestational age were used to establish normal prenatal cranial dimensions by radiography.[4] Upper, lower and total facial height as well as skull base dimensions were measured by their bony components. Although, mean upper and lower facial height data differ, mean total facial height data correspond well with ours. The likely explanation for the difference in the former two, but not the latter measurement, is the choice of the landmark between upper and lower facial height (subnasion).

Furthermore, it should be borne in mind that craniofacial measurements, such as brain weight[5], in fetuses used for post-mortem studies may be influenced by several factors, for instance the preservation technique of the fetal specimen, cause of death, delivery-death interval and presence of traumatic, vascular, inflammatory, or other intracranial pathology. This is likely to cause differences in measurement results when compared to our normal living fetuses in utero.

### 3.1.2 Length of the back of the nose, nasal protrusion, philtrum length, nasal width and mouth width

*Results*

Total coefficient of variation was 7.7% for nasal width. The total coefficient of variation was between 11 and 22% for the length of the back of the nose, nasal protrusion, philtrum length

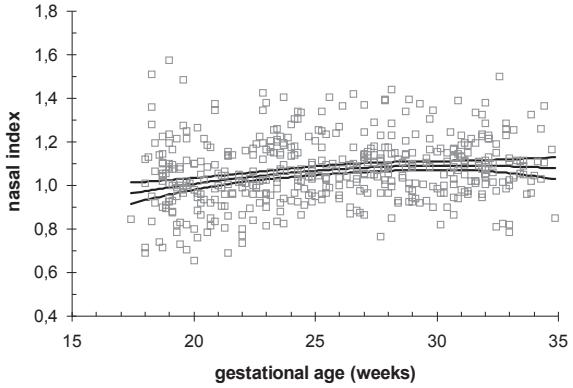


**Figure 6:** Nasal index (nasal width/ upper facial height) relative to gestational age weeks). Curves represent fitted median values with 95% confidence limits.



and mouth width, which we found not acceptable (Table I). Therefore was decided not to further elaborate on these last measurements.

A significant quadratic relation was found for nasal width relative to gestational age (Figure A6; Appendix p183).

The log relation of the nasal index (nasal width/ upper facial height) shows a statistically significant quadratic relation relative to gestational age (Figure 6). The width of the nose increases more than the length (or upper facial height) in the second half of gestation.

*Comment*

The poor reproducibility of the length of the back of the nose, nasal protrusion, philtrum length and mouth width may be explained by the following drawbacks. Firstly, especially early in gestation, the distances are small which increases the relative measurement error. Secondly, as a consequence of the smallness of the dimensions and the limitation in spatial resolution of the 3D ultrasound machine the distances may look larger than they actually are

**Table IV:** Comparison of data on mean nasal width (mm) derived from the literature and current study.

| | | Study period (wk) | Number of subjects | Nasal width (mm) 18w | 34w |
|---|---|---|---|---|---|
| 3D | Current study (95% confidence limits) | 18- 34 | 126 | 8.3 (8.1-8.5) | 20.4 (19.9-21.0) |
| 2D | Goldstein et al (1997)[7] | 14- 40 | 302 | 10.0 | 20.5 |
| | Pinette et al (1997)[8] | 14- 40 | 782 | 8.3 | 19.8 |
| | Ben Ami et al (1998)[9]# | 15- 42 | 229 | ±11 | ±20 |

3D: 3D ultrasound, 2D: 2D ultrasound, w: weeks of gestation.

# Data visually estimated from graphs.

(lateral resolution artifact).[6] Thirdly, the edges of the mouth width in the transverse plane can be difficult to determine.

Other observers in the field of measurement of nasal width have been Goldstein et al[7], Pinette et al[8] and Ben Ami et al[9]. The obtained values correspond fairly well to each other and ours (Table IV). Pinette et al found the nasal width to be over the 97.7$^{th}$ percentile in 4 out of 10 fetuses with Trisomy 21.

### 3.1.3 Palatal length, outer palate width, inner palate width and bigonial breadth

*Results*

Acceptable reproducibility was found for palatal length, outer palate width and bigonial breadth, but not for the inner palate width. The total coefficient of variation for the last measurement was almost 15% and it was decided, therefore, to exclude this measurement from analysis (Table I).

Linear relations were demonstrated for palatal length and bigonial breadth relative to gestational age (Figures A7-A8; Appendix p183). Outer palate width showed a significant quadratic relation relative to gestational age (Figure A9; Appendix p184).

*Comment*

The larger variability for inner and outer palate width measurements may be caused by difficulty in determining the borders of the inner and outer palate in both the sagittal and transverse planes. Scattering of the ultrasound beam due to the bony structures that surround the palate cause the alveolar ridge to look larger (refraction artifact[6]). Furthermore, the smallness of the inner fetal palate may increase the relative measuring error.

Two 3D ultrasound studies have been performed on the fetal maxilla and/ or mandible. Rotten et al (2002) measured the width of both the maxilla and mandible for diagnosing micrognathia.[10] The method for determining the maxillary (outer palate) width and subsequent results agree fairly well with ours. However, in our study the mean bigonial breadth (mandible width) shows a distinctly steeper increment. This difference may be due to the more anteriorly oriented measurement methodology applied by Rotten et al.[10] Also Tsai et al (2004) found considerable lower values on bigonial breadth. They did not obtain their mandible width data in a transverse but in a coronal plane.[11]

Goldstein et al (1999) obtained values on outer palate width (alveolar ridge width) by means of two-dimensional ultrasound that are distinctly below our averages.[12] The authors measure the outer palatal width in a more anterior oriented plane, which will probably explain the divergence. The mandible width (bigonial breadth) has been determined by means of two-dimensional ultrasound by Escobar et al[1], Watson and Katz[13] and Paladini et al[14]. The first author obtained values that do not agree with any of the other data, while averages described by Watson and Katz[13] and Paladini et al[14] correspond very closely with ours. However, Watson

and Katz measure the inner borders of the mandible, which might explain the slight difference. Escobar et al measure the bigonial breadth in the coronal and not the transverse plane, which may explain the divergence.[1]

Figures observed by Goldstein et al (2005) with two-dimensional ultrasound on palatal length (or what they call maxillary bone length) are distinctly lower than ours, although measurement methodology seems to equal ours. No explanation can be given for this divergence.

The post-mortem study performed by Burdi et al (1969) shows mean palatal length values that agree well with ours.[15]

### 3.1.4. Anterior skull base/ palatal plane angle and anterior skull base/ mandibular plane angle



*Results*

Good reproducibility for anterior skull base/ palatal plane angle and anterior skull base/ mandibular plane angle was found (Table I).

For both anterior skull base/ palatal plane angle and anterior skull base/ mandibular plane angle no significant relation relative to gestational age could be established. The mean angles remain at 28 and 31 degrees, respectively, throughout the second half of gestation (Figures A10 and A11; Appendix p184).

*Comment*

Burdi et al (1969)[15] measured an anterior skull base- palatal plane angle of 9 degrees that barely varies during the second half of gestation. Levihn et al (1967)[16] studied both angles in a small population of fetal autopsies and found the anterior skull base- palatal plane angle to decline from 14 to 10 degrees and the anterior skull base- mandibular plane angle from 42- 34 degrees at approximately 18- 34 weeks of gestation.

A different calliper placement is the most likely explanation for this discrepancy between their data and ours. However, a consistency with our observation is that almost no deviation of the mean anterior skull base/ palatal plane angle relative to gestation is found. Apparently the anterior skull base / palatal plane and anterior skull base / mandibular plane relation is formed in the first half of gestation.

### 3.1.5 . Biparietal distance (BPD), fronto-occipital distance (FOD), head circumference (HC), inter ocular distance (IOD) and outer ocular distance (OOD).

*Results*

Good reproducibility was found for all five measurements (Table II). A significant quadratic curve could be fitted for all measurements relative to gestational age (Figures A12 to A16; Appendix p185-186).

Total facial height in relation to head circumference shows a slight decrease relative to gestational age, which was significant ($p < 0.05$) (Figure 7). The relation of cephalic index (CI= BPD/ FOD x 100) and gestational age was found to be significantly quadratic (Figure 8). Mean CI values range between 78.1 and 80.8%.

A quadratic curve gave an optimal fit for both the IOD/ BPD- ratio and the IOD/ OOD-ratio relative to gestational age (Figure 9 and 10). The OOD/ BPD-ratio showed a significant linear decrease relative to gestational age (Figure 11). Figure 9, 11 and 12 demonstrate that the increase in BPD is more pronounced than the increase in IOD and OOD. The same applies to OOD compared with IOD, until the third trimester when a constant seems to have been reached (Figure 10 and 13).

A good agreement was found for 2D- and 3D ultrasound measurement of BPD, FOD, HC and OOD (intra-class correlation coefficient (ICC) = 0.98-0.99). Acceptable agreement was found in measuring the IOD (ICC = 0.89). Significant differences of 0.3- 5.4 mm between 2DUS and 3DUS were found for measurement of BPD, FOD, HC and OOD (Table II).

Figure 14, 15 and 16 present the comparison of data (mean, 5$^{th}$ and 95$^{th}$ percentiles) on BPD, FOD and HC, by Chitty et al[17], Kurmanavicius et al[18] and from the current study.

*Comment*

Nomograms of the above measurements have been developed by a number of authors. Only the ones used in our clinic and those that follow the guidelines described by Altman and Chitty in 1994[19] are mentioned here for comparison.

Our current BPD, FOD and HC data are in close agreement with those derived from 2D ultrasound studies by Chitty et al (1994)[17] and Kurmanavicius et al (1999)[18] for the second trimester of pregnancy (Table V, Figure 14-16). However, in the late second and early third trimester our data are somewhat greater than data from the other two studies.

Most of the divergence in head circumference data can be explained by the clear different measurement techniques. Although, Chitty et al do not explain their ways of measurement, Kurmanavicius estimated the head circumference from the FOD and BPD. Our methodology consisted of manually tracing the head circumference in the 3D View program. However, for our larger mean BPD and FOD in the second trimester compared to theirs, no clear explanation can be given.

Both the cephalometric measurements derived from autopsies[3] and from neonates[20] are remarkably smaller than those derived from ultrasound (Table V). This could point to a difference in measuring methodology before and after birth. Furthermore, fetal weight at autopsies is generally smaller than weight of live born fetuses.[21]

The figures on mean CI data reported by Gray et al (1989)[22], Chitty et al (1994)[17] and Kurmanavicius et al (1999)[18] and ours show the same general tendency. In all three studies the fitted mean displays a parabolic pattern similar to ours, with a lowest value around 26-28 weeks of gestation. The increment among the studies varies slightly (Table VI).

Close agreement is found between the mean values of larger studies on inter and outer ocular distance, published by Merz et al[23] and Trout et al[24] and ours (Table VII).

As can be concluded from Table II, standard biometry can be measured by 3DUS at the same level of reliability as by 2DUS. The small differences between the two techniques are not clinically relevant.



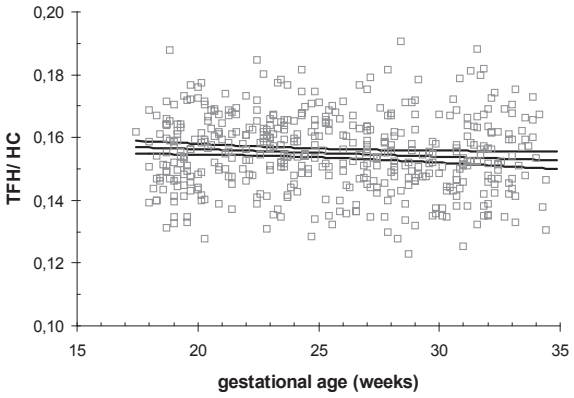


**Figure 7:** Total facial height (TFH)\ head circumference (HC)-ratio relative to gestational age (weeks). Curves represent fitted mean values with 95% confidence limits.

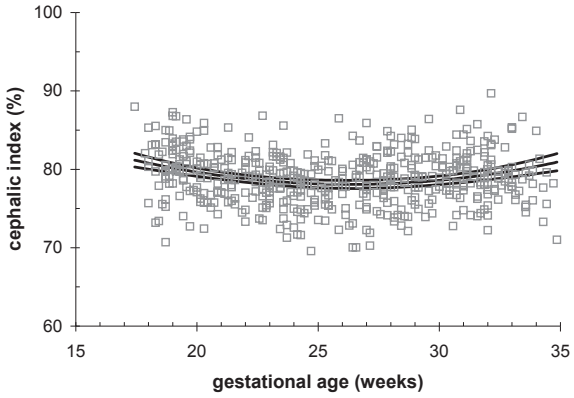


**Figure 8:** Cephalic index (biparietal-/ fronto-occipital distance x 100) relative to gestational age (weeks). Curves represent fitted mean values with 95% confidence limits.

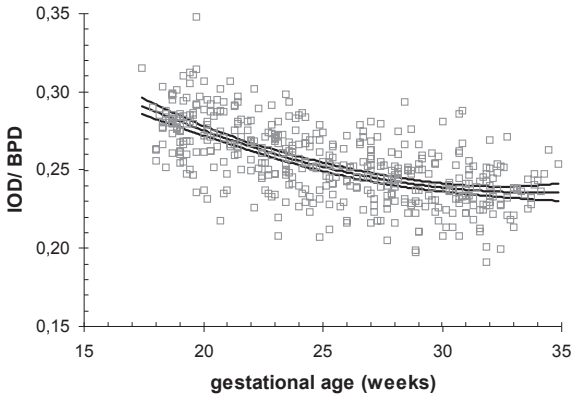


**Figure 9:** Inter ocular distance (IOD)\ biparietal distance (BPD)-ratio relative to gestational age (weeks). Curves represent fitted mean values with 95% confidence limits.

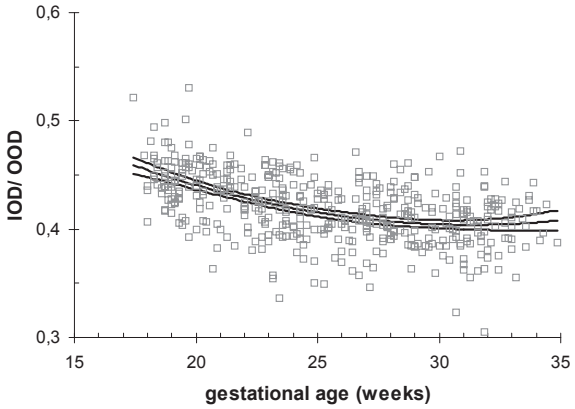


**Figure 10:** Inter ocular distance (IOD)\ outer ocular distance (OOD)-ratio relative to gestational age (weeks). Curves represent fitted mean values with 95% confidence limits.

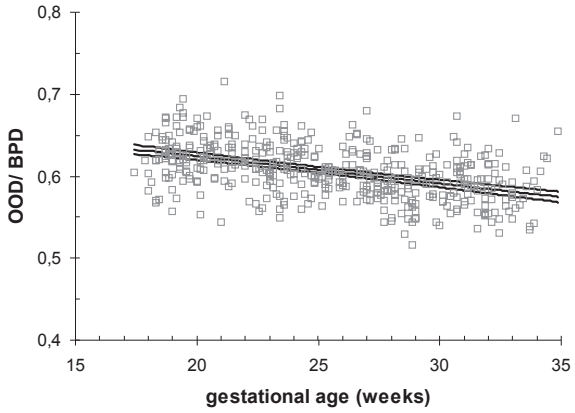


**Figure 11:** Outer ocular distance (OOD)\ biparietal distance (BPD)-ratio relative to gestational age (weeks). Curves represent fitted mean values with 95% confidence limits.

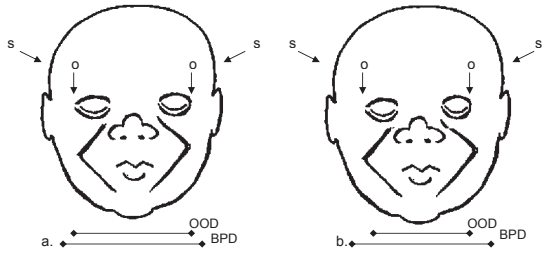


**Figure 12:** Schematic drawing of a coronal view of a fetus at 18 weeks (a) and the effect of a higher increment of biparietal distance (BPD) relative to outer ocular distance (OOD) at 34 weeks (b) of gestation (s: side of the skull, o: outer border of the orbit).

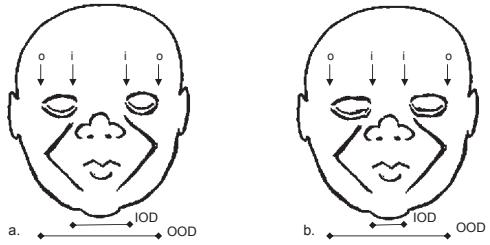


**Figure 13:** Schematic drawing of a coronal view of a fetus at 18 weeks (a) and the effect of a higher increment of outer ocular distance (OOD) relative to inter ocular distance (IOD) at 34 weeks (b) of gestation (o: outer border of the orbit, i: inner border of the orbit).

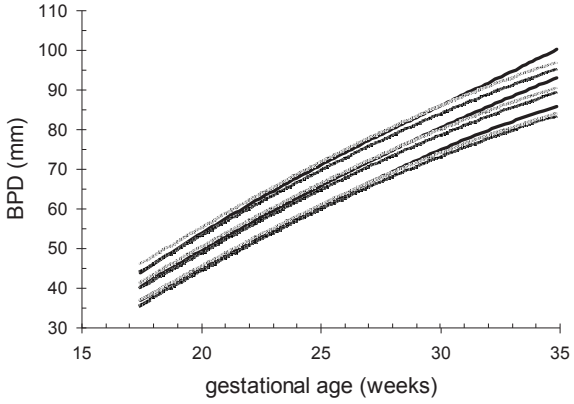


**Figure 14:** Comparison of mean BPD data, 5th and 95th percentiles of Chitty's study (dark gray); Kurmanavicius' study (light gray) and the current study (black lines).

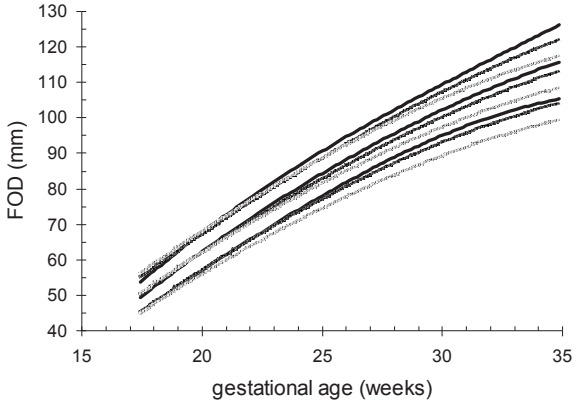


**Figure 15:** Comparison of mean FOD data, 5th and 95th percentiles of Chitty's study (dark gray); Kurmanavicius' study (light gray) and the current study (black lines).

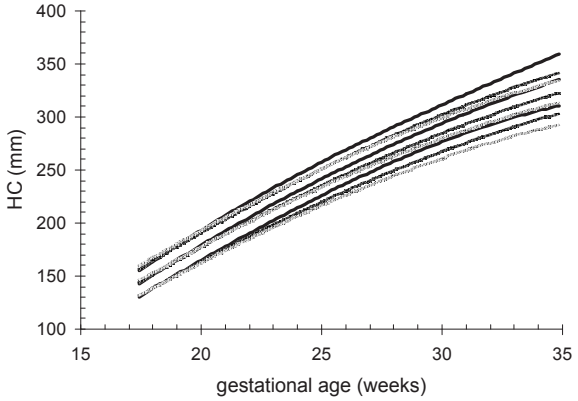


**Figure 16:** Comparison of mean HC data, 5th and 95th percentiles of Chitty's study (dark gray); Kurmanavicius' study (light gray) and the current study (black lines).

**Table V:** Comparison of data on mean biparietal distance (BPD), fronto-occipital distance (FOD) and head circumference (HC) derived from the literature and current study.

| | | Study period (wks) | N | BPD (mm) | | | | FOD (mm) | | | | HC (mm) | | | |
|---|---|---|---|---|---|---|---|---|---|---|---|---|---|---|---|
| | | | | 18w | 26w | 27w | 34w | 18w | 26w | 27w | 34w | 18w | 26w | 27w | 34w |
| 3D | Current study (2005) (95% confidence limits) | 18- 34 | 498 | 42.4 (41.9- 42.9) | 69.9 (69.4- 70.4) | 71.9 (71.4- 72.4) | 90.9 (90.1- 91.7) | 52.3 (51.7- 53.0) | 88.2 (87.6- 88.9) | 92.0 (91.4- 92.7) | 113.7 (112.5- 114.9) | 150.9 (149.3- 152.7) | 252.8 (251.2- 254.4) | 263.7 (262.1- 265.3) | 328.1 (325.4- 331.0) |
| 2D | Chitty et al (1994)[17] | 12- 42 | 594 | 42.4 | 66.1 | 71.4 | 87.6 | 52.9 | 86.8 | 90.8 | 110.9 | 151.3 | 244.8 | 256.1 | 316.1 |
| | Kurmanavicius et al (1999)[18] | 12- 42 | 6557 | 43.5 | 69.4 | 72.2 | 88.9 | 53.2 | 85.1 | 88.4 | 106.9 | | | | |
| PM | Chambers et al (1993)[3] | 13- 26 | 260 | 40 | 61 | | | 52 | 81 | | | 148 | 243 | | |
| Ne | Merlob et al (1984)[20]# | 27-41 | 198 | | | 63 | 82 | | | 84 | 102 | | | 240 | 309 |

3D: 3D ultrasound, 2D: 2D ultrasound, PM: post-mortem, Ne: neonatology, N: Number of subjects, w: weeks of gestation.
# Data visually estimated from graphs.

**Table VI:** Comparison of mean cephalic index (CI) derived from the literature and current study.

| | | Study period (weeks) | Number of subjects | CI (%) | |
|---|---|---|---|---|---|
| | | | | 18w | 34w |
| 3D | Current study (2005) (95% confidence limits) | 18- 34 | 498 | 80.8 (80.0-81.6) | 80.4 (79.7-81.0) |
| 2D | Gray et al (1989)[22] | 14- 40 | 777 | 79.7 | 78.7 |
| | Chitty et al (1994)[17] | 12- 42 | 594 | 80.5 | 79.1 |
| | Kurmanavicius et al (1999)[18] | 12- 42 | 6557 | 82 | 83 |

3D: 3D ultrasound, 2D: 2D ultrasound, w: weeks of gestation.

**Table VII:** Comparison of mean inter ocular distance (IOD) and outer ocular distance (OOD) derived from the literature and current study.

| | | Study period (wks) | N | IOD (mm) | | OOD (mm) | |
|---|---|---|---|---|---|---|---|
| | | | | 18w | 34w | 18w | 34w |
| 3D | Current study (2005) (95% confidence limits) | 18- 34 | 498 | 12.3 (12.1-12.5) | 21.2 (20.6-21.8) | 26.8 (26.5-27.2) | 52.6 (51.9-53.2) |
| 2D | Trout et al (1994)[24] | 12- 47 | 422 | 11 | 20 | 27 | 53 |
| | Merz et al (1995)[23] | 12- 41 | 1090 | 11.0 | 19.3 | 28.3 | 51.7 |

3D: 3D ultrasound, 2D: 2D ultrasound, N: Number of subjects, w: weeks of gestation.

### 3.1.6. Sella- nasion, gonion- sella, bitragal breadth and upper facial depth.

*Results*

Acceptable intra-observer variability was found for sella- nasion, bitragal breadth and upper facial depth. However, the variability in measuring the gonion- sella was considerably larger (Table I). This measurement was therefore not further analyzed.

Best fitted curves for the log transformation (base 10) of sella- nasion and for upper facial depth were quadratic relative to gestational age (Figures A17 and A18; Appendix p186-187). Bitragal breadth data demonstrated a significant linear increase relative to gestational age (Figure A19; Appendix p187).

The log transformation of the bitragal breadth/ biparietal distance(BPD)-ratio showed a significant quadratic relation with gestational age, with a slight decrease in time (Figure 17).

*Comment*

The landmarks gonion and sella are found in different planes in the volume. In order to measure the distance between the two, the calliper has to be moved through these planes. This will invoke an inadequacy that will explain the larger measuring variability.

For comparison with our sella- nasion data only 2D ultrasound and post-mortem studies were available. Most mean values agree well with ours (Table VIII). Eriksen et al found a larger sella- nasion distance than the other authors.[4] An explanation for this difference could not be

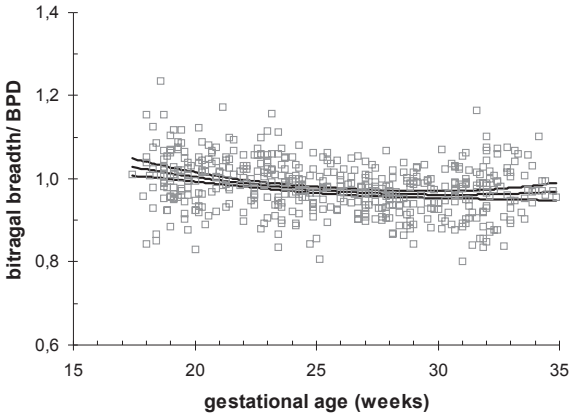


**Figure 17:** Bitragal breadth\ biparietal distance (BPD)-ratio relative to gestational age (weeks). Curves represent fitted median values with 95% confidence limits.



**Table VIII:** Comparison of median/ mean sella- nasion derived from the literature and current study.

| | | Study period (wks) | Number of subjects | Sella- nasion (mm) | | | | | |
|---|---|---|---|---|---|---|---|---|---|
| | | | | 18w | 20w | 22w | 26w | 29w | 34w |
| 3D | Current study (2005) (95% confidence limits)* | 18- 34 | 495 | 18.0 (17.6- 18.3) | 20.4 (20.2- 20.7) | 24.2 (23.9- 24.5) | 29.8 (29.3- 30.1) | 32.3 (31.8- 32.8) | 33.9 (33.2- 34.7) |
| 2D | Escobar et al (1990)[1] | 16, 26, 36 | 89 | - | - | - | 28.8 | - | - |
| PM | Burdi et al (1969)[15]# | 12- 40 | 68 | - | 22.2 | 23.6 | 26.4 | 28.7 | 32.3 |
| | Eriksen et al (1995)[4] | ±13- 22 | 47 | 20.7 | 24.6 | 28.6 | - | - | - |
| | Jeffery and Spoor (2002) [25] | 10- 29 | 46 | 18.2 | 21.7 | 24.1 | 26.1 | 31.0 | - |

3D: 3D ultrasound, 2D: 2D ultrasound, PM: post-mortem w: weeks of gestation.
*Median values for $^{10}$log(sella-nasion) values. This transformation was required to obtain a normal distribution.
#sella-nasion was based on crown-rump length measurement. This was converted to weeks of gestation with help of biometry data on fetal autopsies produced by Singer and Sung (1991)[28] which are available from 20 weeks of gestation.

found. Considering the difference in landmark choice in the study presented by Jeffery and Spoor (the foramen caecum instead of nasion) the agreement between their data and ours is remarkable.[25]

### 3.1.7. Ear length, ear breadth, ear rotation and ear position.

*Results*

Only for ear length total variation was within 11% (Table I). The intra-observer variability of the other measurements was found not to be acceptable. These measurements were therefore not further analyzed.

Ear length data showed a significant quadratic relation relative to gestational age (Figure A 20; Appendix p187).

*Comment*

Several explanations for the large intra-observer variability of the ear measurements can be given. Firstly, determination of all ear measurements, like for gonion-sella, includes different planes and is therefore more susceptible to variation. Secondly, correct calliper placement can be difficult in measuring the ear rotation. A small error in calliper placement may result in a large difference in the actual ear rotation angle (more than for instance in a linear measurement). Thirdly, the nasion, landmark for ear position, is more difficult to visualize in the coronal scan than in the sagittal scan.

In spite of differences in measurement methodology ear length data derived from literature agree well with ours, although the figures of Birnholz and Farell are slightly smaller[26] (Table IX).

**Table IX:** Comparison of mean ear length (mm) derived from the literature and current study.

| | | Study period (wks) | N | Ear length (mm) | | | |
|---|---|---|---|---|---|---|---|
| | | | | 18w | 24w | 27w | 34w |
| 3D | Current study (2005) (95% confidence limits) | 18- 34 | 494 | 11.7 (11.2- 12.2) | 19.4 (19.1-19.7) | 22.8 (22.4-23.2) | 29.7 (28.9-30.5) |
| | Chang et al (2000)[29] | 17- 41 | 113 | 15.7 | 22.3 | 25.2 | 30.8 |
| 2D | Birnholz and Farrell (1988)[26] | 15- 40 | 180 | 10.3 | 16.9 | 20.2 | 27.9 |
| | Shimizu et al (1992)[30]# | 18- 42 | 124 | 11.5 | 19 | 22 | 28 |
| | Lettieri et al (1993)[31] | 14- 25 | 424 | 12 | 19 | | |
| | Chitkara et al (2000)[32] | 15- 40 | 2583 | 11.7 | 19.7 | 22.5 | 29.2 |
| | Yeo et al (2003)[33] | 14- 41 | 447 | 13 | 20 | 25 | 31 |
| PM | Gill et al (1994)[34] | 14- 24 | 106 | 12.6 | 19.5 | | |
| Ne | Sivan et al (1983)[35]# | 27- 41 | 198 | | | 26 | 32.5 |

3D: 3D ultrasound, 2D: 2D ultrasound, PM: post-mortem, Ne: neonatology; N: number of study subjects, w: weeks of gestation

# Data visually estimated from graphs.

### 3.1.8. Conclusions

From this current study it can be concluded that most measurements can be reliably obtained by 3D ultrasound. The same applied to regular craniofacial measurements, such as the biparietal distance. Only the smaller distances, such as philtrum length and nasal protrusion, are less reproducible. Some measurements are more complicated, because they have to be found through movement of the callipers in more than one of the orthogonal 3D planes. Finally, some landmarks, such as the edges of the mouth, are difficult to determine (or are being moved in time), and the measurement is therefore less reliable.

Most of the craniofacial growth charts show fastest growth rates during the beginning of the second trimester with gradual plateauing after midpoint of the second trimester. This is consistent with the growth pattern described by Burdi et al and Escobar et al [1,15].



### 3.1.9. References


1. Escobar LF, Bixler D, Padilla LM, Weaver DD, Williams CJ. A morphometric analysis of the fetal craniofacies by ultrasound: fetal cephalometry. *J Craniofac Genet Dev Biol* 1990; **10**: 19-27.
2. Abramowicz JS, Sherer DM, Bartov E, Woods JR. The Cheek-To-Cheek Diameter in the Ultrasonographic Assessment of Fetal Growth. *Am J Obstet Gynecol* 1991; **165**: 846-852.
3. Chambers HM, Knowles S, Staples A, Tamblyn M, Haan EA. Anthropometric measurements in the second trimester fetus. *Early Hum Dev* 1993; **33**: 45-59.
4. Eriksen E, Bachpetersen S, Solow B, Kjaer I. Midsagittal Dimensions of the Prenatal Human Cranium. *J Craniofac Genet Dev Biol* 1995; **15**: 44-50.
5. Jordaan HV, Dunn LJ. A new method of evaluating fetal growth. *Obstet Gynecol* 1978; **51**: 659-665.
6. Kremkau FW, Taylor KJW. Artifacts in Ultrasound Imaging. *J Ultrasound Med* 1986; **5**: 227-237.
7. Goldstein I, Tamir A, Itskovitz-Eldor J, Zimmer EZ. Growth of the fetal nose width and nostril distance in normal pregnancies. *Ultrasound Obstet Gynecol* 1997; **9**: 35-38.
8. Pinette MG, Blackstone J, Pan YQ, Pinette SG. Measurement of fetal nasal width by ultrasonography. *Am J Obstet Gynecol* 1997; **177**: 842-845.
9. Ben Ami M, Weiner E, Perlitz Y, Shalev E. Ultrasound evaluation of the width of the fetal nose. *Prenat Diagn* 1998; **18**: 1010-1013.
10. Rotten D, Levaillant JM, Martinez H, Ducou le Pointe H, Vicaut E. The fetal mandible: a 2D and 3D sonographic approach to the diagnosis of retrognathia and micrognathia. *Ultrasound Obstet Gynecol* 2002; **19**: 122-130.
11. Tsai MY, Lan KC, Ou CY, Chen JH, Chang SY, Hsu TY. Assessment of the facial features and chin development of fetuses with use of serial three-dimensional sonography and the mandibular size monogram in a Chinese population. *Am J Obstet Gynecol* 2004; **190**: 541-546.
12. Goldstein I, Jakobi P, Tamir A, Goldstick O. Nomogram of the fetal alveolar ridge: a possible screening tool for the detection of primary cleft palate. *Ultrasound Obstet Gynecol* 1999; **14**: 333-337.
13. Watson WJ, Katz VL. Sonographic Measurement of the Fetal Mandible - Standards for Normal-Pregnancy. *Am J Perinatol* 1993; **10**: 226-228.

14. Paladini D, Morra T, Teodoro A, Lamberti A, Tremolaterra F, Martinelli P. Objective diagnosis of micrognathia in the fetus: the jaw index. *Obstet Gynecol* 1999; **93**: 382-386.

15. Burdi AR. Cephhalometric growth analyses of the human upper face region during the last two trimesters of gestation. *Am J Anat* 1969; **125**: 113-122.

16. Levihn WC. A cephalometric roentgenographic cross-sectional study of craniofacial complex in fetuses from 12 weeks to birth. *Am J Orthodontics* 1967; **53**: 822-848.

17. Chitty LS, Altman DG, Henderson A, Campbell S. Charts of fetal size: 2. Head measurements. *Br J Obstet Gynaecol* 1994; **101**: 35-43.

18. Kurmanavicius J, Wright EM, Royston P, Wisser J, Huch R, Huch A, Zimmermann R. Fetal ultrasound biometry: 1. Head reference values. *Br J Obstet Gynaecol* 1999; **106**: 126-135.

19. Altman DG, Chitty LS. Charts of fetal size: 1. Methodology. *Br J Obstet Gynaecol* 1994; **101**: 29-34.

20. Merlob P, Sivan Y, Reisner SH. Anthropometric Measurements of the Newborn Infant (27 to 41 Gestational Weeks). March of Dimes Birth Defects Foundation: White Plains, New York, 1984; 1-52.

21. Gruenwald PM, Minh HN. Evaluation of body and organ weights in perinatal pathology. *Am J Clin Pathol* 1960; **34**: 247-253.

22. Gray DL, Songster GS, Parvin CA, Crane JP. Cephalic Index - A Gestational Age-Dependent Biometric Parameter. *Obstet Gynecol* 1989; **74**: 600-603.

23. Merz E, Wellek S, Puttmann S, Bahlmann F, Weber G. Orbital Diameter, Interorbital and Biocular Diameters - A Growth-Model for Fetal Orbital Parameters. *Ultraschall in der Medizin* 1995; **16**: 12-17.

24. Trout T, Budorick NE, Pretorius DH, McGahan JP. Significance of Orbital Measurements in the Fetus. *J Ultrasound Med* 1994; **13**: 937-943.

25. Jeffery N, Spoor F. Brain size and the human cranial base: a prenatal perspective. *Am J Phys Anthropol* 2002; **118**: 324-340.

26. Birnholz JC, Farrell EE. Fetal Ear Length. *Pediatrics* 1988; **81**: 555-558.

27. Goldstein I, Reiss A, Rajamim BS, Tamir A. Nomogram of maxillary bone length in normal pregnancies. *J Ultrasound Med* 2005; **24**: 1229-1233.

28. Singer DB, Sung CJ, Wigglesworth JS. Fetal Growth and Maturation: with Standards for Body and Organ Development. In *Textbook of Fetal and Perinatal Pathology*, Wigglesworth JS, Singer DB. Blackwell Scientific: Boston, 1991; 11-46.

29. Chang CH, Chang FM, Yu CH, Liang RI, Ko HC, Chen HY. Fetal ear assessment and prenatal detection of aneuploidy by the quantitative three-dimensional ultrasonography. *Ultrasound Med Biol* 2000; **26**: 743-749.

30. Shimizu T, Salvador L, Allanson J, Hughes-Benzie R, Nimrod C. Ultrasonographic measurements of fetal ear. *Obstet Gynecol* 1992; **80**: 381-384.

31. Lettieri L, Rodis JF, Vintzileos AM, Feeney L, Ciarleglio L, Craffey A. Ear Length in 2Nd-Trimester Aneuploid Fetuses. *Obstet Gynecol* 1993; **81**: 57-60.

32. Chitkara U, Lee L, El-Sayed YY, Holbrook RH, Jr., Bloch DA, Oehlert JW, Druzin ML. Ultrasonographic ear length measurement in normal second- and third- trimester fetuses. *Am J Obstet Gynecol* 2000; **183**: 230-234.

33. Yeo L, Guzman ER, Ananth CV, Walters C, Day-Salvatore D, Vintzileos AM. Fetal aneuploidy by sonographic ear length. *J Ultrasound Med* 2003; **22**: 565-576.

34. Gill PP, VanHook J, FitzSimmons J, Pascoe-Mason J, Fantel A. Upper face morphology of second-trimester fetuses. *Early Hum Dev* 1994; **37**: 99-106.

35. Sivan Y, Merlob P, Reisner SH. Assessment of ear length and low set ears in newborn infants. *J Med Genet* 1983; **20**: 213-215.

## APPENDIX TO CHAPTER 3.1: REGRESSION EQUATIONS

The regression equations for means/medians of Figures 1- 17 in Chapter 3.1 in relation to gestational age (GA in weeks) are as follows:

Figure 1: Skull height/ total facial height-ratio
Mean = 1.2873 - 0.0085GA

Figure 3: Upper/ lower facial height- ratio
Mean= 0.1604+0.0374GA-0.00072GA2

Figure 4: Facial index
Mean= 1.0539 - 0.00585GA

Figure 6: Nasal index
Median= 10Y
$Y= -0.2531 + 0.0190\ GA-0.00031GA^2$

Figure 7: Total facial height/ head circumference-ratio
Mean= 0.1611 – 0.00024GA

Figure 8: Cephalic index
Mean = 105.16–2.057GA +0.0391GA2

Figure 9: IOD/ BPD-ratio
Mean=0.4698–0.01379GA+ 0.000203GA2

Figure 10: IOD/OOD-ratio
Mean= 0.6841-0.01790GA+ 0.000286GA2

Figure 11: OOD/BPD-ratio
Mean= 0.6906 – 0.00332GA

Figure 17: Bitragal breadth/BPD-ratio
Median= 10Y
Y= 0.1415 – 0.01038 GA+0.00017GA2

## 3.2 THREE-DIMENSIONAL SONOGRAPHIC MEASUREMENT OF NORMAL FETAL BRAIN VOLUME DURING THE SECOND HALF OF PREGNANCY

N.M. Roelfsema*, W.C.J. Hop#, S.M.E. Boito*, J.W. Wladimiroff*
*Department of Obstetrics and Gynecology, #Department of Epidemiology and Biostatistics, Erasmus MC, University Medical Center Rotterdam, The Netherlands

Published in the American Journal of Obstetrics and Gynecology 2004, 190, 275- 280.

### Summary

**Objectives:** This study was undertaken to develop a three-dimensional (3D) ultrasound method of measuring fetal brain volume.

**Study design:** Serial 3D sonographic measurements of fetal brain volume were made in 68 normal singleton pregnancies at 18 to 34 weeks of gestation. A comparison was made with fetal brain volume estimates from two-dimensional (2D) sonographic measurement of head circumference and published postmortem fetal brain weights.

**Results:** Coefficient of Variation for fetal brain volume (3D) caused by differences between repeated tests was 10.2% and between analyses of the same recorded volume 2.2%. Median brain volume increases from 34 ml at 18 weeks to 316 ml at 34 weeks. Median brain weight represented approximately 15% of total fetal weight. The 3D ultrasound-derived brain weight is larger than postmortem brain weight. However, this is not so for brain weight derived from total fetal weight at autopsy. A good agreement between 3D and 2D brain volume was found.

**Conclusion:** Sonographic measurement of fetal brain volume demonstrated an acceptable intraobserver variability and a nearly 10-fold increase during the second half of gestation.

## Introduction

Both fetal biparietal diameter and fetal head circumference are standard parameters in establishing normal and abnormal fetal biometry.[1] With the use of a three-dimensional (3D) sonographic method, it would be possible to measure fetal brain volume. Recently, a method of 3D sonographic measurement of fetal liver volume was introduced[2-4], which would allow calculation of fetal liver to brain weight ratios in both normal and abnormal fetal development.[5] Moreover, determination of the accuracy of a recently developed and simple two-dimensional (2D) sonographic method for estimating fetal brain volume based on postmortem fetal brain weight data from literature,[5] would be feasible.

The objectives of this study were therefore as follows: (i) to develop a 3D sonographic method of measuring fetal brain volume; (ii) to establish reproducibility and normal data relative to gestational age; (iii) to compare 3D ultrasound data with 2D ultrasound data of brain volume and postmortem data of fetal brain weight at 18 to 34 weeks of gestation.

## Materials and methods

*Study design*

During the period of February 2000- September 2001, 68 women with a normal singleton pregnancy consented to participate in the study, which was approved by the Hospital Ethics Review Board. Pregnancy duration varied between 18 and 34 weeks (median 26 weeks). Maternal age ranged between 19 and 38 years (median 29 years). Women were recruited from the antenatal department and regional midwifery services. Pregnancy duration was determined from the last reliable menstrual period, or in case of uncertainty, adjusted by ultrasound in the first trimester of gestation. Pregnancies were uneventful resulting in the delivery of a normally developed infant. According to the Kloosterman tables[6] 91% of the birth weights were situated between the 5$^{th}$ and the 95$^{th}$ percentiles, adjusted for maternal parity and fetal sex. In each pregnancy, fetal brain volume was established four times at 3- to 5-week intervals.

Intraobserver variability was determined during the same gestational period in 22 normal singleton pregnancies, five of which also participating in the serial study of fetal brain volume.

*Recording technique*

3D sonographic examination of the fetal brain was performed with the use of a standard Voluson 530 D (Kretztechnik AG, Zipf, Austria) with a 3-to 5-MHz annular array transducer (VAW 3-5). An internal mechanism in the transducer sliced through the images and recorded a truncated pyramidal volume. Depth, longitudinal and transverse dimensions were adjustable. An opening angle of 50 to 70 degrees and a sampling angle of 30 to 85 degrees was used, resulting in a maximum volume of 3.2 liter. The depth range for the region of interest was set at 6 to 13 cm. 'Normal' frequency range (mid resolution/ mid penetration) was used in

most patients, but was adjusted to 'penetration' (lower resolution/ high penetration) in case of obesity. Frequency range 'resolution' was used in case of thin women and/or superficial position of the fetus. Scanning time for one recorded volume ranged between 4 and 8 seconds, depending on fetal movement and size of the recorded volume.

The 3D ultrasound data for measurement of brain volume were recorded using a sagittal scan of the head. Acquisition of this scan started at the midsagittal view of the head with the fetus facing the transducer. All data were first stored and processed by the equipment and displayed in three perpendicular planes on the monitor. The volume data were then collected on a transportable magnetic disk for later analysis (Iomega Jaz).

Measurements were made with the use of the 3D view program (Kretztechnik AG, version 4.0) on a personal computer with an Iomega Jaz Drive. 3D brain volume (milliliters) was measured by rotating the recorded volume until the midsagittal plane was displayed on the upper right panel. With the VOCAL mode (method for measuring volume) the internal borders of the head were traced manually with stepwise rotation of 30 degrees, taking the skull base (defined as the line between glabella and opisthion) as the lower border (Figure 1).

For 2D sonographic estimation of brain volume, the head circumference (HC) was measured in the plane described first by Campbell and Thoms.[1] The 2D brain volume was calculated according to the formula: $1/2 \times 1/6\ \pi\ (HC/\pi)^3$, described by Boito et al.[5]

Total fetal weight was estimated using the Hadlock formula[7], which includes measurement of fetal head and upper abdominal circumference as well as femur length. For comparison with estimated fetal weight and with postmortem data, fetal brain weight was estimated by multiplying fetal brain volume measured with 3D ultrasound with brain specific gravity (1.04).[8]

All 2D and 3D ultrasound examinations and measurements were performed by one observer (NR).

The reproducibility study consisted of recording two volume data sets from the same fetus with a time interval of approximately 20 minutes. The first recorded data set was analyzed twice with a minimal time interval of one week.

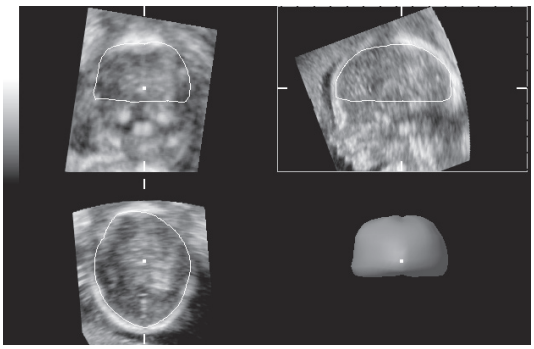

**Figure 1.** Measurement of fetal brain volume with 3D ultrasound.

*Statistical analysis*

Statistical analysis was performed on a personal computer using SPSS version 10.1 (SPSS Corp, Chicago, Ill). Analysis of the reproducibility study consisted of nested analysis of variance to separate the within subjects variation in components caused by differences between repeated tests within patients and differences between analyses of the same recorded volume.

Visual inspection of the scatterplot of 3D fetal brain volume versus gestational age showed roughly quadratic curves for individuals. Therefore, a linear relationship between the square root transformation of 3D brain volume versus gestational age was analyzed with regression analysis for repeated measurements (random coefficients model) using SAS PROC MIXED (SAS Institute, Cary, NC). Weight-specific reference intervals were also calculated according to this model. The random coefficients model was also used for determination of the relationship between fetal brain weight (3D) versus estimated fetal weight and fetal brain weight as a percentage of total estimated fetal weight versus gestational age.

The agreement between both 3D and 2D fetal brain volume was assessed by calculation of the intraclass correlation coefficient (ICC). Systematic differences between 3D and 2D brain volume outcomes were calculated by means of the paired Student *t* test. The 95% confidence limits of 3D fetal brain weight data were calculated for comparison with published postmortem brain weight data relative to gestational age[9-11] and for comparison with published postmortem brain weight relative to total fetal weight.[9,12]

A p value of less than 0.05 was considered significant.

## Results

*3D brain volume measurement*

A complete set of four 3D fetal brain volume measurements was collected in 65 out of 68 women. A recording from the last scan was not available in two women and the last scan was not performed in the remaining woman, resulting in 269 recordings for 3D fetal brain volume measurement. A technically successful measurement was obtained in 245 (91%) out of 269 recordings. The remaining 24 recordings were of insufficient quality mostly due to the limited size of the recorded volume or position of the fetal head.

The reproducibility study showed a coefficient of variation for 3D fetal brain volume measurement of 10.2% caused by differences between repeated tests within women and 2.2% due to differences between analyses of the same recorded volume.

Fetal brain volume data demonstrate a statistically significant linear increase for the square root transformation of fetal brain volume relative to gestational age (Figure 2). The median value (50$^{th}$ percentile) increases from 34 ml at 18 weeks to 316 ml at 34 weeks of gestation (Table I). Weekly increase (50$^{th}$ percentile) in fetal brain volume varies between 9 ml (28%) at 19 weeks to 26 ml (9%) at 34 weeks of gestation (Table I).

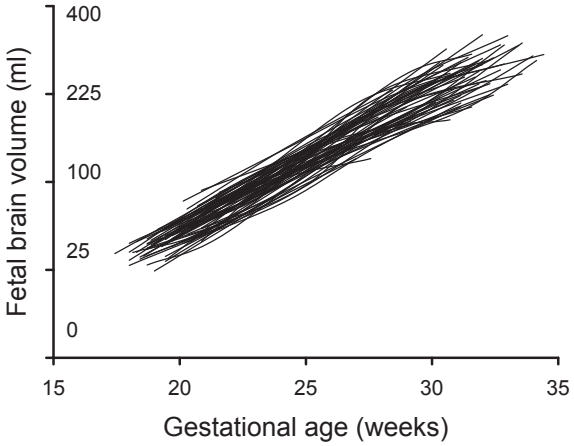


**Figure 2.** Longitudinal representation of fetal brain volume (in milliliters) relative to gestational age (in weeks). Data points (mostly four) are connected by *straight line* segments for individual fetuses. Note the square root-scaled vertical axis.



**Table I.** Fetal brain volume (in milliliters) relative to gestational age (5th, 50th, 95th percentile); weekly increment in fetal brain volume; median fetal brain weight as a percentage of estimated fetal weight.

| GA (wk) | 5% (ml) | 50% (ml)# | 95% (ml) | Weekly increment (ml) | Median fetal brain weight/ estimated fetal weight (%)* |
|---|---|---|---|---|---|
| 18 | 21 | 34 | 49 | - | 16 |
| 19 | 29 | 43 | 59 | 9 (28%) | 16 |
| 20 | 38 | 53 | 71 | 10 (24%) | 16 |
| 21 | 47 | 65 | 85 | 12 (22%) | 16 |
| 22 | 58 | 77 | 100 | 13 (20%) | 17 |
| 23 | 69 | 91 | 116 | 14 (18%) | 17 |
| 24 | 82 | 16 | 133 | 15 (16%) | 17 |
| 25 | 95 | 122 | 152 | 16 (15%) | 17 |
| 26 | 109 | 139 | 173 | 18 (15%) | 17 |
| 27 | 124 | 157 | 194 | 19 (13%) | 17 |
| 28 | 140 | 177 | 218 | 19 (12%) | 16 |
| 29 | 156 | 197 | 243 | 21 (12%) | 16 |
| 30 | 174 | 219 | 269 | 22 (11%) | 16 |
| 31 | 192 | 241 | 297 | 23 (10%) | 15 |
| 32 | 211 | 265 | 326 | 24 (10%) | 15 |
| 33 | 231 | 290 | 356 | 25 (9%) | 15 |
| 34 | 252 | 316 | 389 | 26 (9%) | 14 |

*GA*, gestational age.

#Median fetal brain volume:√ brain volume = 0.75 GA – 7.71

*Median fetal brain weight (BW) as a percentage of estimated fetal weight (EFW): Log (100 x BW/ EFW) = 0.7540 + 0.0388 GA - 0.0008 $GA^2$.

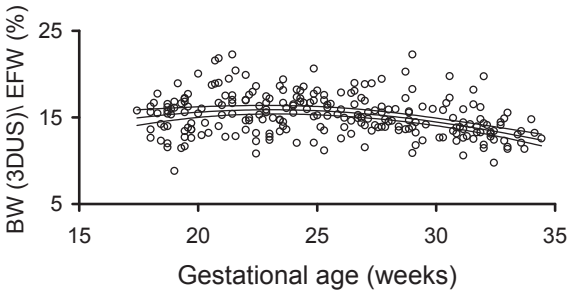


**Figure 3.** Fetal brain weight (*BW*) as a percentage of estimated fetal weight (*EFW*) relative to gestational age (in weeks). Curves represent fitted median values with 95% confidence limits.

The relation between the log transformation (base 10) of brain weight as a percentage of total fetal weight and gestational age appeared nonlinear as evidenced by a significant quadratic fitted curve ($p < 0.001$) (Figure 3). Median fetal brain weight as a percentage of total fetal weight varies between 14% and 17% with a decrease during the first half of the third trimester of pregnancy (Table I; Figure 3).

A clear difference exists between median 3D fetal brain weight and postmortem brain weights, which increases with gestational age (Table II).

When related to estimated fetal weight, mean 3D sonographic fetal brain weight agreed well with brain weight based on equations according to postmortem data from Guihard-Costa et al[9] and Jordaan and Dunn[13] (Table III).

*2D brain volume measurement*

A 2D brain volume measurement was successful in 269 (99%) out of 271 recordings. Mean difference in fetal brain volume between the 3D and 2D sonographic measuring technique was 12 ml, which is statistically significant ($p<0.001$). However, the overall agreement between 3D and 2D measurements of fetal brain volume was good, with an ICC of 0.95.

## Comment

To the best of our knowledge, this is a first longitudinal report on fetal brain volume measured by 3D ultrasound. Measurements on fetal head circumference and Doppler studies on intracerebral blood flow have demonstrated the presence of fetal brain sparing in fetal growth restriction associated with impaired uteroplacental perfusion.[1,14]

The current study shows an acceptable intraobserver variability for differences between repeated tests within women and between analyses of the same recorded volume.

A nearly ten-fold increase in fetal brain volume takes place during the second half of gestation. A similar rise was established by Endres and Cohen[15] in a cross-sectional study design that used a different 3D ultrasound method. At the same time, brain growth demonstrates a marked slow down as expressed by a weekly increment in brain volume at 34 weeks of only one third of the weekly increment at 19 weeks of gestation. When fetal brain weight derived

**Table II.** Comparison of fetal brain weight (50th percentile) (grams) derived from the current 3D sonographic study and three postmortem studies.

| Gestational age (wks) | Fetal brain weight (g) | | | |
|---|---|---|---|---|
| | *Current study (95% confidence limits)* | *Guihard-Costa et al** [9] | *Singer et al* [10] | *Gruenwald and Mingh* [11] |
| 18 | 35 (33-37) | 33 | - | - |
| 20 | 55 (53-57) | 48 | 49 | - |
| 22 | 80 (78-83) | 68 | 65 | - |
| 24 | 110 (107-113) | 91 | 83 | 92 |
| 26 | 145 (141-149) | 118 | 105 | 111 |
| 28 | 184 (179-189) | 147 | 132 | 139 |
| 30 | 228 (221-235) | 181 | 163 | 166 |
| 32 | 277 (268-286) | 219 | 198 | 209 |
| 34 | 330 (319-341) | 260 | 237 | 246 |

* Data visually estimated from graphs in Guihard-Costa et al.[9]

**Table III.** Comparison of fetal brain weight (50th percentile) (grams) derived from the current 3D sonographic study and fetal brain weight from different equations or tables derived from published postmortem studies at the fetal weight range of 500– 2500 grams.

| Fetal weight (g) | Fetal brain weight (g) | | |
|---|---|---|---|
| | *Current study*[§] *(95% confidence limits)* | *Guihard-Costa et al*[9]* | *Jordaan and Dunn*[13#] |
| 500 | 80 (78-83) | 80 | - |
| 750 | 120 (116-123) | 116 | 109 |
| 1000 | 155 (151-160) | 151 | 153 |
| 1250 | 188 (183-193) | 186 | 192 |
| 1500 | 218 (212-224) | 220 | 228 |
| 1750 | 246 (238-253) | 253 | 260 |
| 2000 | 271 (262-281) | 286 | 289 |
| 2250 | 295 (284-307) | 319 | 315 |
| 2500 | 317 (303-332) | 352 | 338 |

*BW*, fetal brain weight; *FW*, (estimated) fetal weight

§ Equation: $\log (BW) = -0.2453 (\log FW)^2 + 2.3496 \log FW - 2.6499$.

* Based on equation: $\log (BW) = 0.92 \log FW - 0.58$.

# Based on equation: $BW = 543.85 - (435.1452)(0.8077)^x$; $x = (FW-750)/500$; fetal weight ≥ 750 g.

from brain volume is examined, this represents 14% to 17% of total estimated fetal weight. Fetal brain weight expressed as a percentage of total fetal weight shows a significant reduction during the first half of the third trimester of pregnancy.

For producing a method that is easy to perform and is reproducible, it is necessary to take borders that are identifiable. The method we present here is based on the method described by Gordon in 1966.[16] It concerns measurement of cranial capacity in children by means of

radiography, taking the frontal pole (in this study "glabella") and the occipital pole (or "opisthion") as the anterior and the posterior border, respectively. Gordon also includes those parts of the brain that are below the level of the skull base. However, in contrast with radiography, this part of the skull is not well visualized with ultrasound and could therefore not be measured. This could induce a small underestimation of the actual brain volume.

However, postmortem fetal brain weights were considerably lower than 3D sonographic fetal brain weights, particularly during the third trimester of pregnancy. These differences were less marked when fetal brain weight relative to total weight was taken into consideration, especially in the lower fetal weight classes. Several factors, such as cooling of the fetal specimen, cause of death, delivery-death interval, presence of traumatic, vascular, inflammatory, or other intracranial pathology, as well as the level at which the brainstem is sectioned, may influence the measured weight of the brain during autopsy.[13] Moreover, fetal death may be associated with loss of water content that will affect fetal weight. This is supported by the observation that total body weight at autopsy is significantly lower than birth weight of live infants at a similar gestational age.[11] This may also explain the good agreement between 3D sonographic and postmortem data when fetal brain weight relative to total weight is compared.

A good agreement, as is expressed by an ICC of 0.95 exists between 3D sonographic measurement and 2D sonographic estimation of fetal brain volume derived from postmortem fetal brain weight. The significantly smaller mean value (difference 12 ml) for 2D sonographic brain volume estimates may be determined by the same limitations associated with postmortem fetal specimen.[13] Because measurement of fetal head circumference is part of routine biometry, the 2D sonographic method of estimating fetal brain volume described here is well applicable, although direct measurement of fetal brain volume with 3D ultrasound should be preferred.

Fetal brain volume measurement in conjunction with fetal liver volume determination could provide insight into the nature of abnormal fetal growth. Measurement of fetal brain volume beyond 34 weeks of gestation may be helpful in determining late onset growth retardation. However, there are several reasons for being increasingly less able of accurately establishing fetal brain volume by 3D ultrasound beyond 34 weeks of gestation. First, there are increasing limitations in recording the entire fetal head because of limited 3D transducer sector size. Second, near term, the fetal head is often situated deep down in the pelvic region, which makes it difficult to obtain the midsagittal plane necessary for correctly recording the volume. Third, the increased bone density of the skull leads to difficulties in visualizing the occipital border of the brain.

It can be concluded that 3D sonographic measurement of fetal brain volume demonstrates an acceptable intraobserver variability. Fetal brain volume shows a nearly 10-fold increase and represents 14% to 17% of total estimated fetal weight during the second half of gestation. Fetal brain weight as derived from 3D sonographic fetal brain volume measurements was higher than that obtained from postmortem fetal specimen. However, this difference becomes less

evident when comparing fetal brain weight relative to total fetal weight. Whereas 2D and 3D sonographic volumes show a good agreement, 2D sonographic estimates were smaller at a mean difference of 12 ml.

## References


1. Campbell S, Thoms A. Ultrasound measurement of the fetal head to abdomen circumference ratio in the assessment of growth retardation. *Br J Obstet Gynaecol* 1977; **84**: 165-174.
2. Chang FM, Hsu KF, Ko HC, Yao BL, Chang CH, Yu CH, Chen HY. Three-dimensional ultrasound assessment of fetal liver volume in normal pregnancy: a comparison of reproducibility with two-dimensional ultrasound and a search for a volume constant. *Ultrasound Med Biol* 1997; **23**: 381-389.
3. Laudy JA, Janssen MM, Struyk PC, Stijnen T, Wallenburg HC, Wladimiroff JW. Fetal liver volume measurement by three-dimensional ultrasonography: a preliminary study. *Ultrasound Obstet Gynecol* 1998; **12**: 93-96.
4. Boito SM, Laudy JA, Struijk PC, Stijnen T, Wladimiroff JW. Three-dimensional US assessment of hepatic volume, head circumference, and abdominal circumference in healthy and growth-restricted fetuses. *Radiology* 2002; **223**: 661-665.
5. Boito SM, Struijk PC, Ursem NTC, Wladimiroff JW. Fetal brain/liver volume ratio and umbilical volume flow parameters relative to normal and abnormal human development. *Ultrasound Obstet Gynecol* 2003; **21**: 256-261.
6. Kloosterman G. On intrauterine growth. *Int J Obstet Gynaecol* 1970; **8**: 895-912.
7. Hadlock FP, Harrist RB, Sharman RS, Deter RL, Park SK. Estimation of fetal weight with the use of head, body, and femur measurements--a prospective study. *Am J Obstet Gynecol* 1985; **151**: 333-337.
8. Duck FA. Mechanical Properties of Tissue. In *Physical properties of tissue: a comprehensive reference book*, Duck FA. Academic Press: London, 1990; 137-65.
9. Guihard-Costa AM, Larroche JC, Droulle P, Narcy F. Fetal Biometry. Growth charts for practical use in fetopathology and antenatal ultrasonography. Introduction. *Fetal Diagn Ther* 1995; **10**: 211-278.
10. Singer DB, Sung CJ, Wigglesworth JS. Fetal Growth and Maturation: with Standards for Body and Organ Development. In *Textbook of Fetal and Perinatal Pathology*, Wigglesworth JS, Singer DB. Blackwell Scientific: Boston, 1991; 11-46.
11. Gruenwald PM, Minh HN. Evaluation of body and organ weights in perinatal pathology. *Am J Clin Pathol* 1960; **34**: 247-253.
12. Jordaan HV, Clark WB. Prenatal determination of fetal brain and somatic weight by ultrasound. *Am J Obstet Gynecol* 1980; **136**: 54-59.
13. Jordaan HV, Dunn LJ. A new method of evaluating fetal growth. *Obstet Gynecol* 1978; **51**: 659-665.
14. Wladimiroff JW, Tonge HM, Stewart PA. Doppler ultrasound assessment of cerebral blood flow in the human fetus. *Br J Obstet Gynaecol* 1986; **93**: 471-475.
15. Endres LK, Cohen L. Reliability and validity of three-dimensional fetal brain volumes. *J Ultrasound Med* 2001; **20**: 1265-1269.

16. Gordon IRS. Measurement of cranial capacity in children. *Br J Radiol* 1966; **39**: 377-381.

## 3.3 THREE-DIMENSIONAL SONOGRAPHY OF PRENATAL SKULL BASE DEVELOPMENT

N.M. Roelfsema*, E.W.M. Grijseels*, W.C.J. Hop#, J.W. Wladimiroff*
*Department of Obstetrics and Gynecology, #Department of Epidemiology and Biostatistics, Erasmus MC, University Medical Center Rotterdam, The Netherlands

Published in the Ultrasound in Obstetrics and Gynecology 2007, 29, 372- 377.

### Abstract

**Objective:** To explore longitudinally the development of the fetal skull base using three-dimensional (3D) sonography.

**Methods:** Serial 3D sonographic measurements of anterior skull base length, posterior cranial fossa length and skull base angle were made in 126 normal singleton pregnancies at 18-34 weeks of gestation. In a sub-study of 22 pregnancies intra-observer variability was determined. Regression analysis for repeated measurements was performed by means of the random coefficients model. Results from an earlier publication on brain volume were extended to the total patient cohort.

**Results**: Measurements were technically successful in 69-94%. The coefficient of variation for differences between repeated tests within women was 3.5- 7.6% and between repeated analyses of the same recorded volume it was 3.0- 5.1%. A statistically significant gestational age-related increase was established for both the anterior skull base length and the posterior cranial fossa length and the skull base angle showed a small but significant flexion of about 6 degrees. A higher increment in posterior cranial fossa length relative to anterior skull base angle was established. A significant quadratic relation could be established for both anterior skull base length ($p<0.0001$) and posterior cranial fossa length ($p<0.0001$), but not for skull base angle, relative to brain volume.

**Conclusion:** The reproducibility was acceptable for all fetal skull base measurements. The more pronounced growth in posterior cranial fossa length relative to anterior skull base length is associated with brain growth. In the small flexion of the skull base angle, however, no association with brain growth was found.

## Introduction

From an evolutionary point of view, we know that the skull base or cranial base of modern men differs markedly from that of other primates. The petrous pyramidas are oriented more coronally and there is a higher degree of midline basicranial flexion. In other words, the basi-occipital base has a more vertically inclined orientation relative to the anterior cranial base, resulting in a deeper and wider posterior cranial fossa (Figure 1)[1,2]. Scientists in this field hypothesised that skull base development is linked to brain expansion, obligatory erect position, and facial orthognathism in *Homo sapiens*[1].

The skull base has an important role in supporting and inducing the formation of craniofacial structures[2-6]. It is related closely to the growth and development of the brain and facial bones. However, the skull base is difficult to measure externally [2]. Different techniques have been used in order to optimize the measurements, varying from the use of radiography to high-resolution magnetic resonance imaging (MRI) in mostly formalin-fixed fetuses. Investigation of skull base development by prenatal ultrasonography has only been employed by Degani et al (2002)[4].

In the literature, there is general agreement on the finding that the anterior and posterior skull base length have distinct growth trajectories, with the anterior exceeding posterior growth[1-6]. Growth in the second trimester is more rapid than in the first trimester, with the fastest growth rates during the 4th and 5th months of gestation[7]. The posterior cranial fossa increases in width and length, the width exceeding length. The posterior cranial fossa becomes progressively broader and shallower.

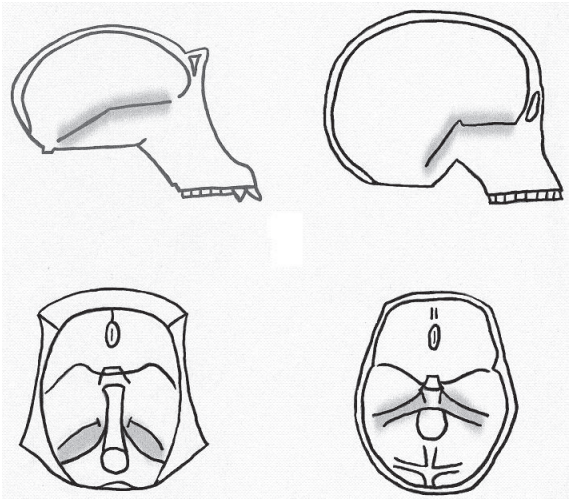

**Figure 1.** Schematic drawing of midline and transverse sections of a chimpanzee (left upper and lower corner) and a modern human (right upper and lower corner). The differences in basicranial flexion (upper row) and petrous pyramids orientation (lower row) are shaded grey. (Drawing based on Figure 1 from Jeffery and Spoor.[1])

However, there is disagreement about the extent to which the angular shapes predominate in skull development. Some studies indicate a moderate decrease in the angle between the anterior and posterior skull base segments, which results in a flexure of the skull base, caused mainly by rapid hind-brain growth. Other studies indicate a retroflexion of the skull base during the second and third trimester of pregnancy [2,8].

In this longitudinal study, we determined anterior skull base length (ASBL), posterior cranial fossa length (PCFL) and skull base angle (SBA) by three-dimensional (3D) ultrasound in order to elucidate prenatal development of the skull base and to obtain insight in the subsequent angular skull base development during the second half of pregnancy. Previously collected brain volume data were used to examine the relationship between brain size and skull base growth.



## Patients and methods

*Study design*

Over a two year period, a total of 129 women with a normal singleton pregnancy consented to participate in this longitudinal study, which was approved by the hospital ethics review board. Women were recruited from the antenatal clinics and regional midwifery services. Pregnancy duration varied between 18 and 34 weeks (median, 26). This was determined from the last reliable menstrual period, adjusted by first-trimester ultrasound in uncertain cases. The Maternal age ranged between 19 and 40 years (median, 30). A total of 126 women remained in the study after three (2%) women were excluded retrospectively from the analysis, due to a fetal malformation detected prenatally (n=1; spina bifida), a congenital malformation or disease recognised after birth (n=1; mildly hydropic child, cause unknown) or there being no follow-up available (n=1). Ninety-five percent of the birth weights were situated between the 5th and 95th percentile, adjusted for maternal parity and fetal sex according to the Kloosterman tables[9]. In each pregnancy, fetal skull base examinations were performed four times at 3- 5 week intervals.

An earlier study on fetal brain volume covered only part of this study cohort, namely the first 68 pregnancies.[10] Fetal brain volume recordings were performed four times in these 68 pregnancies, with a total of 269 recordings (in 3 women a last scan was not available). To be able to compare brain volume measurements to skull base measurements we extended the former study results to the total study cohort of 126 pregnancies.

Intraobserver variability was determined on one occasion in 22 normal singleton pregnancies, six of which also participated in the longitudinal study. Gestational ages at examination were divided equally between 18 and 34 weeks

*Recording technique*

The 3D-ultrasound machine used in the present study was a standard Voluson 530D (Kretztechnik AG, Zipf, Austria) with a 3-5 MHz transducer (VAW 3-5). Depth, longitudinal and transverse dimensions were adjustable. An opening angle of 50 to 70 degrees and a sampling angle of 30 to 85 degrees were used, resulting in a maximum volume of 3.2 litre. The depth range for the region of interest was set at 6-13 cm. Scanning time for one recorded volume ranged between 4 and 8 seconds, depending on fetal movement and size of the recorded volume. The region of interest was defined containing the complete fetal head. Fetal skull base data were recorded by acquisition of a sagittal scan of the face, starting at the mid-sagittal plane, with the fetus facing the transducer. The volume data were collected on a transportable magnetic disk for later analysis (Iomega Corp., Roy, UT, USA). Measurements were made using the 3D view program (Kretztechnik AG, version 4.0) on a personal computer with an Iomega Jaz Drive.

ASBL was defined as the distance in mm between glabella and sella turcica (Figure 2). The sella turcica is located just between the frontal and the occipital part of the spenoid bone in the midsagittal plane and the middle of the cross formed by the spenoid ridge and the otic cartilage in the transverse plane (Figures 3 and 4)

Measurement of the posterior skull base length, the distance between the sella turcica and basion, was not feasible since the basion, the lowest part of the clivus, is often difficult to determine due to scattering by or too much reflection from the surrounding bony tissue. Instead, the PCFL, the distance in mm between the sella turcica and opisthion (the lowest part of the skull), was considered to be an acceptable alternative for determining the development of the posterior part of the skull base (Figure 2). For the SBA (degrees), one arm was defined as the distance between the nasion and the sella turcica, the other arm being the line connecting

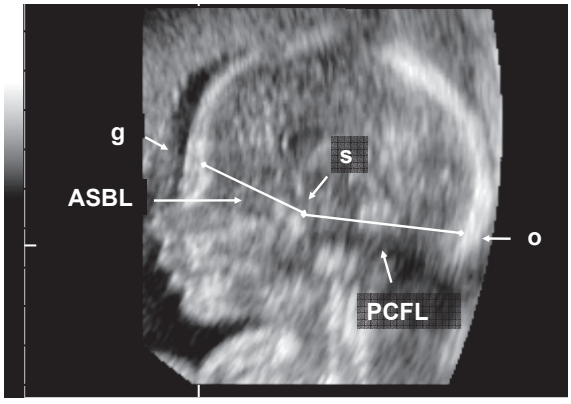


**Figure 2.** Measurement of anterior skull base length (ASBL) and posterior cranial fossa length (PCFL) using three-dimensional ultrasound. (Landmarks: g= glabella, prominence on the frontal bone above the root of the nose at the level of the superior orbital ridges; s= sella turcica, middle of cross formed by sphenoid ridge and the otic cartilage in transverse plane; o= opisthion, lowest posterior point of the skull (inner border))

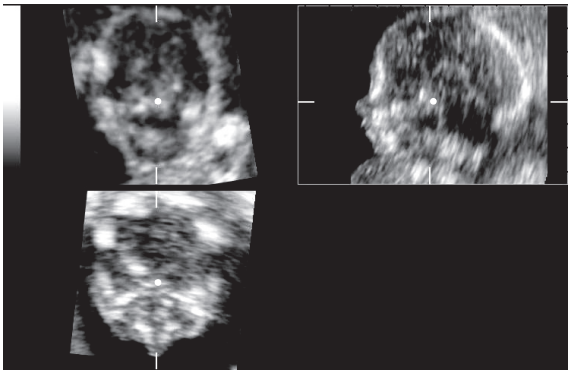

**Figure 3.** Position of sella turcica in the multiplanar view: coronal (top left), sagittal (top right) and transverse (bottom left) planes.



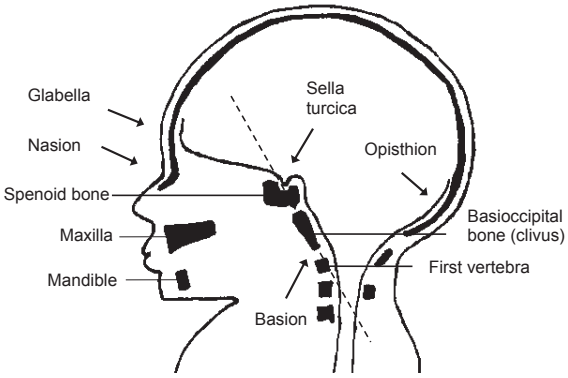


**Figure 4.** Schematic drawing of the midsagittal section of a normal fetus at about 26 weeks' gestation. The dotted line represents the line from the sella turcica, through the clivus to the frontal part of the first vertebra.

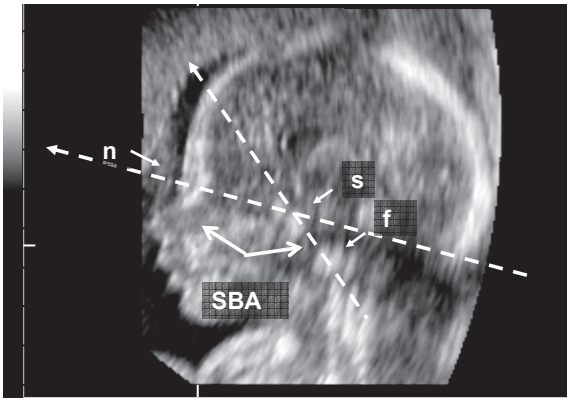


**Figure 5.** Measurement of skull base angle (SBA) with three-dimensional ultrasound. (Landmarks: n= nasion, deepest part of the nasal root; s= sella turcica; f= frontal part of the first vertebra)

the sella through the clivus with the frontal part of the first vertebra (Figures 4 and 5). 3D brain volume (ml) was measured by rotating the recorded volume until the mid-sagittal plane was displayed on the upper-right panel. With the VOCAL mode (method for measuring volume) the internal borders of the head were traced manually with stepwise rotation of 30 degrees, taking the skull base (defined as the line between glabella and opisthion) as the lower border. This method is explained in detail in an earlier report[10].One observer (NR) performed all 3D ultrasound examinations and measurements.

The reproducibility study consisted of recording two volume datasets from the same fetus separated by a time interval of approximately 20 minutes. The first recorded dataset was analyzed twice with a minimal time interval of one week. This second analysis was done whilst with the researcher blinded to the results of the first analysis.

*Statistical analysis*

Statistical analysis was performed on a personal computer using SPSS version 10.1 (SPSS Inc., Chicago, IL, USA). Analysis of the reproducibility study consisted of Nested Analysis of Variance to separate the within subjects variation in components for differences between repeated tests within subjects and differences between repeated analyses of the same recorded volume.

The relationship of the measurements versus gestational age was analyzed with regression analysis for repeated measurements (random coefficients model) using SAS PROC MIXED, version 6.2 (SAS Institute, Cary, NC.). This procedure is a powerful method for analyzing longitudinal data. Data were centered by using the halfway point of gestational age (20 weeks), and calculations used x=gestational age- 20 as the time axis. The advantage of this transformation is twofold: the resulting intercepts represent the mean outcome at around the middle of pregnancy, and a faster convergence of the iterative procedure is achieved. Weight-specific reference intervals were also calculated according to this model. This random coefficients model was used for determination of the relationship between the log-transformed ASBL/PCFL ratio versus gestational age, along with the 95-percent confidence limits of the median. This transformation was required to get a proper fit.

Regression analysis for repeated measurements was also used for analysis of the relationship of the log-transformed brain volume relative to ASBL, PCFL and SBA.

A p value of less than 0.05 was considered statistically significant.

## Results

A complete set of four 3D volume measurements was collected in 117 out of the 126 women (93%). A recording from the last scan was not performed in five women. The last scan was not available in another four women. This resulted in 495 recordings for fetal skull base and brain volume measurements.

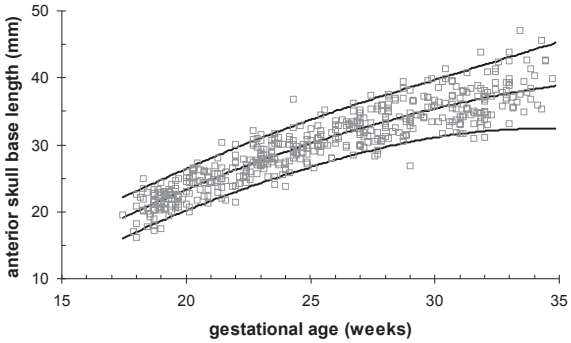


**Figure 6.** Anterior skull base length (mm) relative to gestational age (weeks). Curves represent fitted mean values with 5th and 95th percentiles.



Measurement was technically successful for the ASBL in 466 (94%) recordings, for the PCFL in 454 (92%) recordings and for the SBA in only 341 (69%) recordings. The reproducibility study showed a coefficient of variation (CV) for differences between repeated tests within women of 4.9, 3.5 and 7.6% for ASBL, PCFL and SBA, respectively. The CV for differences between repeated analyses of the same recorded volume was 4.6, 5.1 and 3.0% for ASBL, PCFL and SBA, respectively.

Regression analysis demonstrated a statistically significant quadratic fitted curve for ASBL relative to gestational age (Figure 6). Both PCFL and SBA showed a statistically significant linear relationship with gestational age (Figure 7 and 8). Mean ASBL increased from 20 mm to 38 mm and mean PCFL increased from about 30 mm to 68 mm during the period studied. The mean SBA showed a statistically significant ($p= 0.003$) linear decrease from 138 to 132 degrees, throughout the second half of gestation. Comparing ASBL with PCFL, there was a relatively higher increment of PCFL, resulting in a statistically significant linear decrease of the log-transformed ASBL/ PCFL- ratio relative to gestational age (Figure 9).

A statistically significant quadratic relation was found for the log-transformed brain volume relative to ASBL ($p<0.0001$) and the log-transformed brain volume relative to PCFL ($p<0.0001$) (Figure 10 and 11). However, no statistically significant relationship could be established for brain volume relative to SBA (Figure 12).

## Discussion

To the best of our knowledge this is the first longitudinal report on human fetal skull base development studied by 3D ultrasound.

We demonstrated an acceptable intra-observer variability. High success rates were found for ASBL and PCFL measurements. When the fetus was situated deep in the pelvic region and/ or the fetal face was directed constantly towards the maternal sacrum, it was not possible

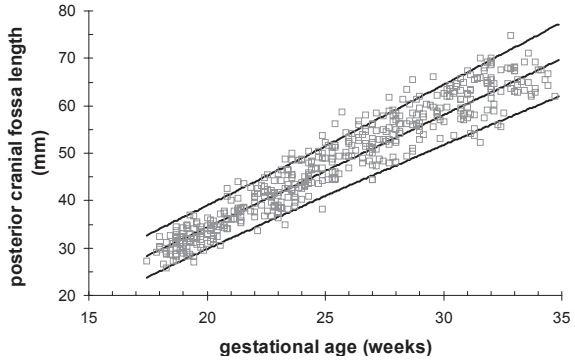


**Figure 7.** Posterior cranial fossa length (mm) relative to gestational age (weeks). Curves represent fitted mean values with 5th and 95th percentiles.

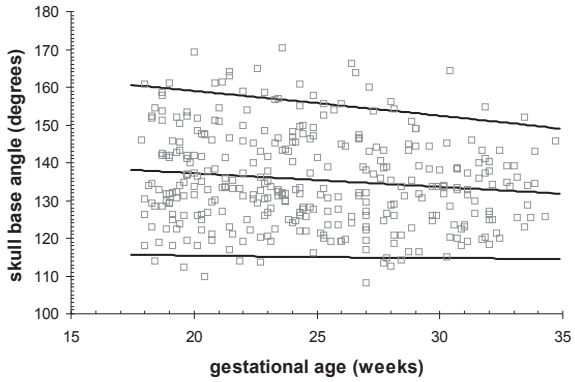


**Figure 8.** Skull base angle (degrees) relative to gestational age (weeks). Curves represent fitted mean values with 5th and 95th percentiles.

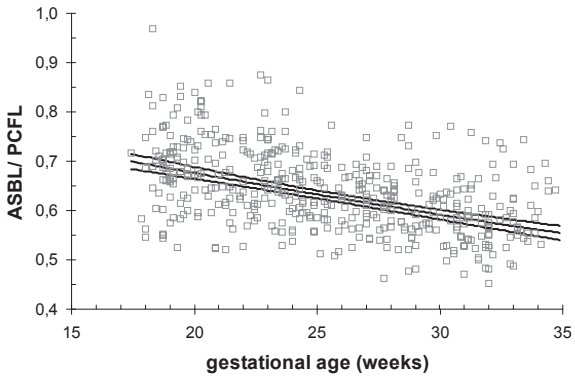


**Figure 9.** Ratio of anterior skull base length (ASBL)/ posterior cranial fossa length (PCFL) relative to gestational age (weeks). Curves represent fitted median values with 95% confidence limits.

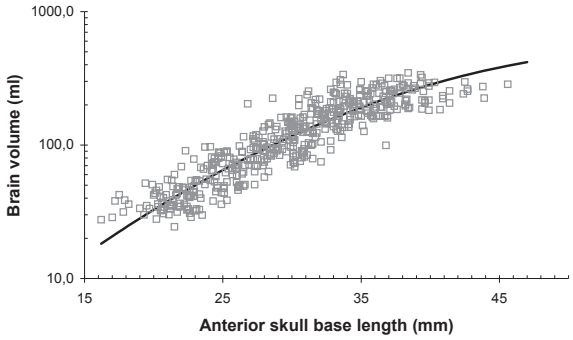


**Figure 10.** Brain volume (BV) relative to anterior skull base length (ASBL). Curve represents fitted median values (log(BV)= 2.0676+0.04687 x (ASBL-30)-0.00084 x (ASBL-30)$^2$; p-value of the quadratic component <0.0001).



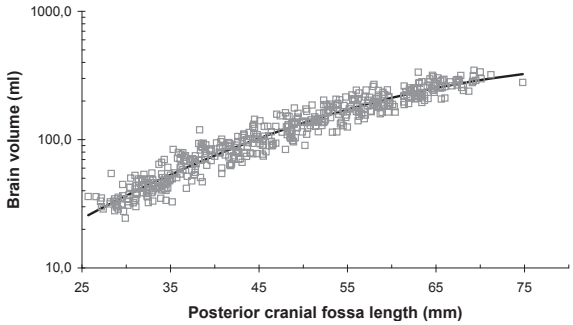


**Figure 11.** Brain volume (BV) relative to posterior cranial fossa length (PCFL). Curve represents fitted median values (log(BV)= 2.0785+0.02381 x (PCFL-47.8)-0.00029 x (PCFL-47.8)$^2$; p-value of the quadratic component <0.0001).

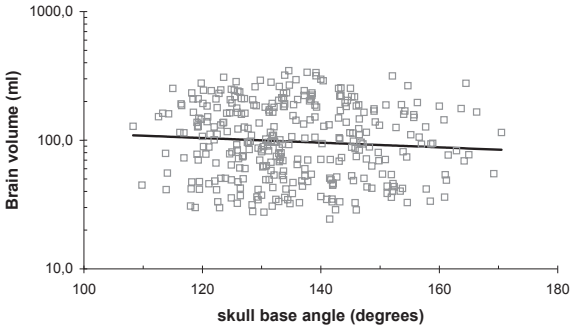


**Figure 12.** Brain volume (BV) relative to skull base angle (SBA). Curve represents fitted median values (non-significant relationship) (log(BV)= 1.99-0.000181 x (SBA-135); p-value of the linear component = 0.15).

to perform any fetal skull base measurements. Obscuring structures in front of the fetal face could also complicate measurement. The relatively lower success rate of the skull base angle measurement can be explained by the difficulty in observing the frontal border of the foramen magnum (or clivus) by ultrasound, as mentioned earlier.

In the evaluation of the skull base, different studies,often use different techniques and therefore different landmarks. Most studies on the fetal skull base are cross-sectionally derived examinations on formalin-fixed fetuses, with fixed landmarks based on ossification detectable by X-ray. However, large proportions of the skull base persist as cartilage throughout the second trimester and thus are not visible by radiography. This applies in particular to the sella turcica, which is used as an important landmark to differentiate between the anterior and the posterior skull base. In more recent studies, high-resolution MRI was used, allowing most tissues to be shown, although considerable practise is necessary to interpret these structures in two dimensions[5]. Our study design had the advantage of obtaining longitudinal information on the development of the prenatal skull base during normal pregnancy and using landmarks suitable for sonographic examination.

Most of the discussions about human skull base development studies are centered around prenatal changes in skull base angle. By using three-dimensional ultrasound, it was possible to pursue serial measurements during normal fetal development and to establish a small but significant flexion of the cranial base during the second half of gestation. Similar results were found by van den Eynde (1992)[11]. This finding is consistent with a well-known (to anthropometrists) model predicting basicranial flexion following increased brain growth relative to slower growth of the midline basicranium [8].

On the other hand, Jeffery and Spoor found basicranial retroflexion during the second half of gestation, as did several other authors [1,6,12,13]. Jeffery and Spoor put forward the hypothesis that the basicranium flexes when the hindbrain undergoes rapid growth in the first trimester, remains stable during the second and retroflexes during the third trimester.[1] The SBA is known to flex again rapidly during the first two years after birth[1,2]. However, why brain size correlates with skull base angle after birth and not before remains unexplained in this hypothesis.[2] Jeffery and Spoor suggest an intrinsic mechanism which is independent of brain growth[1]. Our data indicate that flexion does occur during the second half of gestation. This difference may be explained by the fact that different landmarks were applied, although our study also showed no statistically significant relation between brain volume and SBA, supporting Jeffery and Spoor's suggestion of other factors causing the skull base to flex.

The anterior skull base was compared to the PCFL and not the posterior skull base length for reasons mentioned earlier. The increase in PCFL was more pronounced than that in the ASBL. The sella turcica gained a more anteriorly positioned orientation relative to the back of the skull (opisthion) as gestation progressed. As the ASBL is usually compared with the posterior skull base length and not the PCFL, it is difficult to compare our results with those in literature. However, our findings are consistent with other human fetal studies showing growth along

the skull base to be significantly slower than in other parts of the skull. fetal brain growth to be markedly rapid at the same time[1]. This would result in faster growth of the posterior cranial fossa, allowing the hindbrain to expand. This would also explain the significant relationship between brain volume and PCFL.

The results of Degani *et al* (2002) are in agreement with ours. They studied the skull base in a transverse plane with two-dimensional ultrasound during 14 to 40 weeks' gestation. Their study shows a more pronounced increase in otic cartilage length compared to the sphenoid ridge length, supporting faster backward growth of the skull to increase the space in the posterior part of the skull base[4].

With the introduction of three-dimensional ultrasound, longitudinal studies on fetal skull base development have become feasible. In this study, the more pronounced growth of the PCFL relative to the ASBL was associated with brain growth. However, in the modest flexion of the SBA no association with brain growth was found.



## References


1. Jeffery N, Spoor F. Brain size and the human cranial base: a prenatal perspective. *Am J Phys Anthropol* 2002; 118: 324-340.
2. Lieberman DE, Ross CF, Ravosa MJ. The primate cranial base: ontogeny, function, and integration. *Am J Phys Anthropol* 2000; Suppl: 117-169.
3. Eriksen E, Bachpetersen S, Solow B, Kjaer I. Midsagittal Dimensions of the Prenatal Human Cranium. *J Craniofac Genet Dev Biol* 1995; 15: 44-50.
4. Degani S, Leibovitz Z, Shapiro I, Gonen R, Ohel G. Ultrasound evaluation of the fetal skull base throughout pregnancy. *Ultrasound Obstet Gynecol* 2002; 19: 461-466.
5. Jeffery N. A high-resolution MRI study of linear growth of the human fetal skull base. *Neuroradiology* 2002; 44: 358-366.
6. Burdi AR. Cephhalometric growth analyses of the human upper face region during the last two trimesters of gestation. *Am J Anat* 1969; 125: 113-122.
7. Sherwood TF, Mooney MP, Sciote JJ, Smith TD, Cooper GM, Siegel MI. Cranial base growth and morphology in second-trimester normal human fetuses and fetuses with cleft lip. *Cleft Palate Craniofac J* 2001; 38: 587-596.
8. Jeffery N, Spoor F. Ossification and midline shape changes of the human fetal cranial base. *Am J Phys Anthropol* 2004; 123: 78-90.
9. Kloosterman G. On intrauterine growth. *Int J Obstet Gynaecol* 1970; 8: 895-912.
10. Roelfsema NM, Hop WCJ, Boito SME, Wladimiroff JW. Three-dimensional sonographic measurement of normal fetal brain volume during the second half of pregnancy. *Am J Obstet Gynecol* 2004; 190: 275-280.
11. Van den Eynde B, Kjaer I, Solow B, Graem N, Kjaer TW, Mathiesen M. Cranial Base Angulation and Prognathism Related to Cranial and General Skeletal Maturation in Human Fetuses. *J Craniofac Genet Dev Biol* 1992; 12: 22-32.

12. Dimitriadis AS, Haritantikouridou A, Antoniadis K, Ekonomou L. The human skull base angle during the second trimester of gestation. *Neuroradiology* 1995; 37: 68-71.

13. Levihn WC. A cephalometric roentgenographic cross-sectional study of craniofacial complex in fetuses from 12 weeks to birth. *Am J Orthodontics* 1967; 53: 822-848.

## 3.4 THREE-DIMENSIONAL SONOGRAPHIC DETERMINATION OF NORMAL FETAL MANDIBULAR AND MAXILLARY SIZE DURING THE SECOND HALF OF PREGNANCY

N.M. Roelfsema[a], W.C.J. Hop[b], J.W. Wladimiroff[a]

[a]Department of Obstetrics and Gynecology, [b]Department of Epidemiology and Biostatistics, Erasmus MC, University Medical Center Rotterdam, The Netherlands

Published in the Ultrasound in Obstetrics and Gynecology 2006, 28, 950-957.

### Abstract

**Objective:** To explore the various ways of obtaining fetal maxillary and mandibular size with three-dimensional (3D) ultrasound, with a view of developing a tool for identifying minor anomalies in the lower facial region.

**Methods:** Serial 3D sonographic measurements of the fetal jaws were made in 126 normal singleton pregnancies at 18-34 weeks of gestation for determination of degree of maxillary and mandibular protrusion, maxillary and mandibular corpus lengths, mid- and lower facial depths and maxillary and mandibular curvature. In a sub study the reproducibility of the measurements was evaluated.

**Results:** The coefficient of variation in the reproducibility study varied between 7.1 and 10.5%. For all parameters but maxillary and mandibular protrusion, there was a significant gestational age-related increase. Maxillary/ mandibular protrusion, maxillary/ mandibular corpus lengths, mid-/ lower facial depths and maxillary/ mandibular curvature ratio all showed a significant gestational age-related decrease, with the most distinct decrease in the mid-/lower facial depth ratio.

**Conclusions:** 3D ultrasound measurement of the fetal maxilla and mandible demonstrated an acceptable intraobserver variability for all measurements. The mid-/ lower facial depth ratio appears to be most valuable in determining abnormal mandibular development.

## Introduction

Over the years there has been a considerable number of reports on the prenatal detection of major fetal craniofacial anomalies using two-dimensional (2D) ultrasound[1-6]. Facial structures are formed as early as 8 weeks of gestation. While information on normal facial development is difficult to retrieve by ultrasound this early in embryonic life, using three-dimensional (3D) ultrasound it has now become feasible to conduct fetal facial biometric studies during the second half of pregnancy.

Serial examinations of facial bone structures in three dimensions could provide more detailed knowledge of normal bony facial development and therefore the potential to detect minor facial anomalies. This could contribute to our understanding of certain genetic syndromes and chromosomal anomalies. One particular group of anomalies is characterized by underdevelopment of the chin, or micrognathia, as seen in, for example, Pierre Robin sequence*, several chromosomal deletions and trisomies 13 and 18 and less often in fetal alcohol syndrome* and Noonan syndrome*[5,7,8].

Data on mandibular size and growth as obtained by 2D ultrasound have been reported by several researchers during the last 10-15 years[9-12] and there have been two recent reports on fetal chin development using 3D ultrasound[13,14]. The objective of our study was to explore the various ways of obtaining fetal mandibular and maxillary size during the second half of pregnancy using 3D ultrasound, with a view to developing a tool for identifying minor anomalies in the lower facial region.

## Patients and methods

This was a longitudinal study of 126 women with singleton pregnancies at 18- 34 (median, 26) weeks' gestation. All women consented to participate following approval by the regional ethics review board. Gestational age was determined from the last menstrual period and/or the fetal crown-rump length or biparietal diameter in the first trimester of pregnancy. Maternal age varied between 19 and 40 (median, 30) years. All pregnancies were uncomplicated, resulting in the term delivery of an infant without congenital anomalies. Ninety-five percent of the birth weights were situated between the 5th and 95th percentiles, adjusted for maternal parity and fetal sex according to the Kloosterman tables[15]. Sixty-five (52%) infants were male and 61 (48%) were female. All recordings and measurements were carried out by the same examiner (NR). In each pregnancy, 3D sonographic examinations were performed four times at 3-5 week intervals.

3D sonographic assessment of the fetal head and face was performed using a standard Voluson 530D (Kretztechnik AG, Zipf, Austria) with a 3-5 MHz curved array transducer (VAW 3-5). An internal mechanism in the transducer sliced through the images and recorded a truncated pyramidal volume. Depth, longitudinal and transverse dimensions were adjustable. An

* Syndromes/sequences are identified at p 179-180.

opening angle of 50 to 70 degrees and a sampling angle of 30 to 85 degrees were used, resulting in a maximum volume of 3.2 liter. The depth range for the region of interest was set at 6-13 cm. A 'normal' frequency range (mid resolution/mid penetration) was used in most patients, but was adjusted to 'penetration' (lower resolution/high penetration) in the case of obesity. Frequency range 'resolution' was used in the case of thin women and/or superficial position of the fetus. Scanning time for one recorded volume ranged between 4 and 8 seconds, depending on fetal movement and size of the recorded volume.

Multiple volume datasets were recorded of each fetus (range 2-11, median 5). The region of interest was defined containing the complete fetal head. Two different types of acquisition of the fetal face and head were used for this study: a sagittal scan (frontal view of the face, composed of sagittal planes) and a coronal scan (side of the head, composed of coronal planes). Acquisition of the sagittal scan of the face started at the mid-sagittal plane with the fetus facing the transducer. A coronal scan as performed starting acquisition just in front of the ear. The volume data that displayed the measurements landmarks best, were then collected on a transportable magnetic disk for later analysis (Iomega Corp., Roy, UT, USA).

Measurements were made using a 3D view program (Kretztechnik AG, version 4.0) on a personal computer with an Iomega Jaz Drive. Measurements were based on anthropometric and cephalometric measurements that have been described in the literature and proved useful in the assessment of postnatal (ab)normal craniofacial development.[16-19] The following facial parameters were measured: (i) degree of maxillary and mandibular protrusion, determined by the angle between sella-nasion and nasion-anterior rims of maxilla and mandibula (Figure 1); (ii) maxillary and mandibular corpus lengths represented by the anterior-posterior border of the maxilla, which was extended to the end of the last tooth bud (Figure 2a) and frontal rim of the mandibula-gonion (Figure 2b); (iii) mid facial and lower facial depths, determined by the tragus-anterior rim of the maxilla (Figure 3a) and tragus-gnathion (Figure 3b); (iv) maxillary and mandibular curvature, represented by the curvature from tragus-anterior rim of the maxilla, multiplied by two (Figure 3a) and the curvature from tragus-gnathion, multiplied by two (Figure 3b).

A complete set of 3D sonographic examinations was collected in 116 of the 126 women. A recording of the last scan was not performed in five women, it was not available in four women and it was only partially available in one woman, resulting in 495 and 494 recordings for measurements derived from the sagittal and coronal scan, respectively.

An intraobserver variability study was conducted in 22 uncomplicated singleton pregnancies, six of which also participating in the serial study. The gestational ages of the 22 pregnancies was distributed equally over the period of 18- 34 weeks. Two volume datasets were recorded from the same fetus, separated by a time interval of approximately 20 minutes. The first data set was analyzed twice, separated by a minimal time interval of one week. The second analysis of the first dataset was carried out while being blinded for the first analysis.

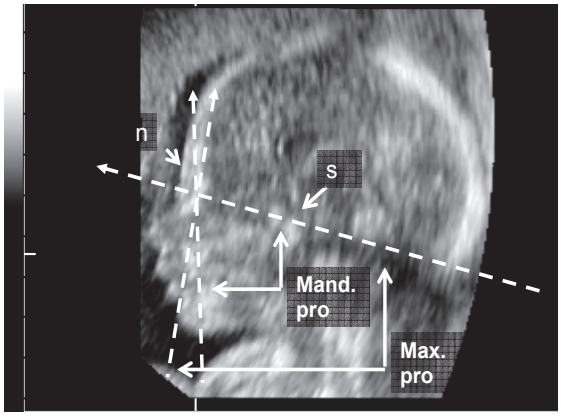


**Figure 1.** Measurement of degree of maxillary (max. pro) and mandibular protrusion (mand. pro) by 3D ultrasound at 20 weeks of gestation. Landmarks are the nasion (n), the deepest part of the nasal root and the sella turcica (s) at the middle of cross formed by the sphenoid ridge and the otic cartilage in transverse plane).

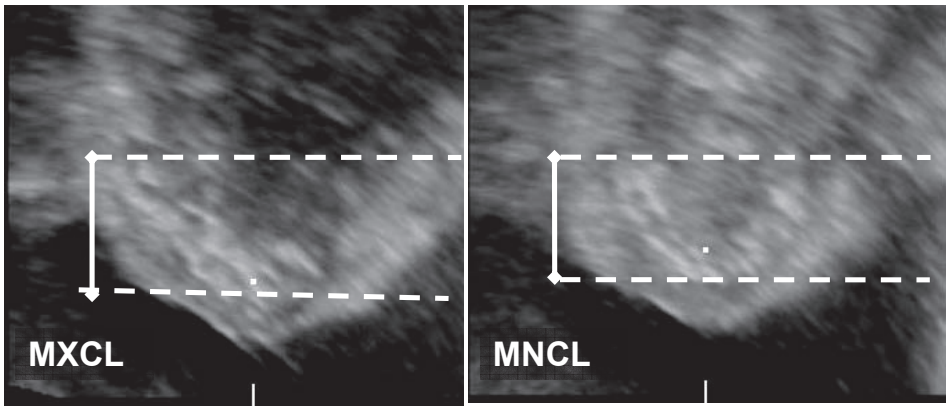


**Figure 2.** Measurement of maxillary corpus length (MXCL) (a) and mandibular corpus length (MNCL) (b) by 3D ultrasound at 20 weeks of gestation.

*Statistical analysis*

Statistical analysis was performed on a personal computer using SPSS for Windows (version 10.1; SPSS Inc., Chicago, IL, USA). Analysis of the reproducibility study consisted of nested analysis of variance to separate the within subjects variation in components for differences between repeated tests within subjects and differences between analyses of the same recorded volume.

The relationship of the maxillary and mandibular measurements versus gestational age was analyzed with regression analysis for repeated measurements (random coefficients model) using SAS PROC MIXED (version 6.2, SAS Institute, Cary, NC). This procedure is a powerful method with which to analyze longitudinal data[20]. Data were centered by using the mid-point

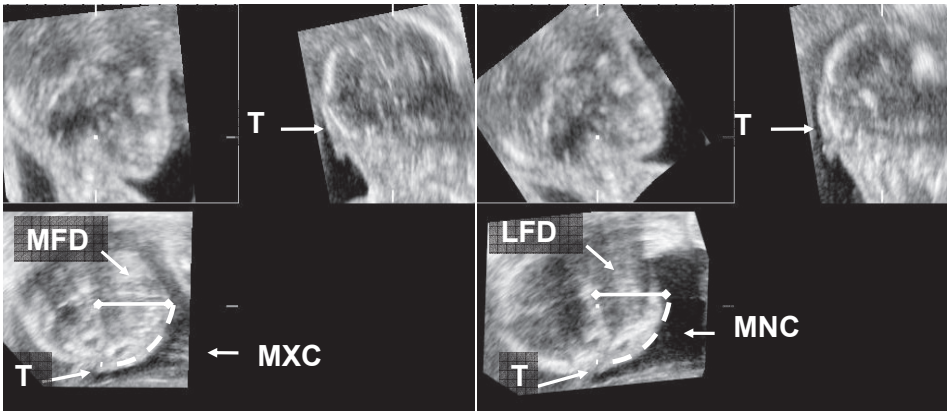


**Figure 3.** Measurement of mid-facial depth (MFD) and maxillary curvature (MXC) (a) and measurement of lower facial depth (LFD) and mandibular curvature (MNC) (b) by 3D ultrasound at 20 weeks of gestation. The landmark is the tragus (T), the middle and most anterior aspect of the ear).



of gestational (20 weeks), and calculations were carried out using x=GA- 20 as the time axis. The advantage of this transformation is two-fold: the resulting intercepts represent the mean outcome at about the middle of pregnancy, and a faster convergence of the iterative procedure is achieved. For various parameters it was required to add a quadratic component of gestational age. Weight-specific reference-intervals were calculated according to this model. This random-coefficients model was also used for determination of the relationship between the different ratios versus gestational age as well as for calculation of the 95-percent confidence limits of the mean values.

A p vale of less than 0.05 was considered significant.

## Results

Table 1 describes for each of the relevant craniofacial parameters: the success rate in obtaining a measurement and the mean and percentage decrease/ increase relative to gestational age (i.e. the percentage change between 18 and 34 weeks) in the 126 women; the coefficient of variation for differences between repeated tests within women (range, 4.1-10.5%), the coefficient of variation for differences between repeated analyses of the same recorded volume (range, 0-6.6%), and the total coefficient of variation (range, 7.1- 10.5%) in the sub study of 22 women. There was a significant gestational age-related increase for each of the craniofacial parameters except for degree of maxillary and mandibular protrusion. Normal reference charts (5th, 50th, 95th percentiles) are provided in Figures 4-7. There was a significant gestational age-related decrease for the maxillary/mandibular protrusion ratio, corpus length ratio and curvature ratio as well as the mid-/lower facial depth ratio. Mean and 95%-confidence intervals of the mean values are depicted in Figures 8-11. The regression equations with standard deviations/ standard errors for Figures 4-11 are presented in Tables 2 and 3.

**Table 1.** Successrate of obtaining measurements and mean measurements with percentage increase or decrease at 34 weeks compared with 18 weeks' gestation, as obtained from regression analyses in 126 pregnancies, and results of reproducibility sub study of 22 pregnancies.

| Measurement | Main study (n=126) | | | | Sub study (n=22) | | |
|---|---|---|---|---|---|---|---|
| | Successful measurements (n (%))* | Mean at 18 wks (mm) | Mean at 34 wks (mm) | % decrease/ increase from 18 to 34 weeks | CV-I (%) | CV-II (%) | $CV_{Total}$ (%) |
| Degree of maxillary protrusion | 462 (93) | 81.2# | 80.9# | - | 6.7 | 4.6 | 8.2 |
| Degree of mandibular protrusion | 455 (92) | 66.7# | 67.9# | - | 5.7 | 5.6 | 8.0 |
| Maxillary corpus length | 471 (95) | 16.5 | 34.5 | 109 | 8.7 | 0.8 | 8.6 |
| Mandibular corpus length | 467 (94) | 13.3 | 29.8 | 124 | 10.5 | 0.0 | 10.5 |
| Mid facial depth | 469 (95) | 27.1 | 56.2 | 107 | 4.1 | 6.6 | 7.8 |
| Lower facial depth | 469 (95) | 25.2 | 55.4 | 120 | 6.1 | 6.1 | 8.6 |
| Maxillary curvature | 469 (95) | 74.5 | 162.0 | 117 | 5.2 | 5.7 | 7.7 |
| Mandibular curvature | 468 (94) | 70.0 | 157.6 | 125 | 7.0 | 1.0 | 7.1 |

* Number of successful measurements out of 496 and 495 recordings for sagittal and coronal measurements, respectively.
# Non-significant change. CV-I: coefficient of variation for differences between repeated tests within women; CV-II : coefficient of variation for differences between analyses of the same recorded volume; $CV_{Total}$: total coefficient of variation.

## Discussion

Serial 3D sonographic images were obtained from the mid and lower facial regions with emphasis on maxillary and mandibular bony size and development during intrauterine life. Knowledge of the relationship between the various bony facial structures during intrauterine development is of interest both for evolutionary reasons and because of the possibility of detecting facial dysmorphology. Abnormal mid- and lower facial development represent phenotypes of a wide range of Mendelian genetic syndromes. For example, trisomy 18, Treacher Collins* and Pierre Robin sequence* are nearly always associated with an abnormal shape or proportions of the mandibula, resulting in micrognathia or retrognathia[8].

The restriction of 2D ultrasound is that bony facial structures can only be viewed in one plane, whether it is transverse or sagittal. The advantage of 3D ultrasound is that it produces a composite image of these structures in all orthogonal planes, allowing a more accurate determination of the biometry of the facial structure of interest.

In our study, the success rate in obtaining an acceptable measurement was always more than 90 percent. Reproducibility was acceptable for all measurements. However, with advancing gestational age the fetus is more often in cephalic position with the chin on the chest. Also, in the presence of a relatively reduced amount of amniotic fluid, the limbs or umbilical

* Syndromes/sequences are identified at p 179-180.

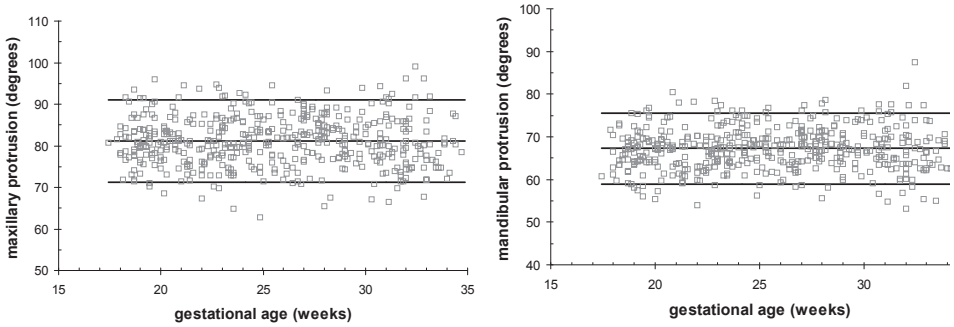


**Figure 4.** Maxillary (a) and mandibular (b) protrusion relative to gestational age. Lines represent fitted mean values with 5th and 95th percentiles.

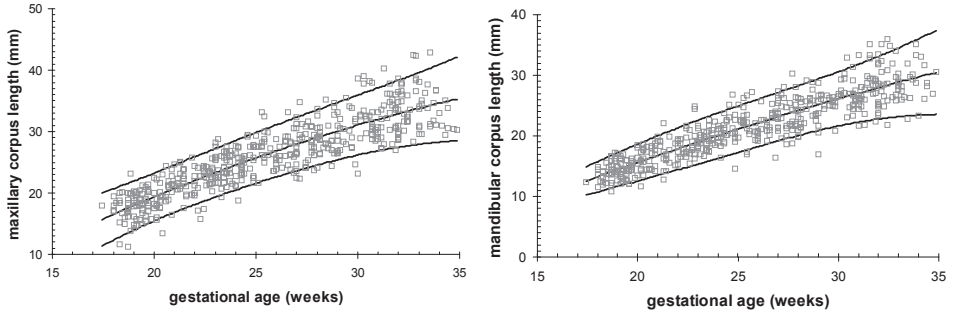


**Figure 5.** Maxillary (a) and mandibular (b) corpus length relative to gestational age. Lines represent fitted mean values with 5th and 95th percentiles.

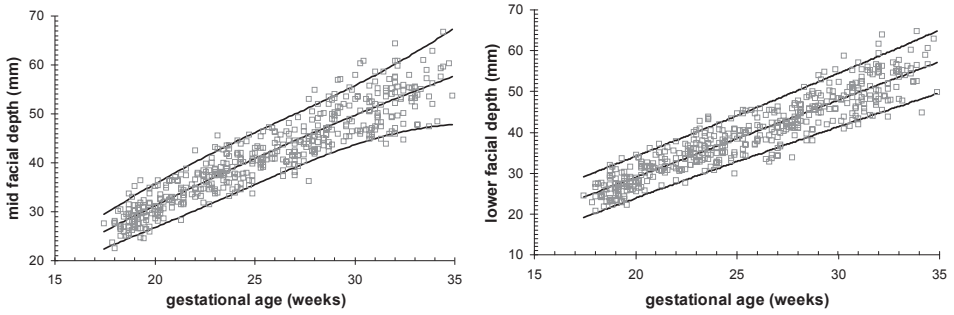


**Figure 6.** Mid- (a) and lower (b) facial depth relative to gestational age. Lines represent fitted mean values with 5th and 95th percentiles. Figure 6. Mid- (a) and lower (b) facial depth relative to gestational age. Lines represent fitted mean values with 5th and 95th percentiles.

cord are more often situated in front of the chin. This can complicate measurement of the mandible, especially the visibility of the gonion.

We used sagittal and coronal scan modes to view the fetal jaws. These two scan modes perform equally well in the transverse plane. However, there is a clearly limited lateral resolution

**Table 2.** Regression equations (mean) and SD around the curves of the fetal maxillary and mandibular measurements relative to adjusted gestational age*

| Measurement | Constant (95% CI) | A (95% CI) | B (95% CI) | SD |
|---|---|---|---|---|
| Maxillary protrusion (°) | 81.08 (80.34 to 81.82) | - | - | 6.02# |
| Mandibular protrusion (°) | 67.25 (66.65 to 67.86) | - | - | 5.09# |
| Maxillary corpus length (mm) | 19.33 (18.94 to 19.72) | 1.373 (1.229 to 1.517) | -0.0206 (-0.0323 to -0.0088) | $\sqrt{}$ (5.62-0.17x+0.118$x^2$-0.012$x^3$+0.0006$x^4$) |
| Mandibular corpus length (mm) | 15.58 (15.30 to 15.86) | 1.154 (1.041 to 1.266) | -0.0102 (-0.0205 to 0.0001) | $\sqrt{}$ (3.42+0.570x-0.014$x^2$-0.0061$x^3$+0.00057$x^4$) |
| Mid-facial depth (mm) | 31.22 (30.82 to 31.63) | 2.011 (1.851 to 2.171) | -0.0163 (-0.0315 to -0.0011) | $\sqrt{}$ (7.37+1.01x-0.060$x^2$-0.0090$x^3$+0.00122$x^4$) |
| Lower facial depth (mm) | 28.97 (28.51 to 29.44) | 1.886 (1.816 to 1.957) | - | $\sqrt{}$ (9.73+0.22x+0.040$x^2$) |
| Maxillary curvature (mm) | 86.46 (85.17 to 87.75) | 5.93 (5.49 to 6.37) | -0.039 (-0.077 to -0.002) | $\sqrt{}$ (66.5+3.5x-0.25$x^2$+0.002$x^3$+0.0011$x^4$) |
| Mandibular curvature (mm) | 80.96 (79.88 to 82.04) | 5.470 (5.295 to 5.644) | - | $\sqrt{}$ (55.79+2.58x+0.221$x^2$) |

*y =constant + Ax or y =Constant + Ax +B$x^2$, where A is the coefficient fro the linear component, B is the coefficient for the quadratic component and x denotes gestational age minus 20 (weeks) in order to center the data with respect to the time axis.

# no relation with gestational age

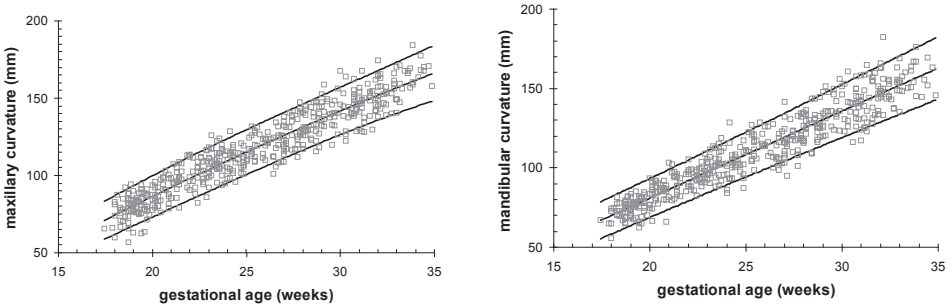


**Figure 7.** Maxillary (a) and mandibular (b) curvature relative to gestational age. Lines represent fitted mean values with 5th and 95th percentiles.

in the transverse image of both the sagittal and coronal scans. This affects in particular the structures further away from the probe. In the sagittal scan (with the fetal nose facing the transducer) the back of the head is more blurred and appears broader than does the frontal part, while in the coronal scan, with one side of the fetal head facing the transducer, the op-

**Table 3.** Regression equations (mean) and standard error of the mean of the fetal maxillary/ mandibular ratios relative to adjusted gestational age*

| Measurement | Constant (95% CI) | A (95% CI) | Standard error of the mean |
|---|---|---|---|
| Maxillary/mandibular protrusion | 1.22 (1.21 to 1.22) | -0.0016 (-0.0025 to -0.0006) | $\sqrt{(1.7\ 10^{-5}-2.8\ 10^{-6}x+2.4\ 10^{-7}\ x^2)}$ |
| Maxillary/mandibular corpus length | 0.09 (0.09 to 0.10)† | -0.0019 (-0.0030 to -0.0007)† | $\sqrt{(2.1\ 10^{-5}-4.0\ 10^{-6}x+3.5\ 10^{-7}\ x^2)}$† |
| Mid-facial/lower facial depth | 1.08 (1.07 to 1.09) | -0.0039 (-0.0052 to -0.0027) | $\sqrt{(1.9\ 10^{-5}-3.8\ 10^{-6}x+4.0\ 10^{-7}\ x^2)}$ |
| Maxillary/mandibular curvature | 1.07 (1.06 to 1.08) | -0.0021 (-0.0036 to -0.0004 ) | $\sqrt{(3.9\ 10^{-5}-8.2\ 10^{-6}x+6.3\ 10^{-7}\ x^2)}$ |

*y =constant + Ax, where A is the coefficient for the linear component, and x denotes gestational age minus 20 (weeks) in order to center the data with respect to the time axis.† median data are for $^{10}$log (MXCL/MNCL) values because this transformation was required to obtain a normal distribution

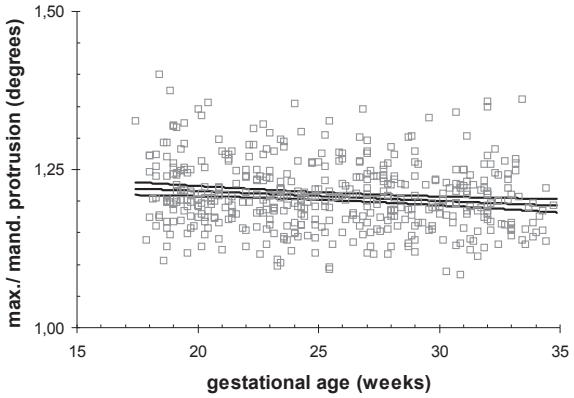


**Figure 8.** Maxillary (max.)/ mandibular (mand.) protrusion ratio relative to gestational age. Lines represent fitted mean values with 95% confidence limits.

posite side is similarly affected. However, the landmarks in the frontal part, as used in this study, can be well visualized and are much less liable to these artifacts.

All non-angular measurements displayed a 2- 2.5 fold increase during the second half of pregnancy. In the 2D ultrasound method of Otto and Platt[9] and Chitty et al[10], the authors measured one ramus of the mandible in a plane that was more coronal than was ours. More comparable 2D ultrasound measurements of the fetal mandible were performed by Watson and Katz[11], who measured the inner length of the mandible without the bony ridge. They found interobserver measurement differences of 10% or less. However, intraobserver variability was not determined.

Paladini et al[12] established good intraobserver variability with a 2D ultrasound method of measuring the mandible corpus length that was equalivalent to our 3D ultrasound method.

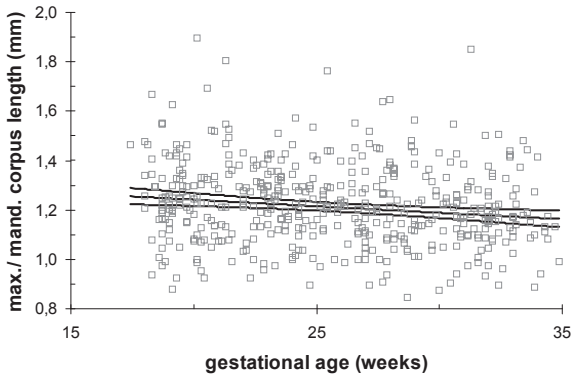


**Figure 9.** Maxillary (max.)/ mandibular (mand.) corpus length ratio relative to gestational age. Lines represent fitted median values with 95% confidence limits.

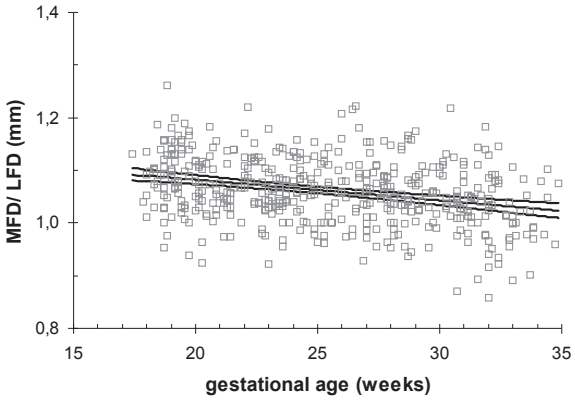


**Figure 10.** Mid-/ lower facial depth ratio relative to gestational age. Lines represent fitted mean values with 95% confidence limits.

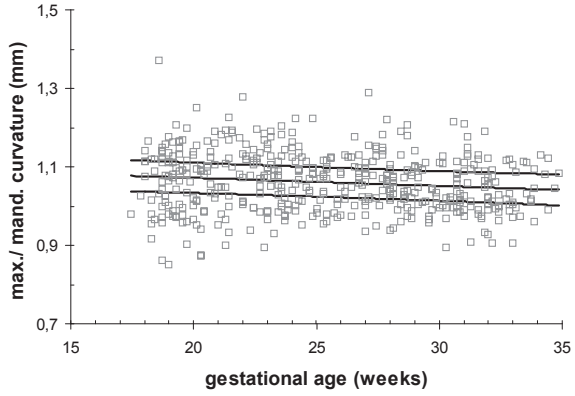


**Figure 11.** Maxillary (max.)/ mandibular (mand.) curvature ratio relative to gestational age. Lines represent fitted mean values with 95% confidence limits.

They found regular lateral growth of the mandible in micrognathia, with growth being impaired primarily in the anteroposterior direction. Although their 2D ultrasound method of measurement of the mandibular corpus length seems to be similar to our 3D ultrasound method, their measurements from normal subjects were smaller than were ours. This could be explained by a slightly different scanning plane.

3D studies on the fetal maxilla and mandible have been performed by Rotten et al[13] and Tsai et al[14]. Both studies concentrated on measurement of maxillary and/ or mandibular width. In line with the finding of Paladini et al[12], the use of these measurements for diagnosing micrognathia can be questioned. Rotten et al[13] also described the application of an inferior facial angle in fetuses with mandibular anomalies. As one arm of this angle is a line orthogonal to the vertical part of the forehead (the other being a line through the tip of the mentum and the anterior border of the more protrusive lip), this measurement would not be useful in fetuses with other facial dysmorphologies, such as frontal bossing. The reference line (the line between nasion and sella turcica) used for our measurement of maxillary and mandibular protrusion is not easily influenced by other facial malformations and would be more valuable in fetuses with multiple (craniofacial) abnormalities.

From postmortem studies it is known that between 10 and18 weeks of gestation the lower jaw recedes relative to the upper jaw. After this period, the lower jaw grows forward again, but does not catch up before birth[21]. In our study this relatively faster growth of the mandible was reflected in a significant decrease of all four ratios when related to gestational age (Figure 8-11). The decrease is most distinct in the mid- to lower facial depth ratio.

It can be concluded that maxillary and mandibular growth can be assessed in various ways. In this study we have described four different methods using 3D ultrasound. Success rate and intraobserver variability were comparable between methods, except for measurement of mandibular corpus length. Forward growth of the mandible is best expressed by the mid- to lower facial depth ratio. These two measurements of maxillary and mandibular growth may be the most valuable ones in determining mandible anomalies. Diagnostic accuracy needs to be determined in future research.



## References


1. Pilu G, Reece EA, Romero R, Bovicelli L, Hobbins JC. Prenatal diagnosis of craniofacial malformations with ultrasonography. *Am J Obstet Gynecol* 1986; 155: 45-50.
2. Hafner E, Sterniste W, Scholler J, Schuchter K, Philipp K. Prenatal diagnosis of facial malformations. *Prenat Diagn* 1997; 17: 51-58.
3. Clementi M, Tenconi R, Bianchi F, Stoll C. Evaluation of prenatal diagnosis of cleft lip with or without cleft palate and cleft palate by ultrasound: experience from 20 European registries. EUROSCAN study group. *Prenat Diagn* 2000; 20: 870-875.
4. Cash C, Set P, Coleman N. The accuracy of antenatal ultrasound in the detection of facial clefts in a low-risk screening population. *Ultrasound Obstet Gynecol* 2001; 18: 432-436.

5. Turner GM, Twining P. The Facial Profile in the Diagnosis of Fetal Abnormalities. *Clin Radiol* 1993; 47: 389-395.
6. Wong GB, Mulliken JB, Benacerraf BR. Prenatal sonographic diagnosis of major craniofacial anomalies. *Plast Reconstr Surg* 2001; 108: 1316-1333.
7. Nicolaides KH, Salvesen DR, Snijders RJ, Gosden CM. Fetal facial defects: associated malformations and chromosomal abnormalities. *Fetal Diagn Ther* 1993; 8: 1-9.
8. Jones KL. Smith's Recognizable Patterns of Human Malformation. W.B. Saunders Company: Philadelphia, 1997.
9. Otto C, Platt LD. The Fetal Mandible Measurement - An Objective Determination of Fetal Jaw Size. *Ultrasound Obstet Gynecol* 1991; 1: 12-17.
10. Chitty LS, Campbell S, Altman DG. Measurement of the fetal mandible--feasibility and construction of a centile chart. *Prenat Diagn* 1993; 13: 749-756.
11. Watson WJ, Katz VL. Sonographic Measurement of the Fetal Mandible - Standards for Normal-Pregnancy. *Am J Perinatol* 1993; 10: 226-228.
12. Paladini D, Morra T, Teodoro A, Lamberti A, Tremolaterra F, Martinelli P. Objective diagnosis of micrognathia in the fetus: the jaw index. *Obstet Gynecol* 1999; 93: 382-386.
13. Rotten D, Levaillant JM, Martinez H, Ducou le Pointe H, Vicaut E. The fetal mandible: a 2D and 3D sonographic approach to the diagnosis of retrognathia and micrognathia. *Ultrasound Obstet Gynecol* 2002; 19: 122-130.
14. Tsai MY, Lan KC, Ou CY, Chen JH, Chang SY, Hsu TY. Assessment of the facial features and chin development of fetuses with use of serial three-dimensional sonography and the mandibular size monogram in a Chinese population. *Am J Obstet Gynecol* 2004; 190: 541-546.
15. Kloosterman G. On intrauterine growth. *Int J Obstet Gynaecol* 1970; 8: 895-912.
16. Ward RE, Jamison PL, Farkas LG. Craniofacial variability index: a simple measure of normal and abnormal variation in the head and face. *Am J Med Genet* 1998; 80: 232-240.
17. Allanson JE, O'Hara P, Farkas LG, Nair RC. Anthropometric craniofacial pattern profiles in Down syndrome. *Am J Med Genet* 1993; 47: 748-752.
18. Garn SM, Smith BH, Lavelle M. Applications of pattern profile analysis to malformations of the head and face. *Radiology* 1984; 150: 683-690.
19. Gorlin RJ, Cohen MM, Levin IS. Cranial measurements (Appendix). In *Syndromes of the Head and Neck*., Gorlin RJ, Cohen MM, Levin IS. Oxford University Press, 1990; 921-939.
20. Littel RC, Milliken GA, Stroub WW, Wolfinger RD. Random coefficients models. In *SAS system for mixed models*, Littel RC, Milliken GA, Stroub WW, Wolfinger RD. SAS Institute Inc.: Cary, NC, 1996; 253-266.
21. Trenouth MJ. Changes in the jaw relationships during human foetal cranio-facial growth. *Br J Orthod* 1985; 12: 33-39.

## 3.5 COMPARISON OF PRENATAL AND POSTNATAL DEVELOPMENT

During the second half of gestation the most distinct growth is seen in head width, especially width of the face, i.e. bizygomatic breadth and nasal width. Less growth is accomplished in depth and height of the head (Table I). This is in contrast to the findings of Escobar et al.[1] These authors found the most active growth axes to be the sagittal and vertical planes or depth and height. However, their study was not longitudinal and they performed ultrasound measurements only at 16, 26 and 36 weeks of gestation.

Different authors hypothesised both prenatal and postnatal craniofacial growth to follow a trend characterised by progressive enlargement of a relatively stable profile.[2] However, this contradicts the clear findings of definite changes in shape, described by for instance Trenouth.[3] Stricker et al describe the growth of the skull to be a continuous development, directed by a single activator, the 'brain'. The sutures being a quasi-exclusive mechanism. However, growth of the face is multifactorial, with successive mechanisms such as synchondroses, sutures and apposition-resorption. The authors describe craniofacial growth to be a continuous phenomenon, taking place with varying speed in separate locations. The adult size at each location is reached at different ages.[4]



### 3.5.1. Height of the head and face

At 6-18 weeks Trenouth found growth of the skull to predominate over growth of the face.[3] However, in the second half of gestation the face starts to grow faster than the skull, which continues after birth (Table II). In adults, skull height is known to be about 50% of the total facial height.[5]

In line of the above we expected to find an increase in the total facial height/ head circumference-ratio. However, a slight decrease was found (Figure 7; sub-Chapter 3.1). Apparently the brain (and skull) still grows strongly during the second half of gestation at a slightly higher rate than facial height.

At 6-22 weeks the maxilla enlarges and moves forward, increasing the lower facial height in relative terms.[3,6] This tendency was not found in the second half of gestation, where a progressive growth of both upper and lower facial depth are found (Table II, Figure 3 in sub-Chapter 3.1). In childhood the upper facial height (or nose height) shows a stronger growth than the lower facial height, resulting in a increase of the upper/ lower facial height-ratio during the period of 6 to 18 years of life (Table II).[7]

### 3.5.2. Facial width

The bizygomatic breadth (or cheek-cheek diameter) relates strongly to the amount of subcuteous adipose tissue in the fetus.[8] The amount of subcuteous adipose tissue increases in the late third trimester fetus, explaining the steeper increase in facial width and decrease in facial index (Table II; Figure 4 and 5 in sub-Chapter 3.1). After birth a powerful increase in

facial height relative to facial width is seen, which continues less strongly after the age of 6 (Table II).[7]

During the second half of gestation the nasal index increases strongly, representing more growth in the width than in height of the nose (Table II; Figure 6 in sub-Chapter 3.1). However, after birth the opposite is visible and a strong decline in nasal index is found between birth and the 5th year of age, further developing between the 6th and 18th year of age (Table II).[7]

The skull base attains adult size at a much earlier state than the skull.[9] This might explain the small decline in the bitragal breadth/ BPD-ratio, representing width of the skull base/ skull width, as found in our study. (Table II; Figure 17 in sub-Chapter 3.1). However, at 6- 18 years the bitragal breadth is found to increase more than the biparietal distance (Table II).[7]

In the embryo the eyes are positioned laterally on the face, and 'move' more medially, by stronger expansion of the lateral regions.[10,11] This trend continues in the fetus as well as after birth resulting in a decline of the IOD/ BPD-, IOD/ OOD- and OOD/ BPD- ratios (Table II; Figure 9-13 in sub-Chapter 3.1).[7] This observation was also made by both Denis and Siebert in a study on second and third trimester fetuses at autopsy.[12,13]

**Table I.** Summary of growth in height, width and length of the face and skull at 18- 34 weeks of gestation.

| Direction of measurement | Measurement | % Increase |
|---|---|---|
| Height of the head and face | Skull height | 86 |
| | Total facial height | 112 |
| | Upper facial height | 116 |
| | Lower facial height | 108 |
| Width of the head and face | Biparietal diameter | 114 |
| | Bitragal breadth | 99 |
| | Outer ocular diameter | 96 |
| | Inter ocular diameter | 72 |
| | Bizygomatic breadth | 132 |
| | Outer palate width | 127 |
| | Bigonial breadth | 109 |
| | Nasal width | 147 |
| Depth of the head and face | Fronto-occipital diameter | 117 |
| | Anterior skull base length | 92 |
| | Posterior cranial fossa length | 128 |
| | Palatal length | 90 |
| | Sella-nasion | 88 |
| | Upper facial depth | 106 |
| | Mid facial depth | 107 |
| | Lower facial depth | 120 |

### 3.5.3. Facial depth

Cephalic index varies little during the second half of gestation. Both width and depth of the skull grow relatively proportionally (Table II; Figure 8 in sub-Chapter 3.1). This trend continues into childhood (Table II).[7]

In the second half of gestation the mandible shows more forward growth than the maxilla, resulting in a decline of both mid/ lower facial depth-ratio and maxillary/ mandibular curvature- ratio (Table II, Figure 10 and 11 in sub-Chapter 3.4). In spite of this forward growth, the mandible is still relatively small compared to the maxilla at birth. More growth is established during childhood (Table II).

**Table II.** Comparison of pre- and postnatal measurement ratios at 18th to 34th week of gestation, 0th to 5th year and 6th to 18th year. Values represent mean values x 100 and percentage increase.

| Index | Mean value at 18w | Mean value at 34w | % in/de-crease | Mean value at 0y# | Mean value at 5y# | % in/de-crease | Mean value at 6y# | Mean value at 18y# | % in/de-crease |
|---|---|---|---|---|---|---|---|---|---|
| Skull height/ total facial height | 113 | 100 | - 12 | - | - | - | 108 | 99 | - 8 |
| Upper/ lower facial height | 60 | 60 | 0 | - | - | - | 66 | 75 | + 12 |
| Facial index | 95 | 86 | - 9 | 70 | 83 | + 19 | 85 | 87 | + 3 |
| Nasal index | 97† | 108† | + 11 | 90 | 74 | -18 | 71 | 65 | - 9 |
| Bitragal breadth/ BPD | 102† | 97† | - 5 | - | - | - | 88 | 95 | + 8 |
| IOD/OOD (intercanthal index)* | 45 | 41 | - 9 | 37 | 39 | - 4 | 38 | 37 | - 4 |
| Cephalic index | 81 | 80 | - 0.5 | 79 | 77 | - 2 | 77 | 78 | + 2 |
| Mid/ lower facial depth | 109 | 103 | - 6 | - | - | - | 95 | 91 | - 4 |
| Maxillary/ mandibular curvature | 108 | 104 | - 4 | - | - | - | 98 | 93 | - 5 |

Facial index: total facial height/ bizygomatic breadth; BPD: biparietal distance; IOD: inter ocular distance; OOD: outer ocular distance; cephalic index: biparietal distance/ fronto-occipital distance; nasal index: nasal width/ upper facial width
#From Farkas et al; mean values of both males and females together.[7]
*Farkas et al: intercanthal index: inter canthal distance/ outer canthal distance. Inter and outer canthal distances (soft tissue measurements) do not equal inter and ocular distances (bony measurements), however the indexes are comparable and give an impression of the changes in the relation of outer and inner borders of the eye.[14]
†Median data for $^{10}$log (bitragal breadth/ BPD) and $^{10}$log (MXCL/MNCL) values. This transformation was required to obtain a normal distribution

## 3.5.4. References


1. Escobar LF, Bixler D, Padilla LM, Weaver DD, Williams CJ. A morphometric analysis of the fetal craniofacies by ultrasound: fetal cephalometry. *J Craniofac Genet Dev Biol* 1990; **10**: 19-27.
2. Burdi AR. Cephhalometric growth analyses of the human upper face region during the last two trimesters of gestation. *Am J Anat* 1969; **125**: 113-122.
3. Trenouth MJ. Shape changes during human fetal craniofacial growth. *J Anat* 1984; **139**: 639-651.
4. Stricker M, Raphael B, van der Meulen J, Mazzola R. Craniofacial development and growth. In *Craniofacial Malformations*, Stricker M, Raphael B, van der Meulen J, Mazzola R. Churchill Livingstone: Edinburgh, 1990; 61-98.
5. Flood J, Byrd HS. Craniofacial anomalies I. *Selected Readings in Plastic Surgery* 1998; **8**: 1-42.
6. Eriksen E, Bachpetersen S, Solow B, Kjaer I. Midsagittal Dimensions of the Prenatal Human Cranium. *J Craniofac Genet Dev Biol* 1995; **15**: 44-50.
7. Farkas LG, Munro IR. Anthropometric facial proportions in medicine. Charles C Thomas Publisher: Springfield Illinois USA, 1987.
8. Abramowicz JS, Sherer DM, Bartov E, Woods JR. The Cheek-To-Cheek Diameter in the Ultrasonographic Assessment of Fetal Growth. *Am J Obstet Gynecol* 1991; **165**: 846-852.
9. Lieberman DE, Ross CF, Ravosa MJ. The primate cranial base: ontogeny, function, and integration. *Am J Phys Anthropol* 2000; **Suppl**: 117-169.
10. Vermeij-Keers C. Craniofacial embryology and morphogenesis: normal and abnormal. In *Craniofacial malformations*, Stricker M, Raphael B, van der Meulen J, Mazzola R. Churchill Livingstone: Edinburgh, 1990; 27-60.
11. Moore KL. The Developing Human. WB Saunders co: Philadelphia, London, Toronto, 1977.
12. Siebert JR. Prenatal growth of the median face. *Am J Med Genet* 1986; **25**: 369-379.
13. Denis D, Burguiere O, Burillon C. A biometric study of the eye, orbit, and face in 205 normal human fetuses. *Invest Ophthalmol Vis Sci* 1998; **39**: 2232-2238.
14. Allanson JE, O'Hara P, Farkas LG, Nair RC. Anthropometric craniofacial pattern profiles in Down syndrome. *Am J Med Genet* 1993; **47**: 748-752.

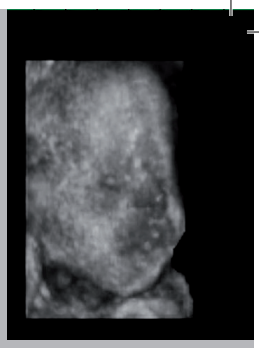

Chapter 4

# Craniofacial Variability Index

## INTRODUCTORY REMARKS

With the introduction of three-dimensional ultrasound in prenatal diagnosis many reports have appeared on the subjective visualisation of (minor) fetal craniofacial malformations. However, rarely more objective approaches to the prenatal diagnosis of fetal craniofacial anomalies appeared. Multivariate analysis (craniofacial pattern profile analysis) in combination with three-dimensional ultrasound offer an objective method for a thorough evaluation of the fetal head and face.

Sub-Chapter 4.1 describes the introduction of craniofacial pattern profile analysis and the Craniofacial Variability Index with three-dimensional ultrasound as a new method to obtain insight into fetal craniofacial development. In sub-Chapter 4.2 these tools were evaluated in a group of fetuses with isolated and syndromal cleft lip/ palate.

## 4.1 CRANIOFACIAL VARIABILITY INDEX IN UTERO; A THREE-DIMENSIONAL ULTRASOUND STUDY.

N.M. Roelfsema[a], W.C.J. Hop[b], L.N.A. van Adrichem[c], J.W. Wladimiroff[a]
[a]Department of Obstetrics and Gynecology, [b]Department of Epidemiology and Biostatistics, [c]Department of Plastic and Reconstructive Surgery, Erasmus MC, University Medical Centre Rotterdam, The Netherlands

Published in the Ultrasound in Obstetrics and Gynecology 2007, 29, 258-264

### Abstract

**Objective:** This study was undertaken to develop a craniofacial pattern profile analysis by Three-dimensional (3D) ultrasound and to introduce a craniofacial variability index (CVI) which can assist in the evaluation of fetal facial anatomy.

**Mehods:** Serial 3D sonographic measurements of 16 different fetal craniofacial parameters were performed at 18- 34 weeks of gestation in 126 normal singleton pregnancies. In another 6 pregnancies complicated by fetal abnormality a single 3D recording was obtained. The 16 measurements cover various aspects of the facial anatomy such as width, depth and height. For each parameter, regression analysis was performed to calculate gestational age-specific Z-scores and normal limits for the CVI (the latter quantifies the variability between the 16 Z-scores).

**Results:** The 95$^{th}$ percentile of normal CVI data increased from 1.08 at 18 weeks to 1.27 at 34 weeks of gestation. The CVI was situated above the 95$^{th}$ percentile in three out of six fetuses with abnormalities. In abnormal subjects, two to eight out of 16 parameters showed abnormal values.

**Conclusion:** Craniofacial pattern profile analysis and the CVI may aid in the evaluation of fetal facial anatomy. They could be a valuable tool in syndrome delineation and for distinguishing between normal and abnormal craniofacial development.

## Introduction

Craniofacial dysmorphology is the keystone to syndrome delineation. Although several authors have attempted to improve prenatal diagnosis of craniofacial malformations by describing normal craniofacial anatomy and centile charts, minor abnormalities can still be difficult to determine by conventional (2D) ultrasound.

Multivariate analysis of different anthropometric (soft-tissue landmarks) or cephalometric (radiographicly derived or bony landmarks) measurements allows craniofacial pattern profile analysis. With this method measurements are translated into Z-scores to allow evaluation of the relationship of different parts of the craniofacial area and follow-up of development in time. Samples of individuals can be compared to the normal population and expressed in Z-scores to illustrate the deviation of 'normality'.[1] Escobar et al (1988, 1990) employed this method for ultrasound-derived cephalometric measurements.[2,3] The authors found that pattern profile analysis may have an additional value in the diagnosis of fetuses with mild abnormalities or abnormality patterns.[4]

The 3-dimensional (3D) ultrasound technique offers potential advantages over 2D ultrasound, especially in the evaluation of complex anatomy, such as the fetal head and face.[5,6] If the advantages of 3D ultrasound and objective assessment and evaluation of craniofacial biometry with pattern profile analysis were to be combined, this could aid in the evaluation of normal and abnormal craniofacial development.

The objectives of this study were therefore as follows: (i) to develop a 3D sonographic method of establishing fetal craniofacial biometry, (ii) to obtain reproducibility and normal growth data relative to gestational age for these measurements, (iii) to conduct craniofacial pattern profile analysis and develop a craniofacial variability index to assist in the evaluation of fetal facial anatomy.



## Patients and methods

*Study design*

In a longitudinal study, a total of 126 women with a normal singleton pregnancy consented to participate, following approval by the Regional Ethics Review Board (both study and informed consent). Another six women with a fetal abnormality known or suspected to affect craniofacial anatomy consented to participate for a single 3D ultrasound examination. Pregnancy duration was determined from the last reliable menstrual period or, in case of uncertainty, adjusted by ultrasound in the first trimester of gestation.

Women with a normal pregnancy were recruited from the antenatal outpatients' and regional midwifery services. Only women without maternal disease known to affect fetal growth, i.e. pre-existent hypertension, diabetes mellitus and pregnancies that were not at risk for craniofacial abnormality were included in the study. All were singleton pregnancies resulting in the term delivery of an infant without congenital anomalies. Pregnancy duration

varied between 18 and 34 weeks (median 26 weeks). Maternal age was 19- 40 years (median 30 years). 95% of the birth weights were situated between the 5th and the 95th percentile, adjusted for maternal parity and fetal sex, according to the Kloosterman Tables.[7]

3D sonographic examinations were performed four times at 3- 5 week intervals. The third or last examination could not be performed in five pregnancies and five records were not, or only partly, available for analysis, resulting in a total of 494 complete recordings.

Pregnancy duration in the six women with a fetal abnormality varied between 22 and 32 weeks (median 27 weeks). Maternal age was 27- 40 years (median 30 years). 3D ultrasound examinations were performed only once after a fetal abnormality was suspected on a detailed two-dimensional (2D) ultrasound scan.

Intraobserver variability was determined in 22 normal singleton pregnancies, six of which were also included in the serial study. Pregnancy duration in these 22 was similar in distribution to that of the participants in the serial study.

*Recording technique*

Three-dimensional sonographic examination of the fetal head and face was performed using a standard Voluson 530 D (Kretztechnik AG, Zipf, Austria) with a 3- to 5-MHz transducer (VAW 3-5). The region of interest was defined, containing the complete fetal head. Three different types of acquisition of the fetal face and head were made. A sagittal scan (frontal view of the face composed of sagittal planes); a coronal scan (side of the head composed of coronal planes); and a transverse scan (side of the head composed of transverse planes). Acquisition of the sagittal scan of the face started at the mid-sagittal plane with the fetus facing the transducer. A coronal scan was made, starting acquisition just in front of the ear. A transverse scan was made by using the regular plane for measurement of the biparietal diameter[8] to start the acquisition. Multiple volume recordings were made of each fetus (range 2-11, median 5) to obtain one good volume for every type of acquisition. The best volume data were then collected on a transportable magnetic disk for later analysis (Iomega Jaz).

Sixteen craniofacial measurements, proven useful in the assessment of postnatal (ab)normal craniofacial development, were extracted from literature on anthropometric and cephalometric measurements (Table I).[2,9-14] Measurements were made using the 3D view program (Kretztechnik AG, version 4.0) on a personal computer with an Iomega Jaz Drive. This took 10- 15 minutes. Measurement methodology is displayed in Table I and Figures 1 to 6. One observer (NR) performed all 3D ultrasound examinations and measurements.

The reproducibility study consisted of recording two volume data sets from the same fetus at a time interval of approximately 20 minutes. The first recorded data set was analyzed twice with a minimal time interval of one week. This second analysis was done while being blinded for the first analysis.

**Table I.** Measurements methodology by direction: landmarks (soft-tissue, unless otherwise mentioned), three-dimensional volume mode by which the measurements were assessed and measurement plane (See also Figures 1- 6).

| Direction | Measurement | Landmarks | Scan mode | Plane |
|---|---|---|---|---|
| Facial width | BPD | Maximal diameter of the skull (outer bony borders)* | Transverse | Transverse |
| | BITRB | Tragus to midline, multiplied by 2* | Coronal | Transverse |
| | BIZYB | Left- right zygoma | Sagittal | Coronal |
| | BIGOB | Left- right gonion (bony border) | Sagittal | Transverse |
| | NASW | Outer borders of the alae nasi | Sagittal | Coronal |
| | IOD | Inner bony borders of the orbits | Transverse | Transverse |
| | OOD | Outer bony borders of the orbits | Transverse | Transverse |
| Facial depth | FOD | Maximal diameter frontal- posterior skull border (outer bony borders)† | Transverse | Transverse |
| | UFD | Tragus- nasion† | Coronal | Transverse |
| | MFD | Tragus- anterior rim of the maxilla† | Coronal | Transverse |
| | LFD | Tragus- gnathion† | Coronal | Transverse |
| | ASBL | Glabella- sella turcica (bony borders) | Sagittal | Sagittal |
| | PCFL | Sella turcica- opisthion (bony borders) | Sagittal | Sagittal |
| Facial height | SH | Vertex-nasion‡ | Sagittal | Sagittal |
| | UFH | Nasion- subnasion‡ | Sagittal | Sagittal |
| | LFH | Subnasion- gnathion‡ | Sagittal | Sagittal |

BPD: biparietal distance; BITRB : bitragal breadth; BIZYB: bizygomatic breadth; BIGOB: bigonial breadth; NASW: nasal width; IOD: inter ocular distance; OOD: outer ocular distance; FOD: fronto-occipital distance; UFD: upper facial depth; MFD: mid facial depth; LFD: lower facial depth; ASBL: anterior skull base length; PCFL: posterior cranial fossa length; SH: skull height; UFH: upper facial heigth; LFH: lower facial heigth.

* measure perpendicular to the midline (which should be parallel to the horizontal axis).

†measure parallel to the midline (which should be parallel to the horizontal axis)

‡ measure perpendicular to the horizontal axis, which is formed by a line connecting the middle of the anterior rim of the maxilla and the 'opisthion'

*Statistical analysis*

Statistical analysis was performed on a personal computer with the SPSS version 10.1 (SPSS Corp, Chicago, Ill). Analysis of the reproducibility study consisted of nested analysis of variance to separate the within-subject variation in components for differences between repeated tests within subjects and differences between repeated analyses of the same recorded volume.

For all 16 craniofacial measurements in the normal subjects, the relationship of the measurement versus gestational age was analyzed by means of analysis for repeated measurements (random coefficients model) using the SAS PROC MIXED statistical program version 6.2 (SAS Institute, Cary, NC). This procedure is a powerful method to analyze longitudinal data[15]. Data were centered by using the halfway point of gestational age (GA) (20 weeks), and calculations were done using x=GA- 20 as the time axis. In most cases a quadratic term was required to obtain a good fit. The resulting gestational age related fitted mean and standard deviation

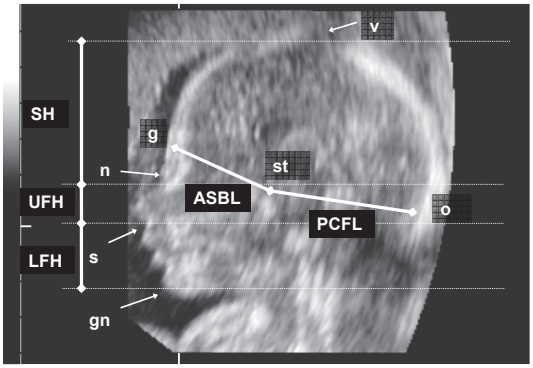


**Figure 1.** Measurement of skull height (SH), upper facial height (UFH), lower facial height (LFH), anterior skull base length (ASBL) and posterior cranial fossa length (PCFL) by 3D ultrasound. (Landmarks: v= vertex, the highest point of the head; g= glabella, prominence on the frontal bone above the root of the nose at the level of the superior orbital ridges; n= nasion, the deepest part of the nasal root; s= subnasion, the deepest point of concavity at the base of the nose; gn= gnathion, lowest median landmark on the lower border of the mandible; st= sella turcica, middle of cross formed by sphenoid ridge and the otic cartilage; o= opisthion, lowest posterior point of the skull (inner border))

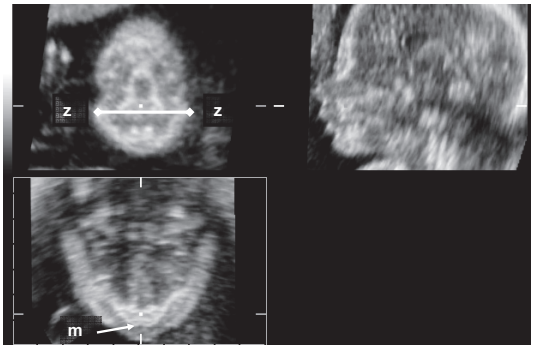


**Figure 2.** Measurement of bizygomatic breadth (BIZYB) by 3D ultrasound. (Landmarks: z= left and right zygoma, the most lateral point of the zygomatic arch). The cursor is placed in the middle of the anterior rim of the maxilla (m).

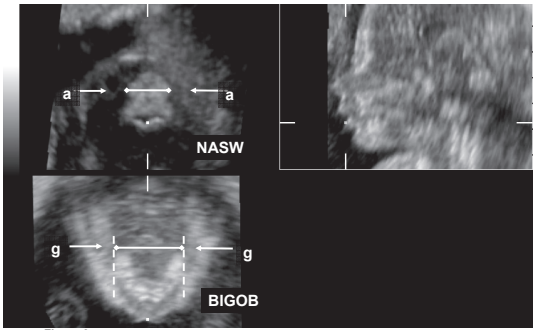


**Figure 3.** Measurement of nasal width (NASW) and bigonial breadth (BIGOB) by 3D ultrasound. (Landmarks: a= left and right alea nasi; g= left and right gonion, the most lateral aspect of the mandible).

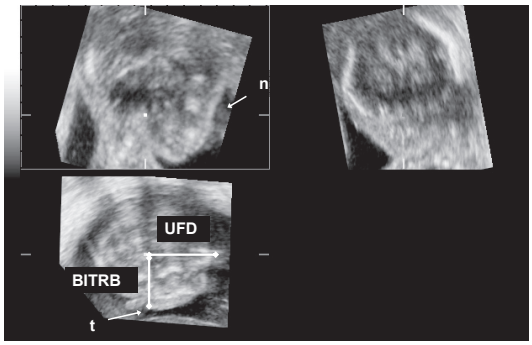


**Figure 4.** Measurement of bitragal breadth (BITRB) and upper facial depth (UFD) by 3D ultrasound. (Landmarks: n= nasion; t= tragus, the middle and most anterior aspect of the ear).

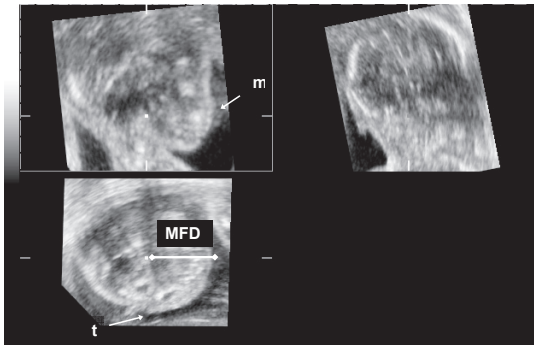


**Figure 5.** Measurement of mid facial depth (MFD) by 3D ultrasound. (Landmarks: m= anterior rim of the maxilla; t= tragus).

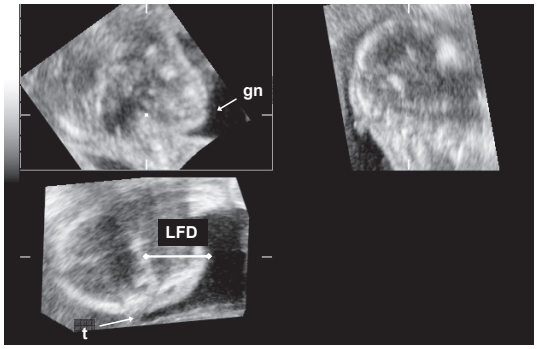


**Figure 6.** Measurement of lower facial depth (LFD) by 3D ultrasound. (Landmarks: gn= gnathion; t= tragus).

**Table II.** Results of reproducibility study and regression analysis of measurements.

| Measurement | CV-I | CV-II | Mean* | Standard Deviation* |
|---|---|---|---|---|
| BPD | 1.5 | 0.6 | $49.49 + 3.446x - 0.0348x^2$ | $\sqrt{(6.99+0.954x-0.0480x^2-0.00646x^3+0.000619x^4)}$ |
| BITRB | 4.2 | 0.3 | $49.98 + 2.754x$ | $\sqrt{(18.24 -0.211x+0.098x^2)}$ |
| BIZYB | 6.0 | 5.7 | $30.27 + 2.145x$ | $\sqrt{(10.61+0.324x+0.0200x^2)}$ |
| BIGOB | 8.6 | 2.8 | $23.16 + 1.392x$ | $\sqrt{(8.42+0.076x+0.0306x^2)}$ |
| NASW | 6.7 | 3.7 | $10.73 + 1.153x -0.0329x^2$ | $\sqrt{(2.38+0.188x-0.0148x^2-0.00088x^3+0.000081x^4)}$ |
| IOD | 4.4 | 2.2 | $13.564+ 0.622x - 0.0057x^2$ | $\sqrt{(1.11+0.146x-0.011x^2-0.0001x^3+0.000064x^4)}$ |
| OOD | 2.4 | 2.1 | $30.82 + 1.932x - 0.0270x^2$ | $\sqrt{(2.72+0.253x-0.0070x^2-0.0018x^3+0.00021x^4)}$ |
| FOD | 2.1 | 0.0 | $62.29 + 4.816x - 0.0818x^2$ | $\sqrt{(10.60+1.29x-0.096x^2-0.0043x^3+0.00094x^4)}$ |
| UFD | 4.5 | 5.6 | $30.63 + 1.938x-0.0142x^2$ | $\sqrt{(7.18+0.49x-0.034x^2+0.0004x^3+0.00035x^4)}$ |
| MFD | 4.1 | 6.6 | $31.22+2.011x-0.0163x^2$ | $\sqrt{(7.37+1.01x-0.060x^2-0.0090x^3+0.00122x^4)}$ |
| LFD | 6.1 | 6.1 | $28.97+1.886x$ | $\sqrt{(9.73+0.22x+0.040x^2)}$ |
| ASBL | 4.9 | 4.6 | $23.28 + 1.552x - 0.0339x^2$ | $\sqrt{(3.61+0.162x+0.025x^2-0.0049x^3+0.00042x^4)}$ |
| PCFL | 3.5 | 5.1 | $34.34 + 2.37x$ | $\sqrt{(7.84+0.30x+0.045x^2)}$ |
| SH | 4.5 | 3.4 | $31.04 + 2.084x - 0.0544x^2$ | $\sqrt{(8.17-0.106x+0.082x^2-0.0030x^3)}$ |
| UFH | 4.8 | 7.9 | $10.62 + 0.916x - 0.0236x^2$ | $\sqrt{(1.83-0.093x+0.052x^2-0.0070x^3+0.00033x^4)}$ |
| LFH | 6.7 | 7.4 | $17.36 + 1.203x - 0.0164x^2$ | $\sqrt{(4.10+0.58x-0.0029x^2-0.0046x^3+0.00030x^4)}$ |

* x denotes gestational age in weeks minus 20.

CV-I: Coefficient of Variation (%) for differences between repeated tests within women; CV-II: Coefficient of Variation (%) for differences between repeated analyses of the same recorded volume; BPD: biparietal distance; BITRB : bitragal breadth; BIZYB: bizygomatic breadth; BIGOB: bigonial breadth; NASW: nasal width; IOD: inter ocular distance; OOD: outer ocular distance; FOD: fronto-occipital distance; UFD: upper facial depth; MFD: mid facial depth; LFD: lower facial depth; ASBL: anterior skull base length; PCFL: posterior cranial fossa length; SH: skull height; UFH: upper facial heigth; LFH: lower facial heigth.

(SD) were used for calculation of individual Z-scores for every measurement at each point in time according to the equation: (measured value – fitted mean value)/SD. A craniofacial pattern profile can be made after calculation of the Z-scores for every measurement. A craniofacial pattern profile is a way of illustrating, classifying and/or comparing Z-scores of different individuals. A Z-score smaller than –2 or greater than +2 is considered abnormal.

The craniofacial variability index (CVI) for each individual at each point in time quantifies the differences between the 16 resulting Z-scores and is defined as the standard deviation of these. To determine normal values relative to gestational age, regression analysis for repeated measurements (random coefficients model) of the calculated CVI-values using SAS PROC MIXED was used again and gestational age-specific reference intervals were calculated according to this model. An index above the 95$^{th}$ percentile was classified as abnormal. Z-scores and the craniofacial variability index were calculated for the abnormal fetuses using the derived equations. A p value of less than 0.05 was considered significant.

## Results

The reproducibility study showed a coefficient of variation of 1.5 to 8.6% for differences between repeated tests within women and 0 to 7.9% for differences between repeated analyses of the same recorded volume (Table II). Means and standard deviations used for calculation of Z-scores and CVI are depicted in Table II.

In the group of normal fetuses the craniofacial variability index (CVI) could be calculated in 349 of 494 (71%) of the cases because the CVI can be determined only in the presence of a complete set of 16 measurements. In pregnancies below 22 weeks this rate was 89%, 22- 26 weeks 82%, 26- 30 weeks 62% and the rate decreased to 47% in pregnancies over 30 weeks of gestation.

CVI data showed a statistically significant linear increase ($p<0.001$) relative to gestational age. Mean CVI (50$^{th}$ percentile) increased from 0.78 at 18 weeks to 0.94 at 34 weeks of gestation (Figure 7). The 95$^{th}$ percentile increased from 1.08 at 18 weeks to 1.27 at 34 weeks of gestation (Figure 7). Figure 8 illustrates the craniofacial pattern variability of the one normally developing fetus with the lowest and the one with the highest craniofacial variability index.

The group of abnormalities known or suspected to affect fetal craniofacial development consisted of cases of holoprosencephaly*, Beckwith-Wiedemann syndrome*, chondrodysplasia punctata*, trisomy 21, Bardet-Biedl syndrome* and Alagille syndrome* (Table III). Follow-

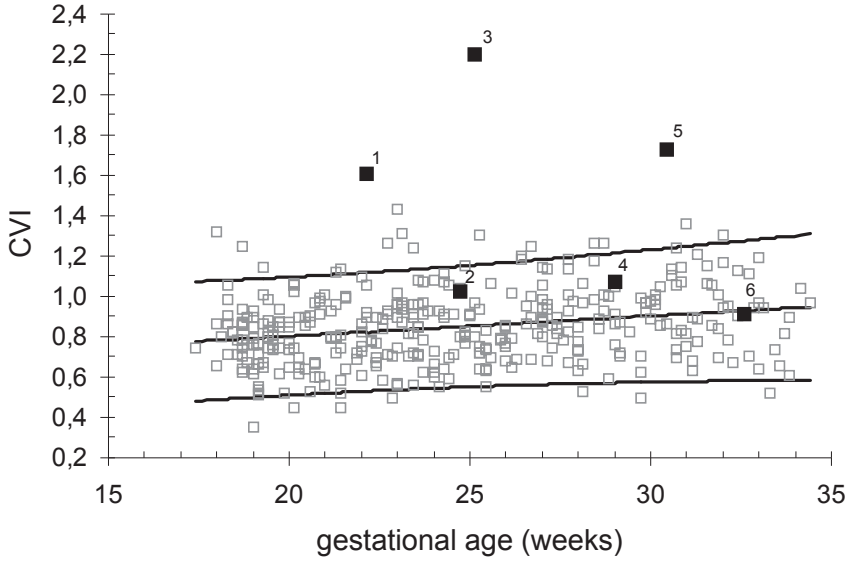


**Figure 7.** Calculated craniofacial variability index according to gestational age in normal (open square) and abnormal fetuses (closed squares; 1 = Chondrodysplasia punctata; 2 = Bardet-Biedl syndrome ; 3 = Holoprosencephaly; 4 = trisomy 21; 5 = Beckwith-Wiedemann syndrome; 6 = Alagille syndrome). Curves represent fitted mean values and the 5$^{th}$ and 95$^{th}$ centiles, calculated from data on normal fetuses.

* Syndromes/sequences are identified at p 179-180.

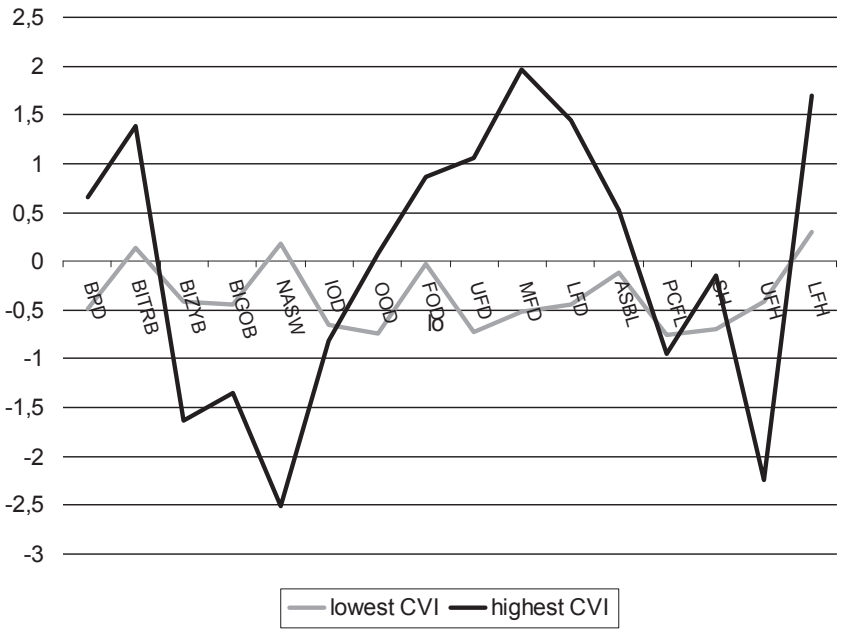


**Figure 8.** Craniofacial pattern variability of the fetus with the lowest and the fetus with the highest craniofacial variability index (CVI) in the group of normal subjects. The abbreviations are identified in Table I.

up was available in all cases and confirmed prenatal findings. Abnormal Z-scores (underlined) were found in all cases. But an abnormal CVI was found in only the first three cases and not in the fetus with Trisomy 21, Bardet-Biedl and Alagille syndrome (Table III). The fetus with holoprosencephaly proved to have the highest CVI (Table III and Figure 7).

The calculation of the CVI is illustrated by the normal fetus with the highest CVI (Figure 8). In this fetus a biparietal diameter (BPD) of 61.5 mm was measured at a gestational age of 23 weeks. The equation for calculation of the Z-score of BPD is: (measured BPD – fitted mean BPD value)/ SD of the BPD values (See Table II for equations). In this case: (61.5- 59.5)/ 3.05= 0.65. The other Z-scores are calculated in the same way. The CVI is calculated by taking the SD out of all 16 Z-scores. In this case: SD (0.65; 1.38; -1.63; -1.35; -2.51; -0.81; 0.07; 0.87; 1.06; 1.96; 1.45; 0.52; -0.95; -0.14; -2.24; 1.70)= 1.43.

## Discussion

Craniofacial involvement is described in over 150 syndromes with clinical implications.[16] Minor involvement or dysmorphism can be difficult to assess in children after birth and often depends upon the clinical impression, which can be misleading.[1] Limited techniques for visualizing the head and face in utero complicate prenatal diagnosis even more. Although three-dimensional ultrasound has improved visibility of the fetal head and face [5,6], discrimination

**Table III.** Craniofacial variability index (CVI) and Z-scores of abnormal fetuses. Abnormal values (CVI: values above 97th percentile; Z-scores: values under –2 or above 2) are underlined.

| | | | Z-scores | | | | | | | | | | | | | | | |
|---|---|---|---|---|---|---|---|---|---|---|---|---|---|---|---|---|---|---|
| | | | Facial width | | | | | | | Facial depth | | | | | | Facial height | | |
| Abnormality | GA | CVI | BPD | BITRB | BIZYB | BIGOB | NASW | IOD | OOD | FOD | UFD | MFD | LFD | ASBL | PCFL | SH | UFH | LFH |
| Holoprosencephaly | $25^{1}$ | 2.20 | -1.97 | -1.79 | 0.09 | -1.33 | -2.64 | -5.55 | -7.16 | -1.43 | -4.18 | -3.30 | -2.38 | -0.21 | -1.83 | 0.26 | 0.00 | 1.01 |
| BWS | $30^{3}$ | 1.73 | -1.15 | 0.36 | 2.08 | 1.93 | 2.77 | 0.05 | 1.5 | -2.09 | 3.46 | 2.40 | 2.43 | -0.21 | -1.11 | -1.79 | 0.75 | 1.85 |
| Chondrodysplasia punctata | $22^{1}$ | 1.61 | 0.00 | 0.40 | 2.06 | -2.62 | -2.52 | -0.83 | 0.71 | 0.58 | -1.62 | -0.51 | -0.85 | \-1.47 | 0.47 | 2.73 | -2.81 | 0.62 |
| Trisomy 21 | $29^{0}$ | 1.07 | -1.83 | -0.60 | -1.82 | -2.23 | -1.35 | -3.80 | -2.47 | -2.92 | -3.25 | -2.80 | -2.37 | -0.56 | -1.12 | -2.16 | -0.03 | -0.74 |
| Bardet-Biedl syndrome | $24^{5}$ | 1.02 | -3.17 | -2.89 | -1.40 | -1.37 | -0.02 | -0.77 | -1.26 | -1.51 | 0.82 | -0.41 | -1.29 | -0.44 | -2.20 | -1.11 | -2.14 | -1.29 |
| Alagille syndrome | $32^{4}$ | .91 | -3.39 | -1.08 | -3.44 | -1.05 | -1.91 | -0.67 | -1.28 | -1.92 | -1.77 | -0.41 | -1.07 | -1.17 | -1.25 | -0.41 | -0.61 | -1.67 |

GA: gestational age in weeks with days in superscript; BPD: biparietal distance; BITRB : bitragal breadth; BIZYB: bizygomatic breadth; BIGOB: bigonial breadth; NASW: nasal width; IOD: inter ocular distance; OOD: outer ocular distance; FOD: fronto-occipital distance; UFD: upper facial depth; MFD: mid facial depth; LFD: lower facial depth; ASBL: anterior skull base length; PCFL: posterior cranial fossa length; SH: skull height; UFH: upper facial heigth; LFH: lower facial heigth; BWS: Beckwith-Wiedemann syndrome.

between normal and abnormal can still be difficult and depends upon skill and experience of the ultrasonographer.

To enable objective assessment of abnormality after birth, different measurement methods have been developed.[1] Anthropometry is a simple, non-invasive method based on surface dimensions, measured with for instance a measuring tape or marking gauge. According to the radiographic cephalometric method, bony landmarks are assessed by X-ray.

For this study we chose different measurements for describing facial width, depth and height from both the anthropometric and cephalometric method, best applicable with 3D ultrasound and based on the craniofacial pattern profile analysis first described by Garn et al.[17] The 3D ultrasound technique allows simultaneous display of the three perpendicular planes in the so-called multiplanar view. This provides exact identification of the biometry planes and the measurement landmarks.

It was not possible to retrieve a complete set of measurements when fetal movement complicated the 3D ultrasound recording. Another limitation was the difficulty in recording the entire fetal head with advancing gestational age as a result of the limited 3D transducer sector size. When the fetus was situated deep in the pelvic region and/ or the fetal face was constantly directed towards the maternal sacrum, it was not possible to perform a sagittal scan. The transverse and coronal scan are often easier to retrieve. Only when the fetus was in cephalic position looking up to the symphysis or down to the sacrum of the mother during the entire examination, was it not possible to obtain the transverse or the coronal scan. This occurred more often in late pregnancy, when the head is situated deep in the pelvis. Structures in front of the fetal face or fetal ear can complicate measurement in the sagittal and coronal scan, respectively. The lower success rates found with advancing gestational age are explained by these limitations.

The craniofacial variability index (CVI) increases only slightly from the 18$^{th}$ to 34$^{th}$ week of gestation. Apparently, the form of the head and face is merely completed and changes little throughout the second half of pregnancy. Also the deviation of the CVI data around the mean shows a minor increase.

When observing the normal fetus with the lowest CVI and that with the highest CVI, the difference in the variability of the Z-scores is obvious (Figure 8). In the interpretation of an individual CVI, it is important to notice that it is the variability of the Z-scores which is indicative for the outcome of the calculation and not the height of the Z-scores. Moreover, when a fetus displays growth retardation with low Z-scores (<2) and a small variation among the measurements, the CVI would still be within the normal range.

Choosing the 95$^{th}$ percentile as the upper limit for 'normality' of the CVI would allow us to delineate three of the six syndromes presented. Trisomy 21, Bardet-Biedl syndrome (characterized by macrocephaly, obesity, retinal pigmentation, polydactyly and renal malformation[18]) and Alagille syndrome (arteriohepatic dysplasia, peripheral pulmonary stenosis and peculiar facies[18]) can display limited dysmorphic symptoms and the CVI will therefore not always be

abnormal. However, the fetus with Trisomy 21 showed 8/16 abnormal Z-scores, the fetus with Bardet-Biedl 4/16 and the fetus with Alagille 2/16. Two or more abnormal Z-scores out of the 16 measurements were found in 13 % of the normal subset at any point in time. Three or more abnormal Z-scores were only found in 4% and would be more indicative of dysmorphology, especially when the fetus has a normal overall growth pattern.

When observing table III the differences in the craniofacial pattern of the Z-scores between the different syndromes is evident. Not surprisingly, the measurements in width (especially in the face) as well as in depth are very small in the fetus with holoprosencephaly (Table II). However, the measurements of facial height are all well within normal limits. The facial width and depth measurements of the fetus that were found to be associated with Beckwith-Wiedemann (characterized by overweight) after birth, were above the normal range (Table II). Chondrodysplasia punctata consists of rhizomelic shortening, vertebral abnormalities and a punctate epiphyseal mineralization.[18] In our case the malformations were very severe and caused a distinctive craniofacial pattern, with extreme flat midfacies, expressed in a small mandible and nose but large bizygomatic breadth, and large skull height but very small upper facial height. (Table III)

Escobar et al (1993) employed Z-scores of 22 craniofacial measurements by 2D ultrasound to describe pattern profile variability in fetal alcohol syndrome*, Crouzon syndrome* and thanatophoric dysplasia*. Although not all fetuses with fetal alcohol syndrome had a variability index in the abnormal range, mid-face measurements in these fetuses were very similar and gave a pattern distinctive for this syndrome.[4]

In conclusion, we have presented a novel method of evaluating fetal facial anatomy by means of 3D ultrasound. Although the number of fetus with abnormalities in our study was small and therefore our conclusions have to be drawn with caution, we believe that craniofacial pattern variability analysis and calculation of the craniofacial variability index could be a valuable tool in syndrome delineation and for distinguishing between normal and abnormal craniofacial development. Three or more abnormal Z-scores may be indicative of dysmorphology in the absence of an intra-uterine growth retardation.



## References

1. Allanson JE. Objective techniques for craniofacial assessment: what are the choices? *Am J Med Genet* 1997; **70**: 1-5.
2. Escobar LF, Bixler D, Padilla LM, Weaver DD. Fetal craniofacial morphometrics: in utero evaluation at 16 weeks' gestation. *Obstet Gynecol* 1988; **72**: 674-679.
3. Escobar LF, Bixler D, Padilla LM, Weaver DD, Williams CJ. A morphometric analysis of the fetal craniofacies by ultrasound: fetal cephalometry. *J Craniofac Genet Dev Biol* 1990; **10**: 19-27.
4. Escobar LF, Bixler D, Padilla LM. Quantitation of craniofacial anomalies in utero: fetal alcohol and Crouzon syndromes and thanatophoric dysplasia. *Am J Med Genet* 1993; **45**: 25-29.

* Syndromes/sequences are identified at p 179-180.

5. Lee A, Deutinger J, Bernaschek G. Three dimensional ultrasound: abnormalities of the fetal face in surface and volume rendering mode. *Br J Obstet Gynaecol* 1995; **102**: 302-306.
6. Pretorius DH, Nelson TR. Fetal face visualization using three-dimensional ultrasonography. *J Ultrasound Med* 1995; **14**: 349-356.
7. Kloosterman G. On intrauterine growth. *Int J Obstet Gynaecol* 1970; **8**: 895-912.
8. Campbell S, Thoms A. Ultrasound measurement of the fetal head to abdomen circumference ratio in the assessment of growth retardation. *Br J Obstet Gynaecol* 1977; **84**: 165-174.
9. Ward RE, Jamison PL, Farkas LG. Craniofacial variability index: a simple measure of normal and abnormal variation in the head and face. *Am J Med Genet* 1998; **80**: 232-240.
10. Allanson JE, O'Hara P, Farkas LG, Nair RC. Anthropometric craniofacial pattern profiles in Down syndrome. *Am J Med Genet* 1993; **47**: 748-752.
11. Hall JG, Froster-Iskenius UG, Allanson JE. Handbook of Normal Physical Measurements. Oxford University Press Inc.: New York, 1995;
12. Goodman RM, Gorlin RJ. Head and facial measurements. In *Atlas of the face in genetic disorders.*, Goodman RM, Gorlin RJ. The C.V. Mosby Company: Saint Louis, 1977; 48-63.
13. Garn SM, Smith BH, Lavelle M. Applications of pattern profile analysis to malformations of the head and face. *Radiology* 1984; **150**: 683-690.
14. Jeffery N. A high-resolution MRI study of linear growth of the human fetal skull base. *Neuroradiology* 2002; **44**: 358-366.
15. Littel RC, Milliken GA, Stroub WW, Wolfinger RD. Random coefficients models. In *SAS system for mixed models*, Littel RC, Milliken GA, Stroub WW, Wolfinger RD. SAS Institute Inc.: Cary, NC, 1996; 253-266.
16. Gorlin RJ, Cohen MM, Levin IS. Syndromes of the Head and the Neck. Oxford University Press, 1990.
17. Garn SM, Lavelle M, Smith BH. Quantification of dysmorphogenesis: pattern variability index, sigma z. *AJR Am J Roentgenol* 1985; **144**: 365-369.
18. Jones KL. Smith's Recognizable Patterns of Human Malformation. W.B. Saunders Company: Philadelphia, 1997.

## 4.2 CRANIOFACIAL VARIABILITY INDEX DETERMINED BY THREE-DIMENSIONAL ULTRASOUND IN ISOLATED VERSUS SYNDROMAL FETAL CLEFT LIP/ PALATE

N.M. Roelfsema[a], W.C.J. Hop[b], L.N.A. van Adrichem[c], J.W. Wladimiroff[a]

[a]Department of Obstetrics and Gynecology, [b]Department of Epidemiology and Biostatistics, [c]Department of Plastic and Reconstructive Surgery, Erasmus MC, University Medical Centre Rotterdam, The Netherlands

Published in the Ultrasound Obstetrics and Gynecology 2007, 29, 265- 270.

### Abstract

**Objective:** This study was undertaken to employ craniofacial pattern profile analysis in fetal facial clefts and to evaluate the craniofacial variability index (CVI) in distinguishing between isolated and syndromal clefts.

**Methods:** Three-dimensional (3D) sonographic assessment of 16 different fetal craniofacial measurements was performed in each of 8 pregnancies complicated by an isolated facial cleft and 7 pregnancies with a syndromal cleft. The measurements covered various aspects of facial width, depth and height. Measured values were compared to gestational age-specific normal values for calculation of Z-scores and the CVI. The number of abnormal Z-scores, i.e. <-2 or >2, found among the measured values and the CVI in the group of isolated facial clefts were compared to those in the group with syndromal clefts.

**Results:** The CVI could be calculated in 14 of 15 fetuses (93%). More abnormal Z-scores and a higher mean CVI were found in the group with more severe (bilateral) facial clefts. Most abnormal values were found in the facial width measurements. Syndromal cleft lip/ palate was associated with significantly more abnormal Z-scores and a higher mean CVI than isolated cleft lip/ palate ($p < 0.05$).

**Conclusion:** Craniofacial variability index may be a valuable tool for distinguishing between isolated and syndromal fetal cleft lip/ palate.

## Introduction

Cleft lip/ palate is the most common craniofacial anomaly.[1] In the Netherlands the incidence is about 1.75 in 1000 live births.[2] Although isolated cheilo-gnatho-palato schisis is not a life-threatening malformation, it requires multiple surgeries and long time follow-up in a multidisciplinary team.[1] A facial cleft can be part of a chromosomal anomaly, for instance trisomy 13 and 18 or syndromes, such as Cornelia de Lange* or Smith-Lemli-Opitz*.[1]

The importance of making a correct prenatal diagnosis is obvious. The prognosis of an isolated facial cleft will be very different from that of a syndromal facial cleft, allowing optimal prenatal counseling and planning of obstetrical and neonatal management. However, especially in the absence of other major malformations, a correct syndrome diagnosis can be difficult to obtain. Minor fetal craniofacial malformations or dysmorphology are often difficult to visualize with conventional two-dimensional (2D) ultrasound.

For craniofacial pattern profile analysis, measurements of the head and face are translated into Z-scores to evaluate the relationship between different parts of the craniofacial area. In an earlier study fetal craniofacial measurements were assessed in a normal population. A craniofacial variability index was developed as a method to express deviation of 'normality'. (Roelfsema et al, this thesis, p116-128)

The objective of the present study was to employ craniofacial pattern profile analysis in fetal facial clefts and to evaluate the craniofacial variability index in distinguishing between isolated cleft lip/ palate and cleft lip/ palate in chromosomal anomalies or syndromes.

## Patients and methods

*Study design*

This study is based on standardized three-dimensional ultrasound measurements derived from a normal population for calculation of a craniofacial variability index.

This normal population consisted on 126 women with a singleton pregnancy recruited from the antenatal department and regional midwifery services. Those included were only women without maternal disease known to affect fetal growth, i.e. pre-existent hypertension, diabetes mellitus and pregnancies that were not at risk for craniofacial abnormality. All pregnancies resulted in the term delivery of an infant without congenital anomalies. Pregnancy duration varied between 18 and 34 weeks (median 26 weeks). Maternal age ranged between 19 and 40 years (median 30 years). 95% of the birth weights were situated between the 5th and the 95th percentile, adjusted for maternal parity and fetal sex, according to the Kloosterman Tables.[3] Three-dimensional (3D) sonographic examinations were performed four times at 3- 5 week intervals. The third or last examination could not be performed in five pregnan-

* Syndromes/sequences are identified at p 179-180.

cies and five records were not, or only partly, available for analysis, resulting in a total of 494 complete recordings. (Roelfsema et al, this thesis, p116-128)

Over a 2 year period, 8 women with a pregnancy complicated by an isolated unilateral or bilateral fetal cleft lip/ palate and 7 women with non-isolated (syndromal) unilateral or bilateral fetal cleft lip/ palate were seen and consented to participate in the study, which was approved by the Hospital Ethics Review Board. Pregnancy duration was determined from the last reliable menstrual period, or in case of uncertainty, adjusted by ultrasound in the first trimester of gestation.

The women were recruited from the Division of Obstetrics and Prenatal Medicine. Pregnancy duration varied between 19 and 34 weeks (median 23 weeks). Maternal age ranged between 20 and 37 years (median 29 years). 3D ultrasound examinations were performed after a fetal cleft lip/ palate was suspected on a detailed two-dimensional (2D) ultrasound scan.

*Recording technique*

Three-dimensional sonographic assessment of the fetal head and face was performed using a standard Voluson 530 D (Kretztechnik AG, Zipf, Austria) with a 3- 5 MHz transducer (VAW 3-5). The region of interest was defined containing the complete fetal head. Three different types of acquisition of the fetal face and head were made. A sagittal scan (frontal view of the face composed of sagittal planes); a coronal scan (side of the head composed of coronal planes); and a transverse scan (side of the head composed of transverse planes). Acquisition of the sagittal scan of the face started at the mid-sagittal plane with the fetus facing the transducer. A coronal scan was made starting acquisition just in front of the ear. A transverse scan was made by using the regular plane for measurement of the biparietal diameter[4] starting the acquisition. Multiple volume recordings were made of each fetus (range 4- 9, median 7) to obtain one good volume for every type of acquisition. The best volume data were then collected on a transportable magnetic disk for later analysis (Iomega Corp., Roy, UT, USA).

Sixteen craniofacial measurements (Table I) proven useful in the assessment of postnatal (ab)normal craniofacial development were extracted from literature on anthropometric and cephalometric measurements.[5-11]

Measurements were made using the 3D view program (Kretztechnik AG, version 4.0) on a personal computer with an Iomega Jaz Drive. This took 10- 15 minutes. Measurement methodology is described in more detail previously (Roelfsema et al, this thesis, p116-128). One observer (NR) performed all 3D ultrasound examinations and measurements.

*Statistical analysis*

Statistical analysis was performed using SPSS version 10.1 (SPSS Corp, Chicago, Ill). For each of the 16 different measurements, individual Z-scores were calculated using the gestational

**Table I.** Measurements methodology by direction: landmarks (soft-tissue, unless otherwise mentioned), three-dimensional volume mode by which the measurements were assessed and measurement plane. (See also Figures 1- 6.)

| Direction | Measurement | Landmarks | Scan mode | Plane |
|---|---|---|---|---|
| Facial width | BPD | Maximal diameter of the skull (outer bony borders)* | Transverse | Transverse |
| | BITRB | Tragus to midline, multiplied by 2* | Coronal | Transverse |
| | BIZYB | Left- right zygoma | Sagittal | Coronal |
| | BIGOB | Left- right gonion (bony border) | Sagittal | Transverse |
| | NASW | Outer borders of the alae nasi | Sagittal | Coronal |
| | IOD | Inner bony borders of the orbits | Transverse | Transverse |
| | OOD | Outer bony borders of the orbits | Transverse | Transverse |
| Facial depth | FOD | Maximal diameter frontal- posterior skull border (outer bony borders)† | Transverse | Transverse |
| | UFD | Tragus- nasion† | Coronal | Transverse |
| | MFD | Tragus- anterior rim of the maxilla† | Coronal | Transverse |
| | LFD | Tragus- gnathion† | Coronal | Transverse |
| | ASBL | Glabella- sella turcica (bony borders) | Sagittal | Sagittal |
| | PCFL | Sella turcica- opisthion (bony borders) | Sagittal | Sagittal |
| Facial height | SH | Vertex-nasion‡ | Sagittal | Sagittal |
| | UFH | Nasion- subnasion‡ | Sagittal | Sagittal |
| | LFH | Subnasion- gnathion‡ | Sagittal | Sagittal |

BPD: biparietal distance; BITRB : bitragal breadth; BIZYB: bizygomatic breadth; BIGOB: bigonial breadth; NASW: nasal width; iOD: inter ocular distance; OOD: outer ocular distance; FOD: fronto-occipital distance; UFD: upper facial depth; MFD: mid facial depth; LFD: lower facial depth; ASBL: anterior skull base length; PCFL: posterior cranial fossa length; SH: skull height; UFH: upper facial heigth; LFH: lower facial heigth.

* measure perpendicular to the midline (which should be parallel to the horizontal axis)

†measure parallel to the midline (which should be parallel to the horizontal axis)

‡ measure perpendicular to the horizontal axis, which is formed by a line connecting the middle of the anterior rim of the maxilla and the 'opisthion'

age-specific mean and standard deviation (SD) for normal fetuses (Roelfsema et al, this thesis, p116-128). This was done according to the formula:

Z-score= (measured value – gestational age-specific mean value for normal fetuses)/SD

Z-scores smaller than -2 or greater than +2 were considered abnormal. In a second step, the craniofacial variability index (CVI) for each individual was calculated as the standard deviation of the 16 resulting separate Z-scores. For this index the reference range of the craniofacial variability index (CVI) was used as previously described (Roelfsema et al, this thesis, p116-128).

Comparison of individual CVI data between the group with isolated and syndromal cleft lip/ palate was done with the T-test. The Mann-Whitney-U test was used to compare the number of abnormal Z-scores (among the 16) between these two groups. The same was done in

comparing the CVI data and number of abnormal Z-scores in unilateral versus bilateral cleft lip/palate. A p value of less than 0.05 was considered significant.

## Results

In the isolated cleft lip/palate group (n=8) the cleft was bilateral in only one case. The facial cleft was limited to the lip in one case, and to both lip and alveolus in another. All remaining cases showed complete cleft lip, alveolus and (secondary) palate (Table II).

**Table II.** Overview of isolated (1-8) and syndromal cases (9-15) of fetal cleft lip/ palate clustered by type of cleft and gestational age (GA). Reported are malformations detected prenatally, postnatal diagnosis and outcome.

| Case | GA | Malformations prenatally detected by ultrasound or genetic testing | Postnatal diagnosis | Outcome |
|---|---|---|---|---|
| 1 | $33^{4}$ | Unilateral cl | Isolated unilateral cl | Alive |
| 2 | $23^{0}$ | Unilateral cl, possibly alveolus | Isolated unilateral cl-alv | Alive |
| 3 | $19^{6}$ | Unilateral cl-p | Isolated unilateral cl-p | Alive |
| 4 | $22^{0}$ | Unilateral cl-p | Isolated unilateral cl-p | Alive |
| 5 | $22^{6}$ | Unilateral cl-p | No follow-up available | Alive |
| 6 | $26^{0}$ | Unilateral cl-alv | Isolated unilateral cl-p | Alive |
| 7 | $32^{0}$ | Unilateral cl-alv | Isolated unilateral cl-p | Alive |
| 8 | $22^{4}$ | Bilateral cl-p | Isolated bilateral cl-p | Alive |
| 9 | $20^{2}$ | Unilateral cl-alv | Unilateral cl-p and hypertelorism | Alive |
| 10 | $30^{2}$ | Unilateral cl-alv, retrognathia , dysplastic ears, AVSD | Unilateral cl-p in CHARGE association† | Alive |
| 11 | $19^{1}$ | Bilateral cl-p, sua: unbalanced chromosome 13-22 translocation | Other malformations: hypertelorism, cystic kidneys, normal umbilical cord | TOP |
| 12 | $22^{1}$ | Bilateral cl-p, diaphragmatic hernia/ thoracic tumour | Fryns syndrome* | ND |
| 13 | $23^{2}$ | Bilateral cl-p, hypertelorism | Confirmation | Alive |
| 14 | $26^{4}$ | Bilateral cl-p, IUGR, micrognathia: 4p– syndrome | No follow-up available | TOP |
| 15 | $26^{6}$ | Bilateral cl-p, microcephaly, holoprosencephaly, hydronefrosis, sandal gap: trisomy 13 | Confirmation | TOP |

GA: gestational age in weeks with days in superscript; cl: cleft lip ; cl-alv: cleft lip and alveolus; cl-p: cleft lip, alveolus and palate; AVSD: atrio-ventricular septal defect; sua: single umbilical artery; IUGR: intra uterine growth restriction; TOP: termination of pregnancy ; ND: neonatal demise.

*hypertelorism, low and small ears, left diaphragmatic hernia; †microcephaly, retrognathia, dysplastic ears, retinoblastoma, complete AVSD, hip dysplasia

**Table III:** Craniofacial variability index (CVI) and number of abnormal Z-scores in fetuses with cleft lip/ palate (1-8: isolated cases, 9-15 syndromal cases). Abnormal CVI values are underlined (upper limit changes with pregnancy duration).

| Case | Diagnosis | GA | CVI | Number of abnormal Z-scores |
|---|---|---|---|---|
| 1 | Unilateral cl | $33^{4}$ | 0.72 | 0 |
| 2 | Unilateral cl-alv. | $23^{0}$ | 0.67 | 0 |
| 4 | Unilateral cl-p | $22^{0}$ | 0.89 | 0 |
| 5 | Unilateral cl-p | $22^{6}$ | 1.11 | 0 |
| 6 | Unilateral cl-p | $26^{0}$ | 1.02 | 1 |
| 7 | Unilateral cl-p | $32^{0}$ | 1.63 | 3 |
| 8 | Bilateral cl-p | $22^{4}$ | 0.84 | 3 |
| 9 | Unilateral cl-p and hypertelorism | $20^{2}$ | 1.21 | 3 |
| 10 | Unilateral cl-p, CHARGE association† | $30^{2}$ | 1.31 | 2 |
| 11 | Bilateral cl-p , Unbalanced Translocation 13- 22 | $19^{1}$ | 1.41 | 1 |
| 12 | Bilateral cl-p, Fryns syndrome* | $22^{1}$ | 1.60 | 4 |
| 13 | Bilateral cl-p and hypertelorism | $23^{2}$ | 1.70 | 4 |
| 14 | Bilateral cl-p, 4p– syndrome | $26^{4}$ | 1.61 | 6 |
| 15 | Bilateral cl-p, trisomy 13 | $26^{6}$ | 2.00 | 11 |

GA: gestational age in weeks with days in superscript; cl: cleft lip ; cl-alv: cleft lip and alveolus; cl-p: cleft lip, alveolus and palate.
*hypertelorism, low and small ears, left diaphragmatic hernia; †microcephaly, retrognathia, dysplastic ears, retinoblastoma, complete AVSD, hip dysplasia

The syndromal group (n=7) consisted of two cases with hypertelorism as the only other anomaly. In the other cases the cleft was part of a chromosomal anomaly (trisomy 13, unbalanced translocation of chromosomes 13 and 22 and 4p– syndrome*) or an association/ syndrome (CHARGE association* and Fryns syndrome*). Unilateral cleft lip/ palate was found in only 2/7 fetuses with syndromal facial cleft (Table II). The other 5 fetuses displayed a bilateral cleft lip/palate.

The total number of abnormal Z-scores among the 16 measurements was highest in case 15 (trisomy 13; Table III). In this fetus only the facial height measurements were in the normal range (Table IV). In 4/8 fetuses with isolated cleft lip/ palate none of the measurements were in the abnormal range (Table III). A statistically significantly higher median number of abnormal Z-scores was found in the syndromal group (median number 4, range 1- 11) compared to the isolated cleft lip/ palate group (median number 0, range 0- 3; p= 0.01). Abnormal values were mostly found in facial width measurements (Table IV). When comparing unilateral and bilateral cleft lip/ palate, again a statistically significant difference was found (median number

* Syndromes/sequences are identified at p 179-180.

**Table IV :** Z-scores in fetuses with cleft lip/ palate and abnormal craniofacial variability index (CVI). Abnormal values are underlined*.

| N | | GA | Z-scores | | | | | | | | | | | | | | | | |
|---|---|---|---|---|---|---|---|---|---|---|---|---|---|---|---|---|---|---|---|
| | | | Facial width | | | | | | | Facial depth | | | | | | Facial height | | | |
| | | | BPD | BITRB | BIZYB | BIGOB | NASW | IOD | OOD | FOD | UFD | MFD | LFD | ASBL | PCFL | SH | UFH | LFH | CVI |
| 7 | Unil | 320 | -1.11 | -1.11 | -2.78 | 2.09 | -3.39 | 0.25 | -0.50 | -1.28 | 1.06 | 1.98 | 1.69 | 1.18 | -1.50 | -0.33 | 0.51 | -0.98 | 1.63 |
| 9 | Unil +hypertelorism | 202 | -0.07 | 0.43 | 2.05 | 2.90 | 0.99 | 1.45 | 1.51 | 1.18 | -0.66 | -0.25 | -0.52 | -0.17 | 2.08 | 1.98 | 1.28 | -1.36 | 1.21 |
| 10 | Unil + CHARGE association† | 302 | -0.60 | 1.65 | -0.66 | -1.92 | 2.20 | 0.73 | 0.79 | -0.90 | -1.15 | -0.98 | -1.68 | -1.96 | 0.21 | -0.29 | -2.19 | 0.59 | 1.31 |
| 11 | Bil + unbalanced translocation 13- 22 | 191 | 0.65 | -1.03 | -1.66 | 1.43 | -0.88 | 0.18 | 1.43 | 0.66 | 0.25 | 1.27 | 0.30 | 1.54 | -1.92 | 3.15 | 0.49 | -1.80 | 1.41 |
| 12 | Bil + Fryns syndrome‡ | 221 | 0.27 | 0.82 | 2.77 | 5.30 | 2.04 | 1.99 | 1.37 | 0.66 | 1.05 | 0.84 | 1.42 | -0.32 | -1.19 | -0.57 | 2.48 | -0.64 | 1.60 |
| 13 | Bil + hypertelorism | 232 | 1.06 | 1.33 | -0.15 | 2.52 | -0.10 | 3.59 | 1.79 | 1.63 | -1.87 | -2.28 | -1.73 | 2.65 | 1.10 | -0.17 | -0.35 | 1.59 | 1.70 |
| 14 | Bil + 4p– syndrome | 264 | -2.17 | -1.28 | -3.73 | -4.19 | -0.40 | 1.69 | -0.43 | -2.74 | -1.14 | -0.13 | -1.00 | -0.01 | -3.05 | -0.18 | -1.12 | -3.27 | 1.61 |
| 15 | Bil + trisomy 13 | 266 | -1.90 | -2.52 | -0.10 | -2.64 | -4.66 | -5.96 | -3.90 | -5.00 | -5.02 | -3.50 | -3.11 | -2.07 | -2.00 | 1.28 | -1.10 | -0.28 | 2.00 |

N: Case number, GA: gestational age in weeks with days in superscript; unil: unilateral cleft lip, alveolus and palate; bil: bilateral cleft lip, alveolus and palate; BPD: biparietal distance; BITRB : bitragal breadth; BIZYB: bizygomatic breadth; BIGOB: bigonial breadth; NASW: nasal width; IOD: inter ocular distance; OOD: outer ocular distance; FOD: fronto-occipital distance; UFD: upper facial depth; MFD: mid facial depth; LFD: lower facial depth; ASBL: anterior skull base length; PCFL: posterior cranial fossa length; SH: skull height; UFH: upper facial heigth; LFH: lower facial heigth.

*A Z-score smaller than –2 or greater than +2 is considered abnormal.

†microcephaly, retrognathia, dysplastic ears, retinoblastoma, complete AVSD, hip dysplasia; ‡hypertelorism, low and small ears, left diaphragmatic hernia

of abnormal Z-scores in the unilateral group was 0.5, range 0- 3; median number of abnormal Z-scores in the bilateral group was 4, range 1- 11; p= 0.009).

Hypertelorism was established after birth in cases 9, 11 (unbalanced translocation of chromosomes 13 and 22), 12 (Fryns syndrome*) and 13. Abnormal values for inter ocular distance or outer ocular distance, however, were measured only in case 13 (Table IV). Anomalies of

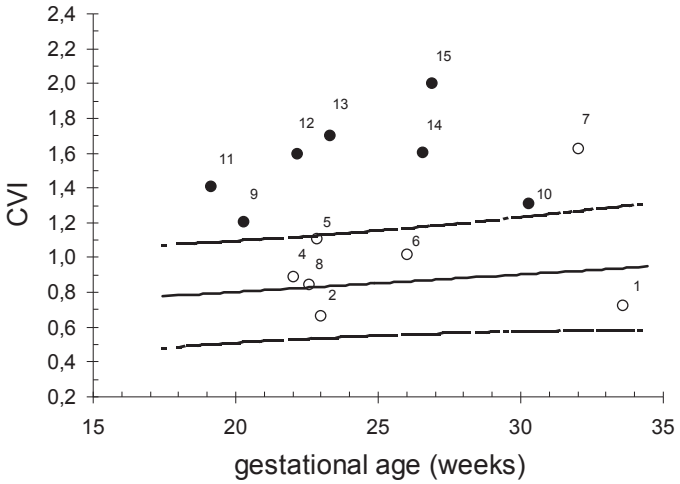


**Figure 1.** Craniofacial Variability Index in fetuses with isolated (open circle) and syndromal cleft-lip palate (closed circle). Numbers represent case number (See Table III; CVI not available in case 3). Solid line= mean expected value in normal fetuses, dotted lines= 5th and 95th percentiles in normal fetuses.

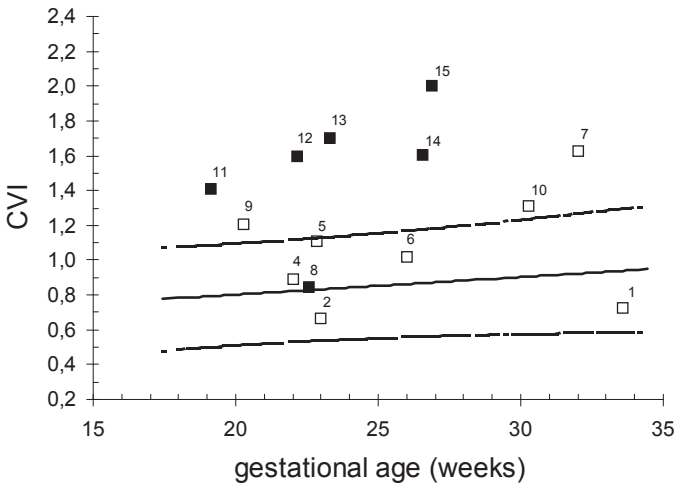


**Figure 2.** Craniofacial Variability Index in fetuses with unilateral (open squares) and bilateral cleft-lip palate (closed squares). Numbers represent case number (See Table III; CVI not available in case 3). Solid line= mean expected value in normal fetuses, dotted lines= 5th and 95th percentiles in normal fetuses.

the mandible were seen after birth in case 10 (retrognathia in CHARGE association*) and 14 (micrognathia in 4p– syndrome*). Abnormal Z-scores of fetal mandible measurements were found only in Case 14 (Table IV) and, of the mandible measurements, it was only bigonial breadth that was abnormal and not the lower facial depth. Bigonial breadth and lower facial depth were small in case 10, but still in the normal range (Table IV).

The CVI could be calculated in 14 out of 15 (93%) of the fetuses. In one fetus, case 3, the whole set of 16 measurements could not be completed. The isolated cases without (secondary) palatal involvement (case 1 and case 2) proved to have the lowest CVI (Table III and Figure 1). The highest CVI was found in case 15 (trisomy 13; Table III and Figure 1).

Abnormal craniofacial variability index (CVI) was found in one case of isolated cleft lip/ palate (14 %) and in all cases of syndromal cleft lip/ palate (100%) (Table III and Figure 1). Mean CVI in the isolated group was 0.98 and in the syndromal group 1.55. This difference was statistically significant (p= 0.004). In comparing the mean CVI between the unilateral and bilateral cleft lip/ palate group a statistically significant difference was again found (mean CVI 1.07 and 1.53 respectively, p= 0.03). Figure 2 shows CVI values for unilateral versus bilateral cleft lip/ palate.

Abnormal measurement of anterior skull base length and posterior cranial fossa length in the fetus with trisomy 13 (case 15, see also Table IV) are presented in Figure 3.



## Discussion

Nearly 300 multiple malformation syndromes have been described with cleft lip/ palate. For making a correct diagnosis family history can be important.[1] In recent literature the rate of associated anomalies found in prenatally diagnosed cleft lip/ palate is in the range 30 - 70%.[12-16]. Chromosomal anomalies are found in 10- 50% of fetuses.[12,13,15,16] However, in the absence of other major congenital anomalies a syndrome diagnosis or chromosomal anomaly can be difficult to obtain.[16]

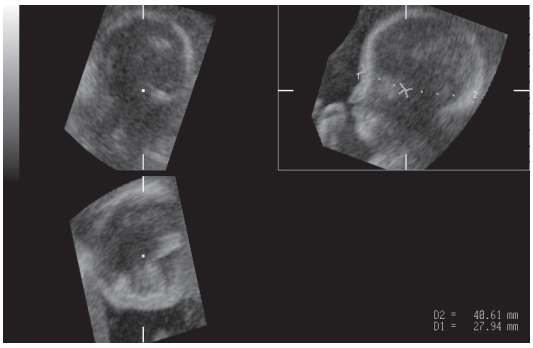


**Figure 3.** Small anterior skull base length (D1) and posterior cranial fossa length (D2) in a fetus with Trisomy 13 (case 15, see Table IV).

Craniofacial pattern profile analysis was first described by Garn et al.[17] This method provides an objective tool to evaluate the relationship of different parts of the craniofacial area; i.e. facial width, depth and height. Samples of individuals can be compared to the normal population and expressed in Z-scores to illustrate deviation of 'normality'.[18] The craniofacial variability index indicates the extent to which the craniofacial measurements of the individual are more variable than might be expected for its age.[17]

This method was applied by Escobar et al (1993) using 2D ultrasound in fetal alcohol syndrome*, Crouzon syndrome* and thanatophoric dysplasia*. They stressed the potential value of this method for documenting craniofacial dysmorphology in utero.[19]

We combined the advantages of craniofacial pattern profile analysis and three-dimensional ultrasound for exact identification of craniofacial measuring planes. In an earlier study two or more abnormal Z-scores out of the 16 measurements were found in 13% at any point in time in a normal population, whereas three or more abnormal Z-scores were found in only 4% (Roelfsema et al, this thesis, p116-128). The 95$^{th}$ percentile of normal CVI data increased from 1.08 at 18 weeks to 1.27 at 34 weeks of gestation (Roelfsema et al, this thesis, p116-128).

Not surprisingly, most abnormal Z-scores were found in the facial width measurements, as a cleft will distort the fetal face especially in the breadth. One explanation for the finding of only one abnormal fetal interocular distance in four cases with hypertelorism after birth, could be that the hypertelorism developed later in pregnancy. The same applies to the discrepancy in normal fetal mandible measurements in case 10 with retrognathia after birth. Interestingly, in case 15 (trisomy 13) abnormal Z-scores were found in both facial width and depth measurements but not in height. This fetus with holoprosencephaly was found to have an identical pattern of abnormal measurements as a fetus with holoprosencephaly without trisomy 13 that was presented by us in an earlier report (Roelfsema et al, this thesis, p116-128). Also in other anomalies as soon as these specific patterns become clear, pattern profile analysis could be an valuable tool for syndrome diagnosis.

In this study we compared the isolated to the syndromal group and the unilateral to the bilateral group with facial clefts. More abnormal Z-scores and higher CVI were found in both the syndromal clefts and the bilateral clefts. These groups clearly have a more pronounced craniofacial distortion. Because the groups are relatively small and the type of clefts are not equally distributed among the groups (the syndromal group contained more bilateral clefts than the isolated group) we could not separate the four groups. While one isolated bilateral cleft was found to have a normal CVI, all syndromal clefts (also the two unilateral clefts) were found to have an abnormal CVI.

Therefore a higher CVI might be more discriminative for syndromal versus isolated clefts than for bilateral versus unilateral clefts.

* Syndromes/sequences are identified at p 179-180.

Only one isolated case was found to have an abnormal CVI (case 7). This case showed a remarkably small bizygomatic breadth and a large bigonial breadth (Table III). However, after birth no anomalies other than the unilateral cleft lip/ palate were apparent. This case would therefore be considered a false positive one, although it is possible that the cleft will prove to be part of a syndrome later in life.

It can be concluded that the CVI may serve as a valuable tool for distinguishing between mild and more pronounced craniofacial pathology. The presence of three or more abnormal Z-scores can also be helpful in directing towards more complicated pathology, especially in the absence of abnormal fetal growth. Evaluation of the pattern profile might help in making the correct syndrome diagnosis.

## References


1. Martin WL, Gornall P, Kilby MD. Cleft lip and palate. Fetal and Maternal Medicine Review 1999; **11**: 91-104.
2. Spauwen PH. [Fifty years of plastic surgery in the Netherlands. IV. Treatment of children with cleft lip and palate]. Ned Tijdschr Geneeskd 2000; **144**: 973-980.
3. Kloosterman G. On intrauterine growth. Int J Obstet Gynaecol 1970; **8**: 895-912.
4. Campbell S, Thoms A. Ultrasound measurement of the fetal head to abdomen circumference ratio in the assessment of growth retardation. Br J Obstet Gynaecol 1977; **84**: 165-174.
5. Ward RE, Jamison PL, Farkas LG. Craniofacial variability index: a simple measure of normal and abnormal variation in the head and face. Am J Med Genet 1998; **80**: 232-240.
6. Allanson JE, O'Hara P, Farkas LG, Nair RC. Anthropometric craniofacial pattern profiles in Down syndrome. Am J Med Genet 1993; **47**: 748-752.
7. Escobar LF, Bixler D, Padilla LM, Weaver DD. Fetal craniofacial morphometrics: in utero evaluation at 16 weeks' gestation. Obstet Gynecol 1988; **72**: 674-679.
8. Hall JG, Froster-Iskenius UG, Allanson JE. Handbook of Normal Physical Measurements. Oxford University Press Inc.: New York, 1995.
9. Goodman RM, Gorlin RJ. Head and facial measurements. In Atlas of the face in genetic disorders., Goodman RM, Gorlin RJ. The C.V. Mosby Company: Saint Louis, 1977; 48-63.
10. Garn SM, Smith BH, Lavelle M. Applications of pattern profile analysis to malformations of the head and face. Radiology 1984; **150**: 683-690.
11. Jeffery N. A high-resolution MRI study of linear growth of the human fetal skull base. Neuroradiology 2002; **44**: 358-366.
12. Stoll C, Dott B, Alembik Y, Roth MP. Evaluation of prenatal diagnosis of cleft lip/palate by foetal ultrasonographic examination. Ann Genet 2000; **43**: 11-14.
13. Berge SJ, Plath H, Van de Vondel PT, Appel T, Niederhagen B, Von Lindern JJ, Reich RH, Hansmann M. Fetal cleft lip and palate: sonographic diagnosis, chromosomal abnormalities, associated anomalies and postnatal outcome in 70 fetuses. Ultrasound Obstet Gynecol 2001; **18**: 422-431.
14. Cash C, Set P, Coleman N. The accuracy of antenatal ultrasound in the detection of facial clefts in a low-risk screening population. Ultrasound Obstet Gynecol 2001; **18**: 432-436.

15. Perrotin F, de Poncheville LM, Marret H, Paillet C, Lansac J, Body G. Chromosomal defects and associated malformations in fetal cleft lip with or without cleft palate. Eur J Obstet Gynecol Reprod Biol 2001; **99**: 19-24.

16. Chmait R, Pretorius D, Moore T, Hull A, James G, Nelson T, Jones M. Prenatal detection of associated anomalies in fetuses diagnosed with cleft lip with or without cleft palate in utero. Ultrasound Obstet Gynecol 2006; **27**: 173-176.

17. Garn SM, Lavelle M, Smith BH. Quantification of dysmorphogenesis: pattern variability index, sigma z. AJR Am J Roentgenol 1985; **144**: 365-369.

18. Allanson JE. Objective techniques for craniofacial assessment: what are the choices? Am J Med Genet 1997; **70**: 1-5.

19. Escobar LF, Bixler D, Padilla LM. Quantitation of craniofacial anomalies in utero: fetal alcohol and Crouzon syndromes and thanatophoric dysplasia. Am J Med Genet 1993; **45**: 25-29.

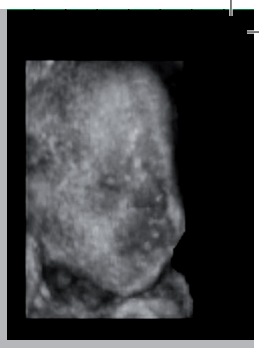

Chapter 5

# Fetal cranial sutures and fontanels

## INTRODUCTORY REMARKS

One of the advantages that becomes noticeable when working with three-dimensional ultrasound in studying the fetal head and face is the improvement in observing the sutures and fontanels. The reconstruction of the fetal skull in three-dimensions allows a far better overview than possible with conventional two-dimensional ultrasound. To be able to optimize three-dimensional scanning circumstances for visualization of the fetal sutures and fontanel the question was raised which factors would influence image quality. In this Chapter, volume recordings out of a sub population of 30 normal pregnancies were evaluated to answer this question.

# THE ROLE OF THREE-DIMENSIONAL ULTRASOUND IN VISUALIZING THE FETAL CRANIAL SUTURES AND FONTANELS DURING THE SECOND HALF OF PREGNANCY.

C.M. Dikkeboom[a]; N.M. Roelfsema[a]; L.N.A. van Adrichem[b]; J.W. Wladimiroff[a]
[a]Department of Obstetrics and Gynaecology, [b]Department of Plastic and Reconstructive Surgery, Erasmus MC, University Medical Centre Rotterdam

Published in the Ultrasound in Obstetrics and Gynecology 2004;24:412- 416.

## Abstract

**Objectives**: The aim of this study was to evaluate the significance of three-dimensional (3D) ultrasound in visualizing fetal cranial sutures and fontanels and to determine factors that could influence visualization and image quality.

**Methods**: Serial 3DUS examinations were evaluated for visibility of fetal cranial sutures and fontanels, image quality and possible influencing parameters in the second half of pregnancy. Thirty fetuses were scanned at four different gestational ages providing a data set of 120 cases.

**Results**: Most (82-100%) cranial sutures and fontanels could be visualized with 3D ultrasound. However, the sagittal suture and posterior fontanel were visualized in only 47% and 42%, respectively. Gestational age significantly influenced the visibility of the sutures and fontanels, image quality decreasing with advancing gestational age.

**Conclusions**: 3D ultrasound can be a reliable technique for visualizing most fetal cranial sutures and fontanels. By performing a sagittal and a transverse scan, most of the sutures and fontanels can be made visible during the second half of pregnancy. Visualization depends on gestational age.

## Introduction

The three main functions of cranial sutures and fontanels are to allow expansion of the skull so that it can accommodate the enlarging brain, to permit moulding of the skull when the human head becomes compressed during passage through the birth canal, and to absorb mechanical stress of minor head trauma[1]. Abnormal development of the sutures and fontanels is found in association with different chromosomal abnormalities and syndromes[1], but more often may result in isolated craniosynostosis[2].

Sutures represent boundaries of curvilinear cranial bones, which may be difficult to visualize by two-dimensional (2D) ultrasound[3]. The diagnosis of craniosynostosis is primarily based on the detection of associated abnormalities or by identifying an abnormal shape of the cranium instead of visualization of the premature closure of the suture and/ or fontanel[3]. Isolated craniosynostosis is less frequently diagnosed *in utero*[2].

In addition to direct visualization of the fetal sutures and fontanels, the use of the cephalic index (the ratio of the biparietal diameter to occipitofrontal diameter) can aid in the prenatal diagnosis of skull deformities. The cephalic index is a quantitative parameter that supplies information of the shape of the fetal head[4-7].

By scanning adjoining section planes and therefore obtaining a volume, three-dimensional (3D) ultrasound allows a better understanding of fetal anatomy both in the multiplanar view (all three orthogonal views visualized at once) and by rendering volume data, for example, to demonstrate curved sutures[8].

There has been one previous study by Pretorius and Nelson on the visualization of the cranial sutures and fontanels with 3D ultrasound in which eight normal fetuses were examined[9]. The objective of the present study was to expand on their findings by visualizing fetal cranial sutures and fontanels in 30 normal pregnancies between 18 and 34 weeks of gestation and to determine which factors may influence image quality.

## Methods

*Study design*

Thirty women with a normal singleton pregnancy consented to participate in a study on 3D ultrasound evaluation of the fetal cranial sutures and fontanels. The study was approved by the Hospital Ethics Review Board. The median pregnancy duration was 26 (range 18- 34) weeks and the median maternal age was 29 (range 19-38) years. Women were recruited from the antenatal department and regional midwifery services.

Gestational age was determined from the last reliable menstrual period, or in case of uncertainty, adjusted by ultrasound in the first trimester of gestation. All pregnancies were uneventful resulting in the delivery of a normally developed infant. Most (91%) of the birth weights were situated between the 5$^{th}$ and the 95$^{th}$ percentile (according to the Kloosterman tables[10]) adjusted for maternal parity and fetal sex.

3D sonographic examination of the fetal head and face was performed four times at 3-5 week intervals in each pregnancy.

*Recording technique*

Ultrasound examinations were performed using the Voluson 530D (Kretztechnik AG, Zipf, Austria) with an abdominal 3-5 MHz annular array transducer (VAW 3-5). For 3D ultrasound scanning an internal mechanism in the transducer is used for recording a truncated pyramidal volume by slicing through the images. Depth, longitudinal and transverse dimensions were adjustable in defining a region of interest. In this study an opening angle of 50 to 70 degrees and a sampling angle of 30 to 85 degrees was used resulting in a maximum volume of 3.2 litre. The depth range for the region of interest was set between 6 and 13 cm. 'Normal' frequency range (mid resolution/ mid penetration) was used in most patients and adjusted to 'penetration' (lower resolution/ high penetration) in case of obesity or 'resolution' in case of thin women and/or superficial position of the fetus. Scanning time for one recorded volume ranged between 4 and 8 seconds, depending on fetal movement and size of the recorded volume.

Multiple volume datasets were recorded of each fetus (range 3–11; median 6). The region of interest was defined and contained the complete fetal head. Three different types of acquisition of the fetal face and head were made; a sagittal scan (frontal view of the face composed of sagittal planes), a coronal scan (side view of the head composed of coronal planes), and a transverse scan (side view of the head composed of transverse planes). For a sagittal scan of the face acquisition started at the mid-sagittal plane with the fetus facing the transducer. For a coronal scan acquisition started just in front of the ear, and for a transverse scan acquisition started at the plane used for measurement of the biparietal diameter[11]. The data were collected on a transportable magnetic disk for later analysis (Iomega Corp. Roy, UT, USA). All sonographic examinations were performed by one observer (N.R.).

Each record was evaluated using a 3D-view computer program (Kretztechnik AG, version 3.0) on a personal computer with an Iomega Jaz Drive. A 3D image was analyzed using the surface mode, after all adjacent structures were removed from the image with the 'electronic scalpel' option. The image was rotated in all directions to obtain a complete 3D impression of the fetal skull.

To determine factors influencing visualization of the sutures and fontanels, maternal body mass index (BMI = weight before pregnancy / height$^2$), as well as gestational age, fetal presentation and amniotic fluid volume at each examination were recorded.

The visibility of five different principal sutures and four fontanels was evaluated (of which three and two, respectively, are located on both sides of the head): metopic, sagittal, coronal, lambdoid and squamosal suture, and anterior, posterior, sphenoid and mastoid fontanel (Figures 1 and 2). A suture/ fontanel was categorized as visible if seen on at least one side of the head. Image quality was categorized as good or poor, which depended on clarity of the 3D

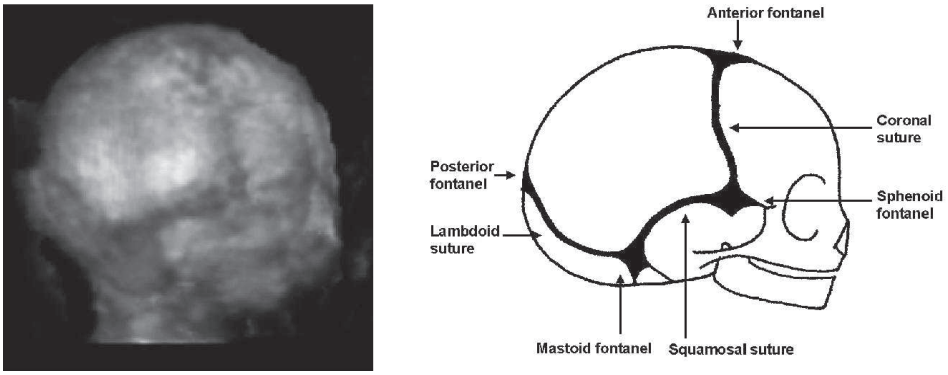


**Figure 1.** Left: three-dimensional reconstruction of the lateral side of the fetal skull (17 weeks of gestation). Right: schematic drawing of the sutures and fontanels of the side of the skull.

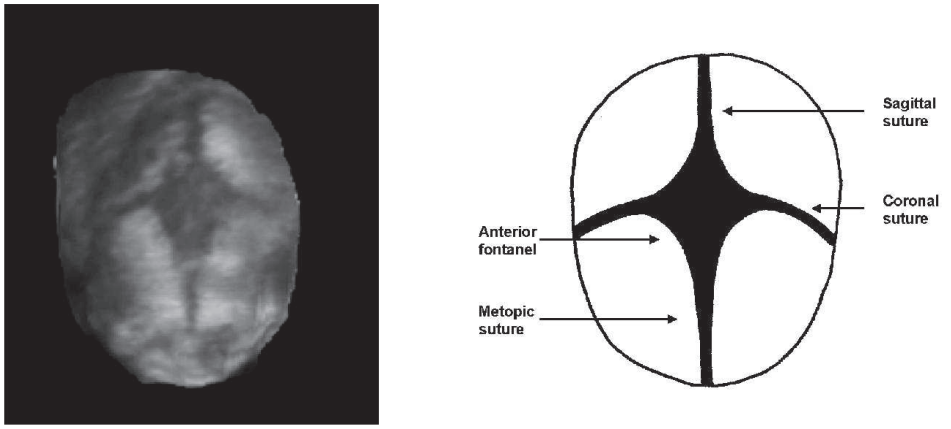


**Figure 2.** Left: three-dimensional reconstruction of the cranial side of the fetal skull (19 weeks of gestation). Right: schematic drawing of the sutures and fontanels of the top of the skull.

image and the influence of artifacts (caused by, for instance, movement during data acquisition or shadowing) on the ability to visualize the sutures and fontanels. Evaluation of visibility and categorization of image quality was performed by a different observer (C.D.).

*Statistical analysis*

Statistical analysis was performed on a personal computer using SPSS (for Windows, version 10.1; SPSS Inc., Chicago, IL, USA). To analyze the association between visibility of the different sutures and fontanels and gestational age, gestational age was divided in four different periods (Table 2). The McNemar test was applied to determine the significance of the differences of visibility between the four different periods. The Fisher's exact test was applied to determine if a suture or fontanel was better visualized in vertex, breech or transverse position of the fetus. The Wilcoxon signed-ranks test was used to determine the significance of the

differences in image quality between the four different periods. Spearman's correlation coefficient was used for analysis of a relation between the BMI and image quality. P < 0.05 was considered significant.

## Results

In all 120 3D ultrasound examinations a transverse scan could be recorded. A sagittal scan could be recorded in 116 (97%) and a coronal scan in 117 (98%).

The metopic, coronal, squamosal and lambdoid suture and anterior, sphenoid and mastoid fontanel could be seen in at least one of the different scans in almost all cases (range, 82-100%). Only the sagittal suture and posterior fontanel were difficult to visualize (47% and 42%, respectively). The metopic and sagittal suture and anterior fontanel were best visualized in the sagittal scan. In the coronal and transverse scan-mode the sutures and fontanels could be seen in almost the same frequencies (Table 1).

Visualization of most of the sutures and fontanels decreased significantly with advancing gestational age ($P < 0.05$). No association was found between gestational age and visualization of the coronal and squamosal suture and the sphenoid and mastoid fontanel ($P > 0.05$) (Table 2).

The anterior fontanel was significantly more often visible in breech position (in all 30 cases of breech position; 100%) than in cephalic (62/82 cases; 76%) or transverse position (5/7 cases; 71%) ($P = 0.001$). In one of the 120 sonographic examinations the position of the fetus was not described. No relation was found between other sutures/ fontanels and position of the fetus.

Image quality was significantly influenced by gestational age. In all three types of acquisition the image quality was significantly more often categorized as poor when the gestational age was advanced ($P < 0.05$). This difference in image quality was only significant when non-adjacent periods of gestational age were compared.

**Table 1.** Frequency of visualization of the sutures and fontanels, subdivided in the three different recording modes. Thirty fetuses were scanned four times during pregnancy. ($n = 120$).

| *Suture/ Fontanel* | *Total (%)* | *Sagittal scan (%)* | *Transverse scan (%)* | *Coronal scan (%)* |
|---|---|---|---|---|
| Metopic suture | 111 (93) | 110 (92) | 14 (12) | 9 (8) |
| Sagittal suture | 56 (47) | 51 (43) | 3 (3) | 10 (8) |
| Coronal suture | 119 (99) | 63 (53) | 111 (93) | 113 (94) |
| Squamosal sut. | 119 (99) | 32 (27) | 115 (96) | 114 (95) |
| Lambdoid sut. | 110 (92) | 13 (11) | 94 (78) | 81 (68) |
| Anterior fontanel | 98 (82) | 93 (78) | 23 (19) | 22 (18) |
| Posterior font. | 50 (42) | 22 (18) | 25 (21) | 24 (20) |
| Sphenoid font. | 120 (100) | 53 (44) | 113 (94) | 115 (96) |
| Mastoid fontanel | 118 (98) | 19 (16) | 112 (93) | 106 (88) |

**Table 2.** Visualization of sutures/ fontanels during different periods of gestation.

| *Suture/ fontanel* | Total<br>*n = 120 (%)* | *< 22 wk*<br>*n = 30 (%)* | *22 – 26 wk*<br>*n = 30 (%)* | *26 – 30 wk*<br>*n = 30 (%)* | *≥ 30 wk*<br>*n = 30 (%)* |
|---|---|---|---|---|---|
| Metopic suture | 111 (93) | 30 (100) | 30 (100) | 27 (90) | 24 (80) |
| Sagittal suture | 56 (47) | 23 (77) | 17 (57) | 12 (40) | 4 (13) |
| Coronal suture | 119 (99) | 30 (100) | 30 (100) | 30 (100) | 29 (97) |
| Squamosal sut. | 119 (99) | 30 (100) | 29 (97) | 30 (100) | 30 (100) |
| Lambdoid suture | 110 (92) | 30 (100) | 30 (100) | 27 (90) | 23 (77) |
| Anterior fontanel | 98 (82) | 29 (97) | 29 (97) | 24 (80) | 16 (53) |
| Posterior fontanel | 50 (42) | 21 (70) | 13 (43) | 10 (33) | 6 (20) |
| Sphenoid font. | 120 (100) | 30 (100) | 30 (100) | 30 (100) | 30 (100) |
| Mastoid fontanel | 118 (98) | 30 (100) | 29 (97) | 29 (97) | 30 (100) |

The mean maternal BMI was 23.3 (range, 18.8 – 38.7). No statistically significant association was found between BMI and image quality in any of the three different scan-modes ($P > 0.05$).

In all cases the amniotic fluid volume was normal. The effect of decreased amniotic fluid on visibility and image quality could therefore not be analyzed.

Table 3 shows a comparison of the data from this study with the data from Pretorius and Nelson[9].

**Table 3.** Comparison of data from Pretorius and Nelson (1994)[9] with data from this study.

| *Suture / fontanel* | *Pretorius & Nelson*<br>*n = 9 (%)* | *Current study*<br>*n = 120 (%)* |
|---|---|---|
| Metopic suture | 1 (11) | 111 (93) |
| Sagittal suture | 2 (22) | 56 (47) |
| Coronal suture | 8 (89) | 119 (99) |
| Squamosal suture | 6 (66) | 119 (99) |
| Lambdoid suture | 9 (100) | 110 (92) |
| Anterior fontanel | 4 (44) | 98 (82) |
| Posterior fontanel | 5 (55) | 50 (42) |
| Sphenoid fontanel | 7 (77) | 120 (100) |
| Mastoid fontanel | 6 (66) | 118 (98) |

## Discussion

Craniosynostosis can present as a complicated medical problem. Besides the necessary surgery after birth, it can be associated with increased intracranial pressure putting at risk normal mental development[12]. The skull deformity can also cause airway obstruction and impairment of vision and hearing[13]. Recognition of craniosynostosis may be important in prenatal

screening of families with a history of a syndrome associated with craniosynostosis. Therefore, correct prenatal diagnosis is important. However, in spite of the enormous progress that has been made in prenatal diagnosis with 2D ultrasound in the last few decades, visualization of sutures and fontanels remains difficult.

The 3D ultrasound records that were analyzed in this study were performed for assessment of fetal craniofacial anatomy in general. At volume recording no particular attention was directed towards evaluation of the fetal cranial sutures and fontanels.

The surface mode and maximum mode proved equal in demonstrating fetal sutures and fontanels throughout gestation and, as the surface mode is more visually pleasing, we preferred to use this mode.

By recording a volume in a sagittal, coronal and transverse scan, it became possible to visualize most sutures and fontanels. The sagittal suture and the posterior fontanel were more difficult to visualize. As would be expected, the metopic suture and anterior fontanel were best seen in the sagittal scan. A transverse scan shows generally the same information as a coronal scan and is more often feasible. Therefore, this scanning mode could suffice in visualization of the sutures and fontanels at the side of the fetal head. The posterior fontanel could often not be seen in any of the scan modes. However, if a 3D ultrasound scan of the back of the head was to be included, the posterior fontanel, the lambdoid sutures and possibly even the sagittal suture could be evaluated better.

Sutures and fontanels that are present bilaterally were categorized as visible if seen on at least one side of the head. With advancing gestational age it might be more difficult to see the suture or fontanel bilaterally in one scanning mode. Therefore, if wanting to exclude unilateral craniosynostosis (for instance in plagiocephaly) it might be necessary to include volume scans of both sides of the head. The proximal aspect of the head is generally more easily visualized as a result of reduced shadowing.

Gestational age clearly influenced the ability to visualize the cranial sutures and fontanels. 3D ultrasound identified fewer sutures and fontanels with advanced gestational age. This was mostly due to difficulties obtaining the whole fetal head because of the limited transducer sector size. Moreover, both reduced image quality caused by the position of the fetal head (cephalic presentation: 60% at a gestational age $< 22$ weeks as opposed to 87% at a gestational age $\geq 30$ weeks) and gestational age related reduction of amniotic fluid volume may influence the ability of 3D ultrasound to show the sutures and fontanels. Visualization may also be affected by the size of the sutures which become smaller later in fetal development. At least one of the coronal and squamosal sutures and at least one of the sphenoid and mastoid fontanels could be seen under all circumstances. Mostly because these structures are easily displayed on a transverse scan, which was feasible in all cases.

In contrast to what one would expect, the maternal BMI did not influence the image quality. This could be explained by the fact that the sutures are part of the skull and therefore a lesser resolution is necessary, than for instance in case of visualization of soft tissue.

Pretorius and Nelson (1994) evaluated the use of 3D ultrasound for visualization of fetal cranial sutures and fontanels[9]. In their study, they evaluated eight normal volunteer pregnant women (one woman was scanned twice) ranging from 16- 39 weeks' gestational age. Multiple volume data acquisitions were made (range, 12-19). In our study a higher frequency of visualization was possible with fewer volume data acquisitions in one examination. This difference may be explained by the greater numbers of cases in our study ($n$ = 120 vs. $n$ = 9).

We conclude that 3D ultrasound can be a reliable technique for visualizing the fetal cranial sutures and fontanels. With the recording of a sagittal and a transverse scan most of the sutures and fontanels can be made visible during the second half of pregnancy. The addition of a sagittal scan visualizing the back of the head of the fetus could improve visualization of the sagittal suture and posterior fontanel. Visualization becomes more difficult with advancing gestational age.

## References


1. Cohen MM, Jr. Sutural biology and the correlates of craniosynostosis. Am J Med Genet 1993;47(5):581-616.
2. van der Ham LI, Cohen-Overbeek TE, Paz y Geuze HD, Vermeij-Keers C. The ultrasonic detection of an isolated craniosynostosis. Prenat Diagn 1995;15(12):1189-1192.
3. Miller C, Losken HW, Towbin R, Bowen A, Mooney MP, Towbin A, Faix RS. Ultrasound diagnosis of craniosynostosis. Cleft Palate Craniofac J 2002;39(1):73-80.
4. Gray DL, Songster GS, Parvin CA, Crane JP. Cephalic index: a gestational age-dependent biometric parameter. Obstet Gynecol 1989;74(4):600-603.
5. Hall JG, Froster-Iskensius, U.G., Allanson, J.E. Handbook of normal physical measurements. Oxford medical publications: Oxford, New York, Toronto; 1995.
6. Jeanty P, Cousaert E, Hobbins JC, Tack B, Bracken M, Cantraine F. A longitudinal study of fetal head biometry. Am J Perinatol 1984;1(2):118-128.
7. Kurmanavicius J, Wright EM, Royston P, Wisser J, Huch R, Huch A, Zimmermann R. Fetal ultrasound biometry: 1. Head reference values. Br J Obstet Gynaecol 1999;106(2):126-135.
8. Merz E, Bahlmann F, Weber G, Macchiella D. Three-dimensional ultrasonography in prenatal diagnosis. J Perinat Med 1995;23(3):213-222.
9. Pretorius DH, Nelson TR. Prenatal visualization of cranial sutures and fontanelles with three- dimensional ultrasonography. J Ultrasound Med 1994;13(11):871-876.
10. Kloosterman G. On intrauterine growth. Int J Obstet Gynaecol 1970;8:895-912.
11. Campbell S, Thoms A. Ultrasound measurement of the fetal head to abdomen circumference ratio in the assessment of growth retardation. Br J Obstet Gynaecol 1977;84(3):165-174.
12. Renier D, Sainte-Rose C, Marchac D, Hirsch JF. Intracranial pressure in craniostenosis. J Neurosurg 1982;57(3):370-377.
13. Wilkie AO. Craniosynostosis: genes and mechanisms. Hum Mol Genet 1997;6(10):1647-1656.

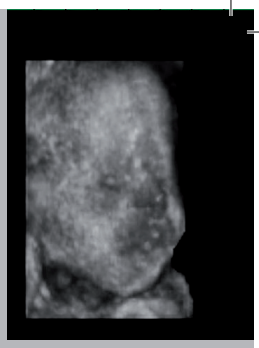

Chapter 6

# General discussion and conclusions

## 6.1 INTRODUCTION

Many researchers have been studying the applicability of 3D ultrasound in prenatal diagnosis, pointing out the complex anatomy of the fetal head and face as an area where the technique could be especially advantageous.[1-8]. For a more objective evaluation, different fetal craniofacial measurements by both two-dimensional (2D) and three-dimensional (3D) ultrasound have been suggested.[9-27] However, these studies were performed in a cross-sectional design and only part of the fetal head was investigated.

This thesis contains a longitudinal 3D sonographic study of the development of the width, depth and height of the fetal head and face in the second half of pregnancy. We chose to study anthropometric and cephalometric measurements that had proven to be useful in postnatal studies and were applicable using 3D ultrasound. Reproducibility of the measurements was established and normal data were obtained and compared with those reported in literature. Normal development of the fetal head and face was compared with postnatal craniofacial development. We used z-scores to develop a craniofacial pattern profile and introduced a craniofacial variability index (CVI) that may aid in the diagnosis of abnormal fetal craniofacial development. These tools were also applied in a group of fetuses with isolated and syndromal cleft lip-palate. Finally, the visualization of fetal cranial sutures and fontanels with 3D ultrasound was evaluated.

## 6.2 METHODOLOGY

Most studies on fetal biometry are of a cross-sectional nature. Our longitudinal set-up was chosen to be able to study development over time as well as producing nomograms. About 500 measurements in 126 subjects were obtained. Since for most measurements, the changes over time are fairly consistent (smooth changes), we think that not much of the efficiency is lost by our longitudinal study design when compared with for instance 500 subjects and one measurement each in a cross-sectional study design. It is realized, however, that for proper growth curves based on a longitudinal study design, more data are needed.

Three different scan modes were used in this study: a sagittal, coronal and transverse scan mode. The best resolution in a 3D volume is obtained in the original section planes. In the orthogonal planes there clearly is a limited lateral resolution. This is especially so for the elevational resolution (resolution in the C-plane, obtained in the direction of the acquisition) and for the structures further away from the probe. For measurements with landmarks in the frontal part of the head, which were mostly in the (mid-)sagittal plane, we used the sagittal scan

mode. For measurements with landmarks at the side of the head (the ear) the coronal scan mode was used, which proved to adequately visualize all necessary landmarks. The transverse scan mode was added for specific transverse measurements such as the biparietal distance. Possibly, measurements such as the inner and outer palatal width, would have shown a better reproducibility when a transverse scan with the fetus facing the transducer would have been used. However, this would have taken considerably more time in both obtaining the 3D volumes and the procedure of post-processing.

Both bony and soft-tissue landmarks were used in this study, depending on the landmark used after birth and on visiblity with 3D ultrasound prenatally. Although after birth, bony landmarks are often more reliable than soft-tissue landmarks, in-utero with (3D) ultrasound this is not necessarily so. Bony landmarks can be liable to scattering, especialy when further away from the probe. However, soft-tissue landmarks are only visible when enough amniotic fluid is present to separate the landmark from the surrounding tissue.

## 6.3 NORMAL FETAL CRANIOFACIAL MEASUREMENT

For most measurements (skull and facial height measurements, nasal and facial width, palatal length and outer palatal width, angle measurements, facial depth measurements, ear length, standard craniofacial biometry, brain volume, measurements of the mandible and maxilla and skull base measurements) a good reproducibility was obtained. Not surprisingly, the measurement of smaller distances (i.e. philthrum length), the measurements that were derived by movement of the calipers through more than one orthogonal plane and measurements that contained landmarks that proved difficult to obtain (i.e. mouth breadth) were less reliable.

Most of the growth charts of the measured distances and the head circumference showed a common pattern, as described earlier by others.[28,29] Fastest growth is seen during the beginning of the second trimester with gradual plateauing after midpoint. Remarkably, the measured angles showed little or no significant relation with gestational age. Although distances do grow at a different rate resulting in a changing spatial relationship of different parts of the fetal head and face, not enough change is accomplished to affect the angles. Only skull base angle showed a small change during the second half of gestation.

Standard fetal craniofacial biometry could be measured by three-dimensional ultrasound at the same degree of reliability as by two-dimensional ultrasound. Also for 3D and 2D fetal brain volumes a good agreement was found.

Brain volume showed a nearly 10-fold increase during the second half of gestation with fastest growth rates in the third trimester. Brain volume represents about 15 percent of total estimated fetal weight during the second half of gestation. Brain growth was strongly

associated with growth of the posterior cranial fossa. However, variation in skull base angle was less associated with brain growth. In this study the focus was on the development of the fetal head and face in time and less on which factors cause the head and face to grow. With progress in resolution and post-processing techniques, 3D ultrasound may be helpful in answering more developmental questions.

In evaluating different methods of determining maxillary and mandibular development, the mid/ lower facial depth ratio appeared to be the most valuable parameter because it showed a distinct decrease relative to gestational age. Interestingly, in a fetus with micrognathia in a 4p– syndrome*, bigonial breadth showed an abnormal value, whereas lower facial depth was situated in the normal range (Chapter 4.2, Table IV) This is in contrast to the results of Paladini et al.[27] In a population of 11 cases of micrognathia these authors found the growth to be primarily impaired in the antero-posterior direction (all cases) and not in the lateral direction (only in 7 out of 11 cases). Rotten et al concentrated on measuring maxillary and mandibular width in diagnosing micrognathia and found abnormal values in 8 out of 12 fetuses with micrognathia.[30] Unfortunately, our population of fetuses with mandible abnormalities was too small to evaluate these different approaches in establishing micro/ retrognathia.

Anthropometric studies on fetal craniofacial development are scarce, which makes comparison of our findings difficult. When comparing our data to data on head and face development after birth (Chapter 3.5, Table 2), the differences in relative growth between the prenatal period, the first five years and the period of 6- 18 years are remarkable. During the second half of gestation most growth is accomplished in width, especially in the facial area (soft-tissue region). In the region of the skull base the lowest growth rate is accomplished. These findings confirm the statement of Stricker et al[31], that craniofacial growth is a continuous phenomenon but takes place with varying speed on separate locations.

## 6.4 CRANIOFACIAL VARIABILITY INDEX

The original 41 measurements were selected from postnatal anthropometric and cephalometric literature[32-39] on the basis of applicability with 3D ultrasound and covering the various aspects of fetal facial anatomy. They were reduced to 16 measurements for pattern profile analysis and calculation of a craniofacial variability index. The remaining 16 measurements were selected on the basis of literature on pattern profile analysis[35,37,40,41], reproducibility and relevance (covering best the facial height, width and depth). For facial depth measurements, mid and lower facial depth were chosen, because these measurements appeared to be the



* Syndromes/sequences are identified at p 179-180.

most valuable ones in determining maxillary and mandibular growth. This combination of 16 measurements was tested in a series of different craniofacial abnormalities. Abnormal CVI was established in 3 out of 6 abnormalities. This does not rule out that another combination of fetal facial measurement may give a better result.

The variability among these sixteen measurements for every normal fetus was represented by the craniofacial variability index (CVI). The upper limit (95th percentile) of the CVI varied from 1.08 at 18 weeks to 1.27 at 34 weeks of gestation. The mild increase in the mean CVI as well as the mild variation around the mean would suggest a progressive enlargement of a relatively stable fetal profile proposed by for instance Burdi in the second half of gestation.[28] However, it should be realized that the CVI represents a standard deviation of Z-scores of 16 different fetal facial measurements. Looking at the individual components of the CVI, marked gestational age related changes are noted.

In a group of pregnancies complicated by a fetal abnormality the CVI proved abnormal in three out of six fetuses. Two to eight out of 16 parameters showed abnormal values in this subset. However, also in the normal subset abnormal values for one or more of the 16 parameters could be found. Thirteen percent of the normal population showed 2 or more out of 16 abnormal values and 4 % even 3 or more out of 16 abnormal values. Three or more abnormal Z-scores would therefore be more indicative for dysmorphology, especially when the fetus has a normal general growth pattern.

In the study of cleft lip/ palate, more abnormal Z-scores and a higher mean CVI were found in the group of bilateral facial clefts compared with unilateral clefts. Most abnormal values were found in the facial width measurements. In the group of syndromal cleft lip/ palate significantly more abnormal Z-scores and a higher mean CVI were found compared with the group with isolated cleft lip/ palate ($p < 0.05$).

For both studies it was apparent that the CVI was higher in abnormalities associated with more severe craniofacial involvement, for instance in holoprosencephaly* without known cause and holoprosencephaly* in trisomy 13. In these two fetuses comparable craniofacial pattern profiles were seen. The CVI may serve as a valuable tool for distinguishing between mild and more pronounced craniofacial pathology. The role of CVI in identifying minor dysmorphology needs to be elucidated, since minor dysmorphology is often part of a syndrome with considerable consequences for the outcome of the affected fetus and the recurrence risk in future offspring. The presence of three or more abnormal Z-scores can also be helpful in pointing at more complicated pathology, especially in the presence of an otherwise normal fetal growth pattern. Evaluation of the pattern profile might help in arriving at the correct syndrome diagnosis.

* Syndromes/sequences are identified at p 179-180

## 6.5 FETAL CRANIAL SUTURES AND FONTANELS

In a subset of 30 pregnancies, image quality, visibility of fetal cranial sutures and fontanels and possible influencing parameters were studied. Recording of both a sagittal and a transverse scan permitted visualization of most of the sutures and fontanels during the second half of pregnancy. Visibility of fetal cranial sutures and fontanels depended on gestational age. The addition of a sagittal scan displaying the back of the skull may improve visualization of the sagittal suture and posterior fontanel.

The use of the surface mode instead of the maximum mode is controversial. We started off by evaluating the optimal settings for this study. In contrast to what would be expected, the surface mode and maximum mode proved equal in demonstrating fetal sutures and fontanels throughout gestation. The surface mode is more relaxing to the eyes. We therefore preferred to use this mode.

## 6.6 FINAL REMARKS

For this research we used the Voluson 530D. The Voluson 730D, which is in use at this moment, has improved much in resolution and might improve even more with advancing technology. This will result in improved reliability of 3D measurements, the diagnostic accuracy of craniofacial pattern profile analysis and the CVI as well as visibility of cranial sutures and fontanels.

Furthermore, post-processing still tends to be time-consuming. However, this can be restricted with: i) improved experience in handling the equipment and understanding fetal anatomy; ii) standardization of the process of obtaining the required volumes ; iii) more efficient programs for data analysis; and iv) proper archiving of the obtained volumes and processing data. Inevitably, if 3D ultrasound becomes more common practice, the focus will shift from actual scanning to post-processing. In other words, less time will be spent with the patient and more time behind the computer. This will require an approach comparable to CT or MRI-scanning, in which results are shared with the patient not by the ultrasonographer, but by their own physician on a later occasion. Promising new possibilities have been developed over the last few years in 3D ultrasound technology. For instance, spatio-temporal image correlation (STIC) allows a 3D evaluation of the moving heart, which may further improve antenatal diagnosis of congenital heart disease.[42] Applying real-time 3D ultrasound (or 4D ultrasound) movements of the fetus are better appreciated and can be studied more intensively, which will further improve our knowledge of normal and abnormal fetal development.[43]

The data presented in this thesis will further improve our understanding of normal fetal craniofacial development and the suggested craniofacial pattern profile analysis and craniofacial variability index may help in more reliably identifying abnormal fetal craniofacial morphology.

## 6.7 REFERENCES


1. Lee A, Deutinger J, Bernaschek G. Three dimensional ultrasound: abnormalities of the fetal face in surface and volume rendering mode. *Br J Obstet Gynaecol* 1995; **102**: 302-306.
2. Pretorius DH, Nelson TR. Fetal face visualization using three-dimensional ultrasonography. *J Ultrasound Med* 1995; **14**: 349-356.
3. Merz E, Weber G, Bahlmann F, Miric-Tesanic D. Application of transvaginal and abdominal three-dimensional ultrasound for the detection or exclusion of malformations of the fetal face. *Ultrasound Obstet Gynecol* 1997; **9**: 237-243.
4. Rotten D, Levaillant JM. Two- and three-dimensional sonographic assessment of the fetal face. 2. Analysis of cleft lip, alveolus and palate. *Ultrasound Obstet Gynecol* 2004; **24**: 402-411.
5. Lin HH, Liang RI, Chang FM, Chang CH, Yu CH, Yang HB. Prenatal diagnosis of otocephaly using two-dimensional and three- dimensional ultrasonography. *Ultrasound Obstet Gynecol* 1998; **11**: 361-363.
6. Manabe A, Hata T, Aoki S, Matsumoto M, Yanagihara T, Yamada Y, Irikoma S, Miyazaki K. Three-dimensional sonographic visualization of fetal facial anomaly. *Acta Obstet Gynecol Scand* 1999; **78**: 917-918.
7. Lai TH, Chang CH, Yu CH, Kuo PL, Chang FM. Prenatal diagnosis of alobar holoprosencephaly by two-dimensional and three-dimensional ultrasound. *Prenat Diagn* 2000; **20**: 400-403.
8. Shipp TD, Mulliken JB, Bromley B, Benacerraf B. Three-dimensional prenatal diagnosis of frontonasal malformation and unilateral cleft lip/palate. *Ultrasound Obstet Gynecol* 2002; **20**: 290-293.
9. Degani S, Leibovitz Z, Shapiro I, Gonen R, Ohel G. Ultrasound evaluation of the fetal skull base throughout pregnancy. *Ultrasound Obstet Gynecol* 2002; **19**: 461-466.
10. Mielke G, Dietz K, Franz H, Reiss I, Gembruch U. Sonographic assessment of the fetal palpebral fissure slant--an additional tool in the prenatal diagnosis of syndromes. *Prenat Diagn* 1997; **17**: 323-326.
11. Birnholz JC, Farrell EE. Fetal Ear Length. *Pediatrics* 1988; **81**: 555-558.
12. Shimizu T, Salvador L, Allanson J, Hughes-Benzie R, Nimrod C. Ultrasonographic measurements of fetal ear. *Obstet Gynecol* 1992; **80**: 381-384.
13. Lettieri L, Rodis JF, Vintzileos AM, Feeney L, Ciarleglio L, Craffey A. Ear Length in 2Nd-Trimester Aneuploid Fetuses. *Obstet Gynecol* 1993; **81**: 57-60.
14. Chitkara U, Lee L, El-Sayed YY, Holbrook RH, Jr., Bloch DA, Oehlert JW, Druzin ML. Ultrasonographic ear length measurement in normal second- and third- trimester fetuses. *Am J Obstet Gynecol* 2000; **183**: 230-234.
15. Yeo L, Guzman ER, Ananth CV, Walters C, Day-Salvatore D, Vintzileos AM. Fetal aneuploidy by sonographic ear length. *J Ultrasound Med* 2003; **22**: 565-576.
16. Goldstein I, Tamir A, Itskovitz-Eldor J, Zimmer EZ. Growth of the fetal nose width and nostril distance in normal pregnancies. *Ultrasound Obstet Gynecol* 1997; **9**: 35-38.
17. Pinette MG, Blackstone J, Pan YQ, Pinette SG. Measurement of fetal nasal width by ultrasonography. *Am J Obstet Gynecol* 1997; **177**: 842-845.
18. Ben Ami M, Weiner E, Perlitz Y, Shalev E. Ultrasound evaluation of the width of the fetal nose. *Prenat Diagn* 1998; **18**: 1010-1013.

19. Guis F, Ville Y, Vincent Y, Doumerc S, Pons JC, Frydman R. Ultrasound evaluation of the length of the fetal nasal bones throughout gestation. *Ultrasound Obstet Gynecol* 1995; **5**: 304-307.

20. Bunduki V, Ruano R, Miguelez J, Yoshizaki CT, Kahhale S, Zugaib M. Fetal nasal bone length: reference range and clinical application in ultrasound screening for trisomy 21. *Ultrasound Obstet Gynecol* 2003; **21**: 156-160.

21. Sonek JD, McKenna D, Webb D, Croom C, Nicolaides K. Nasal bone length throughout gestation: normal ranges based on 3537 fetal ultrasound measurements. *Ultrasound Obstet Gynecol* 2003; **21**: 152-155.

22. Gamez F, Ferreiro P, Salmean JM. Ultrasonographic measurement of fetal nasal bone in a low-risk population at 19-22 gestational weeks. *Ultrasound Obstet Gynecol* 2004; **23**: 152-153.

23. Goldstein I, Jakobi P, Tamir A, Goldstick O. Nomogram of the fetal alveolar ridge: a possible screening tool for the detection of primary cleft palate. *Ultrasound Obstet Gynecol* 1999; **14**: 333-337.

24. Sherer DM, Sokolovski M, Santoso PG, Dalloul M, Abulafia O. Nomograms of sonographic measurements throughout gestation of the fetal hard palate width, length and area. *Ultrasound Obstet Gynecol* 2004; **24**: 35-41.

25. Otto C, Platt LD. The Fetal Mandible Measurement - An Objective Determination of Fetal Jaw Size. *Ultrasound Obstet Gynecol* 1991; **1**: 12-17.

26. Chitty LS, Campbell S, Altman DG. Measurement of the fetal mandible--feasibility and construction of a centile chart. *Prenat Diagn* 1993; **13**: 749-756.

27. Paladini D, Morra T, Teodoro A, Lamberti A, Tremolaterra F, Martinelli P. Objective diagnosis of micrognathia in the fetus: the jaw index. *Obstet Gynecol* 1999; **93**: 382-386.

28. Burdi AR. Cephhalometric growth analyses of the human upper face region during the last two trimesters of gestation. *Am J Anat* 1969; **125**: 113-122.

29. Escobar LF, Bixler D, Padilla LM, Weaver DD, Williams CJ. A morphometric analysis of the fetal craniofacies by ultrasound: fetal cephalometry. *J Craniofac Genet Dev Biol* 1990; **10**: 19-27.

30. Rotten D, Levaillant JM, Martinez H, Ducou le Pointe H, Vicaut E. The fetal mandible: a 2D and 3D sonographic approach to the diagnosis of retrognathia and micrognathia. *Ultrasound Obstet Gynecol* 2002; **19**: 122-130.

31. Stricker M, Raphael B, van der Meulen J, Mazzola R. Craniofacial development and growth. In *Craniofacial Malformations*, Stricker M, Raphael B, van der Meulen J, Mazzola R. Churchill Livingstone: Edinburgh, 1990; 61-98.

32. Goodman RM, Gorlin RJ. Head and facial measurements. In *Atlas of the face in genetic disorders.*, Goodman RM, Gorlin RJ. The C.V. Mosby Company: Saint Louis, 1977; 48-63.

33. Hall JG, Froster-Iskenius UG, Allanson JE. Handbook of Normal Physical Measurements. Oxford University Press Inc.: New York, 1995;

34. Jeffery N. A high-resolution MRI study of linear growth of the human fetal skull base. *Neuroradiology* 2002; **44**: 358-366.

35. Ward RE, Jamison PL, Farkas LG. Craniofacial variability index: a simple measure of normal and abnormal variation in the head and face. *Am J Med Genet* 1998; **80**: 232-240.

36. Stengel-Rutkowski S, Schimanek P, Wernheimer A. Anthropometric definitions of dysmorphic facial signs. *Hum Genet* 1984; **67**: 272-295.

37. Garn SM, Smith BH, Lavelle M. Applications of pattern profile analysis to malformations of the head and face. *Radiology* 1984; **150**: 683-690.

38. Gorlin RJ, Cohen MM, Levin IS. Syndromes of the Head and the Neck. Oxford University Press, 1990;

39. Gordon IRS. Measurement of cranial capacity in children. *Br J Radiol* 1966; **39**: 377-381.

40. Hunter AG. Craniofacial anthropometric analysis in several types of chondrodysplasia. *Am J Med Genet* 1996; **65**: 5-12.

41. Allanson JE. Objective techniques for craniofacial assessment: what are the choices? *Am J Med Genet* 1997; **70**: 1-5.

42. Devore GR, Falkensammer P, Sklansky MS, Platt LD. Spatio-temporal image correlation (STIC): new technology for evaluation of the fetal heart. *Ultrasound Obstet Gynecol* 2003; **22**: 380-387.

43. Campbell S. 4D, or not 4D: that is the question. *Ultrasound Obstet Gynecol* 2002; **19**: 1-4.

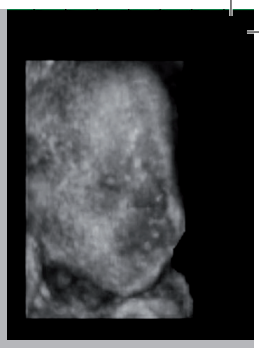

# Summary

## CHAPTER 1

This Chapter reviews the literature on three-dimensional ultrasound with emphasis on fetal head and face. Furthermore, an overview on prenatal diagnosis of craniofacial anomalies by means of ultrasonography and on methods for assessment of craniofacial development is presented. The research objectives are presented at the end of this Chapter.

## CHAPTER 2

This Chapter describes the study population and the methodological aspects of obtaining fetal craniofacial measurements and their reproducibility. The assessment of three-dimensional ultrasound recordings, the computer-based post-processing as well as statistical aspects are outlined. The selection of 16 measurement for craniofacial pattern profile analysis and the calculation of the craniofacial variability index is presented.

## CHAPTER 3

Results on the assessment of normal fetal craniofacial measurements are presented as well as limitations that were established in obtaining the volume recordings. Most measurements, including standard craniofacial biometry, could be reliably obtained. For all, but the angle measurements, a significant gestational age-related increase was found. Fastest growth rates were merely seen at the beginning of the second trimester, reaching a plateau thereafter. Comparison of measurements described in this study and literature was often complicated by differences in methodology.

The first paper shows fetal brain volume to increase nearly 10-fold in the second half of gestation. Fetal brain weight was estimated by multiplying fetal brain volume measured with 3D ultrasound and brain specific gravity (1.04). Median brain weight represents approximately 15% of total fetal weight. Although, 3D ultrasound derived brain weight was found to be larger than postmortem brain weight, there was no difference when comparing fetal brain weight relative to total fetal weight. A good agreement was found between 3D and 2D ultrasound derived brain volume.

The second paper focuses on skull base development. The relatively more pronounced growth in the posterior cranial fossa length relative to anterior skull base length is strongly associated with brain growth. This was not so for the small but significant flexion of the skull base angle, which may be caused by other factors.

In the third paper various ways of obtaining fetal maxillary and mandibular size with 3D ultrasound are explored. Growth of the mandibula was significantly larger than that of the

maxilla. A distinct decrease was found for mid/ lower facial depth ratio, which appears to be most valuable in determining normal mandibular development. However, the diagnostic accuracy of this ratio still needs to be determined.

During the second half of gestation the most distinct growth is seen in facial width. When comparing prenatal and postnatal development, craniofacial growth seems to take place with varying velocities in different craniofacial regions.

## CHAPTER 4

In this Chapter craniofacial pattern profile analysis and the craniofacial variability index (CVI) are introduced as a new method to evaluate fetal facial anatomy with 3D ultrasound. In a first study of 126 normal fetuses and six fetuses with anomalies, sixteen measurements were selected for calculation of gestational age-specific Z-scores and a CVI, which quantifies the variability between the 16 Z-scores. The 95$^{th}$ percentile values of the CVI demonstrated an increase from 1.08 to 1.27 between the 18th and 34th week of gestation. In the abnormal subjects two to eight out of 16 parameters showed abnormal values. Abnormal CVI was found in three out of six fetuses with anomalies.

The second paper evaluated these methods in eight fetuses with isolated and seven fetuses with syndromal cleft lip/ palate. Values of facial width measurements were often abnormal. In more severe (bilateral) clefts and syndromal cleft lip/ palate more abnormal Z-scores and a higher mean CVI were found.

These studies show that the CVI may serve to distinguish between normal and abnormal fetal facial anatomy and between mild and pronounced craniofacial pathology. More complicated pathology may be present if three or more abnormal Z-scores are found. Evaluation of the pattern profile might assist in making the correct syndrome diagnosis.

## CHAPTER 5

In this Chapter serial volume recordings of 30 pregnant women were evaluated for visibility of fetal cranial sutures and fontanels in the second half of pregnancy. All cranial sutures and fontanels, except for the sagittal suture and posterior fontanel, could be regularly demonstrated. Visualization was mostly influenced by a gestational age-related reduction in image quality. A sagittal and transverse scan allowed visualization of the majority of sutures and fontanels. It was concluded that 3D ultrasound is a reliable technique for demonstrating the fetal cranial sutures and fontanels during the second half of pregnancy.

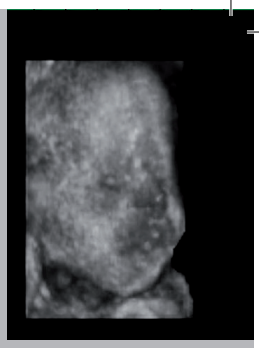

# Samenvatting

## HOOFDSTUK 1

Dit hoofdstuk geeft een overzicht van de literatuur op het gebied van de driedimensionale echoscopie, met name wat betreft het foetale hoofd en aangezicht. Tevens wordt een overzicht gegeven van de prenatale diagnostiek met behulp van echoscopie van craniofaciale afwijkingen en de methoden die gebruikt worden om ontwikkeling van hoofd en aangezicht vast te stellen. Aan het einde van dit hoofdstuk worden de onderzoeksdoelstellingen gepresenteerd.

## HOOFDSTUK 2

Dit hoofdstuk beschrijft de studie populatie en de methodologische aspecten van de foetale craniofaciale metingen en bijbehorende reproduceerbaarheid. Hier wordt uitgelegd hoe de driedimensionale echo-opnamen werden gemaakt, hoe deze nadien werden verwerkt op de computer en welke statistische methoden werden gebruikt voor de verwerking van de data. Tenslotte wordt gepresenteerd hoe 16 metingen werden geselecteerd voor de analyse van een zogenaamd 'craniofaciale patroon profiel' en de berekening van een 'craniofaciale variabiliteitsindex'.

## HOOFDSTUK 3

De resultaten van de normale foetale hoofd- en aangezichtsmetingen worden in dit hoofdstuk gepresenteerd, evenals de beperkingen in het verkrijgen van de volumeopnamen. De meeste metingen, inclusief de standaard craniofaciale biometrie, konden betrouwbaar worden verkregen. Behalve de hoeken, vertoonden alle metingen een significante toename in de loop van de zwangerschap. De meeste groei werd gezien aan het begin van het tweede trimester en bereikte een plateau vlak daarna. Verschillen in methodiek bemoeilijkte de vergelijking van de metingen in deze studie met die in de literatuur.

Het eerste artikel toont een bijna tienvoudige toename van de foetale hersenvolume in de tweede helft van de zwangerschap. Foetaal hersengewicht werd geschat door het foetale hersenvolume dat gemeten was met 3D echoscopie te vermenigvuldigen met de hersendichtheid (1,04). De mediaan van het hersengewicht is ongeveer 15% van het totale foetale gewicht. Het verschil tussen het foetale hersengewicht verkregen met 3D echoscopie (dit was groter) en het hersengewicht dat bij obductie wordt verkregen, verdween als beiden werden gedeeld door het totale foetale gewicht. Hersenvolume gemeten met behulp van driedimensionale echoscopie kwam goed overeen met hersenvolume berekend op basis van tweedimensionale echoscopische metingen.

Het tweede artikel beschrijft de schedelbasisontwikkeling. De relatief meer uitgesproken groei in de lengte van de fossa cranii posterior in vergelijking met de voorste schedelbasislengte is sterk geassocieerd met hersengroei. De kleine significante flexie in de schedelbasishoek niet en wordt vermoedelijk niet door hersengroei veroorzaakt.

In het derde manuscript worden verschillende manieren onderzocht om de boven- en onderkaak op te meten met 3D echoscopie. De groei in de onderkaak was significant groter dan in de bovenkaak. De meest duidelijke afname werd gevonden in de 'mid/ lower facial depth' (middelste/ onderste gezichtsdiepte) ratio. In het aantonen van normale mandibula ontwikkeling lijkt deze ratio daarmee de meest waardevolle. De diagnostische betrouwbaarheid van deze ratio moet nog worden vastgesteld.

In de tweede helft van de zwangerschap is de meest uitgesproken groei te zien in de breedte van het foetale gezicht. Als prenatale en postnatale ontwikkeling worden vergeleken valt op dat de craniofaciale groei met verschillende snelheden op verschillende gebieden van hoofd en aangezicht plaatsvindt.

## HOOFDSTUK 4

In dit hoofdstuk worden de craniofaciale patroon profiel analyse en de craniofaciale variabiliteitsindex (CVI) geïntroduceerd als nieuwe methodes om met 3D echoscopie de anatomie van het foetale gezicht te bestuderen. In een eerste studie van 126 normale foetussen en 6 foetussen met afwijkingen, werden 16 metingen geselecteerd voor de berekening van Z-scores die specifiek zijn voor een bepaalde zwangerschapsduur en voor de berekening van een CVI, die de variabiliteit tussen deze 16 Z-scores weergeeft. Tussen de 18$^{e}$ en 34$^{e}$ week van de zwangerschap nam de 95$^{e}$ percentiel van de CVI toe van 1,08 tot 1,27. In de groep met afwijkingen waren 2 tot 8 van de 16 parameters afwijkend. In 3 van de 6 foetussen met malformaties werd een afwijkende CVI gevonden.

Het tweede artikel geeft een evaluatie van de toepassing van deze twee technieken in acht foetussen met geïsoleerde en zeven foetussen met syndromale lip/ kaak en/ of gehemelte spleet. Metingen in de breedte van het gezicht waren het vaakst afwijkend. In de ernstigere (bilaterale) spleten en de syndromale lip/ kaak en gehemelte spleten werden meer abnormale Z-scores en een hogere gemiddelde CVI gevonden.

Deze studies laten zien dat de CVI kan fungeren als een middel om onderscheid te maken tussen normale en abnormale anatomie van het foetale aangezicht en tussen milde en meer uitgesproken craniofaciale afwijkingen. Ernstigere pathologie kan aanwezig zijn als 3 of meer afwijkende Z-scores gevonden worden. Het evalueren van de patroon profielen kan helpen bij het maken van een juiste syndroom diagnose.

## HOOFDSTUK 5

In dit hoofdstuk worden opeenvolgende volume opnamen van 30 zwangere vrouwen onderzocht op zichtbaarheid van de foetale schedelnaden en fontanellen in de tweede helft van de zwangerschap. Behalve de pijlnaad en de achterste fontanel, waren alle schedelnaden en fontanellen regelmatig zichtbaar. Zichtbaarheid werd het meest beïnvloed door een aan de zwangerschap gerelateerde afname in kwaliteit van de 3D plaatjes. Op een sagittale en transversale opname konden de meeste schedelnaden en fontanellen zichtbaar worden gemaakt. Driedimensionale echoscopie is een betrouwbare techniek voor het in beeld brengen van de foetale schedelnaden en fontanellen in de tweede helft van de zwangerschap.

# Dankwoord

Mijn eerste gedachte gaat naar alle zwangeren die hun medewerking hebben verleend aan dit onderzoek en de verloskundigen die hen direct of indirect op het onderzoek gewezen hebben. Dank jullie wel, zonder jullie was dit boekje er niet geweest!

Vervolgens wil ik professor Wladimiroff bedanken voor zijn niet aflatende steun in het realiseren van dit werk. Uw vertrouwen in mij en in het onderzoek, op de momenten dat ik dat zelf niet meer had, hebben mij zeer geraakt en, zoals u ziet, hun vruchten afgeworpen.

Wim Hop heeft een geweldige bijdrage geleverd aan de statistische uitwerking van dit proefschrift, waarvoor heel veel dank. Ik kijk met veel plezier en een warm hart terug naar de vele momenten op jouw rokerige en rommelige kamertje.

Léon, dank voor jouw enthousiaste ideeën en het kunnen belichten van dit boekje vanuit een heel ander perspectief. Professor Hovius, bedankt dat u bereid was op het laatste moment uw medewerking aan dit onderzoek te verlenen.

Alle medewerkers van de prenatale diagnostiek dank ik voor hun interesse en hun medewerking in het verzamelen van zwangeren voor dit onderzoek. En natuurlijk voor de collegialiteit en de fijne tijd die ik bij jullie heb gekend. Met naam wil ik nog noemen mijn oud-kamergenootjes Jurgen en Els, met wie ik lach en traan heb gedeeld. Dank voor jullie betrokkenheid! Speciale dank aan de onderzoeksafdeling op de 22e van de hoogbouw, Piet, Nicolette en Sandra voor tips en gezelligheid! Simona, thank you for the nice times we spent and laughs we had together!

Christine Verwoerd- Dikkeboom, Joost Riphagen en Sanne Moolenburgh dank ik voor hun medewerking aan dit onderzoek. Jammer dat niet al onze inspanningen in dit boekje konden worden opgenomen! Christine, leuk dat je een beetje mijn plek bij de prenatale hebt ingenomen! Veel succes!

Manon, Aagje, en alle andere dames en heren medeonderzoekers met wie ik in de jaren op de 5-Noord borrelde en lunchte, dank voor de gezelligheid en het kunnen delen van onderzoeksfrustraties!

Lieve broertjes, schoonzusjes, vriendjes en vriendinnetjes, met name Hilmar, dank voor jullie lieve en wijze adviezen en steun op de momenten dat ik het allemaal niet meer zag zitten… Ik houd van jullie!

Pap en mam, het is af en jullie zijn trots en dat is fijn. Ik houd heel veel van jullie!

En…Court… wat fijn dat jij er bent!

# Publication List

Roelfsema NM and Cobben JM. The EEC syndrome: a literature study. *Clin Dysmorphol 1996*;**5(2)**:115-127.

Roelfsema NM, Tan-Sindhunata MB, van Hagen JM, Cobben JM. Genetische Risico's bij de ICSI-procedure. *Patient Care 1999*;**26(5)**:49-53.

Roelfsema NM, Wildschut HIJ, Wladimiroff JW. Commentaar op 'Het recht om te weten'. *Medisch Contact 2000*;**55(38)**:1310-1311.

Roelfsema NM, Hop WCJ, Boito S, Wladimiroff JW. Three-dimensional sonographic measurement of normal fetal brain volume during the second half of pregnancy. *Am J Obstet Gynecol 2004*;**190(1)**:275-280.

Dikkeboom CM, Roelfsema NM, van Adrichem LNA, Wladimiroff JW. The role of three-dimensional ultrasound in visualizing the fetal cranial sutures and fontanels during the second half of pregnancy. *Ultrasound Obstet Gynecol 2004*;**24(4)**:412-416.

Roelfsema NM, Hop WCJ, Wladimiroff JW. Three-dimensional sonographic determination of normal fetal mandibular and maxillary development during the second half of pregnancy. *Ultrasound Obstet Gynecol 2006*;**28**:950-957

Roelfsema NM, Hop WCJ, van Adrichem LNA, Wladimiroff JW. Craniofacial variability index in utero; a three-dimensional ultrasound study. *Ultrasound Obstet Gynecol 2007*;**29**:258-264

Roelfsema NM, Hop WCJ, van Adrichem LNA, Wladimiroff JW. Craniofacial Variability Index determined by three-dimensional ultrasound in isolated versus syndromal fetal cleft lip/ palate. *Ultrasound Obstet Gynecol 2007*;**29**:265-270

Roelfsema NM, Hop WCJ, Wladimiroff JW. Three-dimensional sonography of prenatal skull base development. *Ultrasound Obstet Gynecol 2007*;**29**:372-377

# Curriculum Vitae

Nanette Roelfsema wordt geboren op 26 december 1972 te Norg. In 1985 gaat zij naar het Dr. Nassau College in Assen, waar zij in 1991 haar diploma (VWO) haalt, om vervolgens geneeskunde te gaan studeren aan de Rijksuniversiteit te Groningen. De co-schappen worden in het St. Elisabeth Hospitaal te Willemstad op Curaçao gevolgd, het keuze co-schap bij de afdeling klinische genetica van het VU-ziekenhuis in Amsterdam. Zowel de wetenschappelijke stage, literatuurstudie naar het EEC-(Ectrodactylie, Ectodermale Dysplasie, Clefting)-syndroom, als dit keuze co-schap eindigen in een publicatie. Eind 1998 wordt het artsexamen (cum laude) behaald, waarna zij werk vindt als arts prenatale diagnostiek in het Erasmus MC te Rotterdam tot maart 2005. In 1999 wordt naast dit werk met het promotieonderzoek "Three-dimensional ultrasound study of fetal craniofacial anatomy" begonnen. Van 2001 tot 2003 geeft zij onderwijs aan verpleegkundigen die de Specialistische Vervolgopleiding Obstetrie en Gynaecologie Verpleegkunde in Rotterdam volgen. Van juli tot september 2005 werkt zij als arts-assistent psychiatrie bij de crisisdienst van Parnassia in Den Haag en vanaf januari 2007 als basisarts verpleeghuisgeneeskunde bij de Frankelandgroep te Schiedam.

# List of syndromes mentioned in thesis[1]

**(MOST CHARACTERISTIC FEATURES)**

**Achondroplasia:** short limbs, low nasal bridge, caudal narrowing of spinal canal
**Bardet-Biedl syndrome:** retinal pigmentation, obesity, polydactyly
**Beckwith-Wiedemann syndrome:** macroglossia, omphalocele, macrosomia, ear creases
**Brachmann-de Lange syndrome/ Cornelia de Lange syndrome:** synophrys, thin downturning upper lip, micromelia, mental retardation
**Camptomelic dyplasia:** bowed tibiae, hypoplastic scapulae, flat facies
**Cat-eye syndrome:** coloboma of iris, down-slanting papebral fissures, anal atresia caused by duplication of chromosome 22q11 region.
**CHARGE association:** *c*oloboma, *h*eart disease, *a*tresia choanae, *r*etarded growth and development and/ or central nervous system anomalies , *g*enital anomalies and/or hypogonadism, and *e*ar anomalies and/ or deafness
**Chondrodysplasia punctata:** short humeri and femora, coronal cleft in vertebrae, punctate epiphyseal mineralization, mental deficiency
**Congenital ichthyosis:** thickened keratin layer of skin, flattened ears, diffuse platelike scales, lethal disorder[2]
**Crouzon syndrome:** shallow orbits, premature craniosynostosis, maxillary hypoplasia
**Diastrophic dysplasia:** short tubular bones (especially first metacarpal), joint limitation with talipes, hypertrophied auricular cartilage
**Fetal alcohol syndrome:** prenatal onset growth deficiency, microcephaly, short palpebral fissures caused by (severe) alcohol exposure in utero
**4p– syndrome (deletion 4p syndrome):** ocular hypertelorism with broad and beaked nose, microcephaly and/or cranial asymmetry, low-set simple ear with preauricular dimple and severe mental deficiency caused by partial deletion of the short arm of chromosome 4.
**Frontonasal malformation (frontonasal dysplasia sequence):** unknown primary defect in midfacial development with incomplete anterior appositional allignment of eyes (hypertelorism, cranium bifidum occultum, nose abnormalities)
**Fryns syndrome:** diaphragmatic abnormalities, coarse facies, distal digital hypoplasia

**Goldenhar syndrome (oculo-auriculo-vertebral spectrum/ hemifacial microsomia):** predominant (asymmetric) defects (nonrandom) in morphogenesis of first and second branchial arches.

**Holoprocencephaly sequence:** arhinencephaly, cebocephaly, cyclopia, primary defect in prechordal mesoderm

**Hypohidrotic ectodermal dysplasia syndrome:** defect in sweating, alopecia, hypodontia

**Larsen syndrome:** Multiple joint dislocation, flat facies, short fingernails

**Noonan syndrome:** webbing of the neck, pectus excavatum, cryptorchidism, pulmonic stenosis

**Oculoauriculofrontonasal syndrome:** features of both oculoauriculovertebral spectrum and frontonasal syndrome[3]

**Otocephaly:** extreme hypoplasia/ absence mandible, synotia, microstomia and aglosia, lethal anomaly[4]

**Pfeiffer syndrome:** brachycephaly, mild syndactyly, broad thumbs and toes

**Pierre Robin sequence:** micrognathia, glossoptosis, cleft soft palate, primary defect-early mandibular hypoplasia

**Smith-Lemni-Opitz:** anteverted nostrils and/or ptosis of eyelids, syndactyly of second and third toes, hypospadias, cryptorchidism, mental deficiency caused by defect in cholesterol biosynthesis

**Thanatophoric dysplasia:** short limbs, flat vertebrae, large cranium with low nasal bridge, usually die short after birth

**Treacher Collins syndrome:** malar hypoplasia with down-salnting palpebral fissures, defect of lower lid, malformation of external ear

## References


1. Jones KL. Smith's Recognizable Patterns of Human Malformation. W.B. Saunders Company: Philadelphia, 1997;
2. Vohra N, Rochelson B, Smith-Levitin M. Three-dimensional sonographic findings in congenital (harlequin) ichthyosis. *J Ultrasound Med* 2003; **22**: 737-739.
3. Johnson JM, Benoit B, Pierre-Louis J, Keating S, Chitayat D. Early prenatal diagnosis of oculoauriculofrontonasal syndrome by three-dimensional ultrasound. *Ultrasound Obstet Gynecol* 2005; **25**: 184-186.
4. Lin HH, Liang RI, Chang FM, Chang CH, Yu CH, Yang HB. Prenatal diagnosis of otocephaly using two-dimensional and three- dimensional ultrasonography. *Ultrasound Obstet Gynecol* 1998; **11**: 361-363.

# Appendix

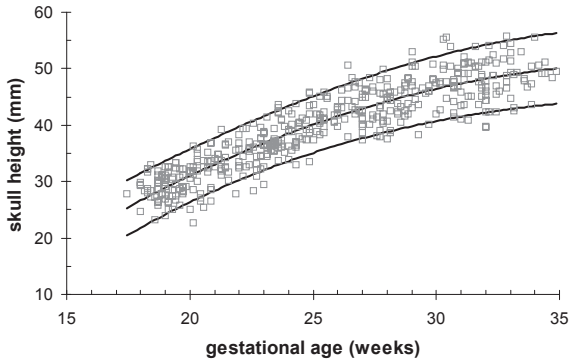


**Figure A1:** Fetal skull height (mm) relative to gestational age (weeks). Curves represent fitted mean values with 5th and 95th percentiles.

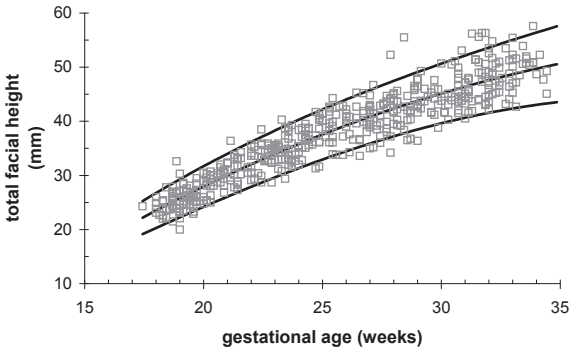


**Figure A2:** Fetal total facial height (mm) relative to gestational age (weeks). Curves represent fitted mean values with 5th and 95th percentiles.

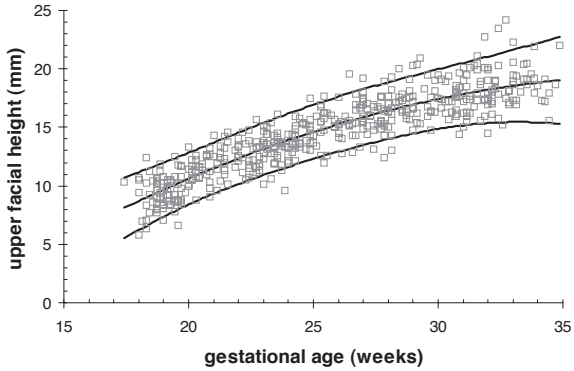


**Figure A3:** Fetal upper facial height (mm) relative to gestational age (weeks). Curves represent fitted mean values with 5th and 95th percentiles.

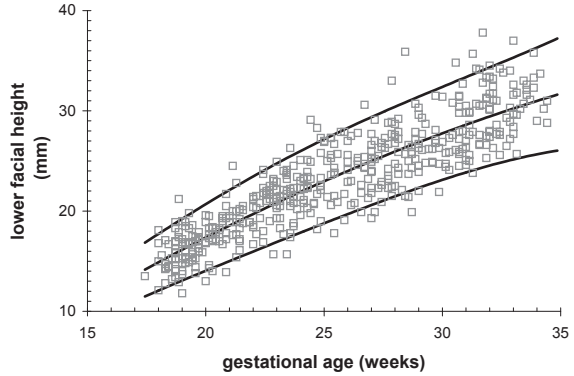


**Figure A4:** Fetal lower facial height (mm) relative to gestational age (weeks). Curves represent fitted mean values with 5th and 95th percentiles.

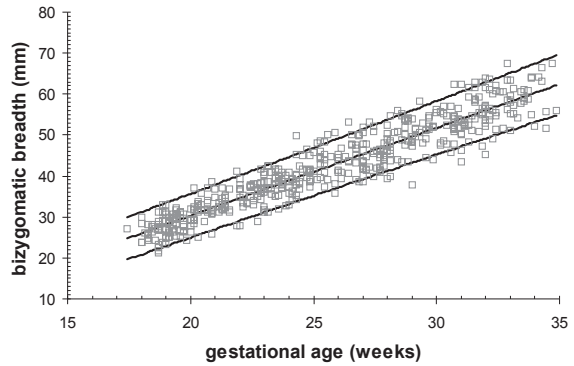


**Figure A5:** Fetal bizygomatic breadth (mm) relative to gestational age (weeks). Curves represent fitted mean values with 5th and 95th percentiles.

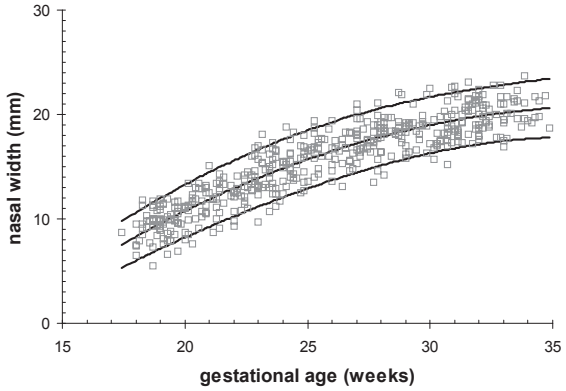


**Figure A6:** Fetal nasal width (mm) relative to gestational age (weeks). Curves represent fitted mean values with 5th and 95th percentiles.

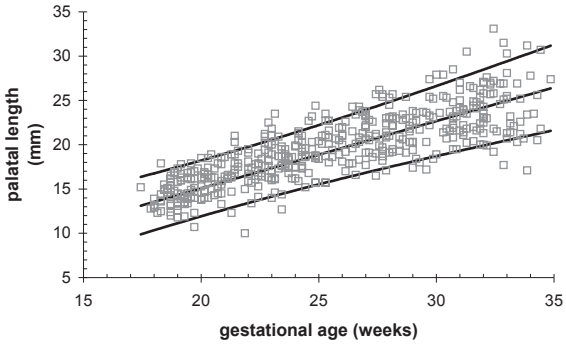


**Figure A7:** Fetal palatal length (mm) relative to gestational age (weeks). Curves represent fitted mean values with 5th and 95th percentiles.

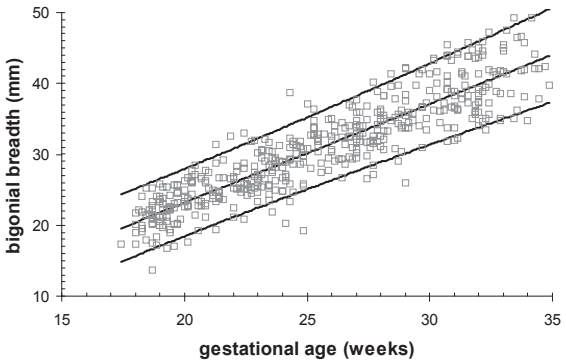


**Figure A8:** Fetal bigonial breadth (mm) relative to gestational age (weeks). Curves represent fitted mean values with 5th and 95th percentiles.

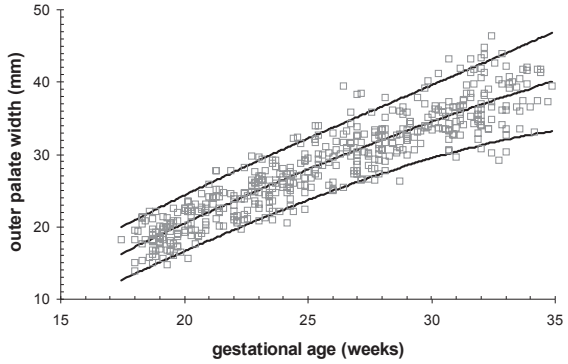


**Figure A9:** Fetal outer palate width (mm) relative to gestational age (weeks). Curves represent fitted mean values with 5th and 95th percentiles.

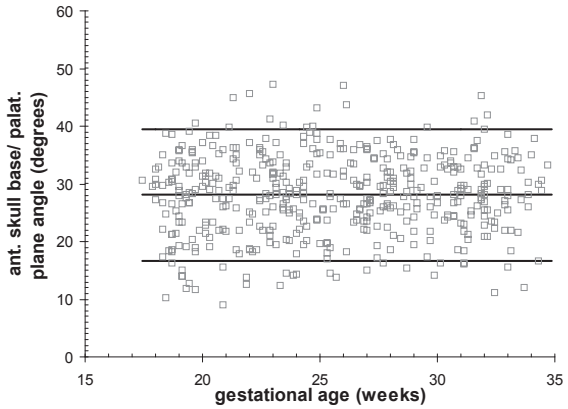


**Figure A10:** Anterior skull base/ palatal plane agle (degrees) relative to gestational age (weeks). Curves represent fitted mean values with 5th and 95th percentiles.

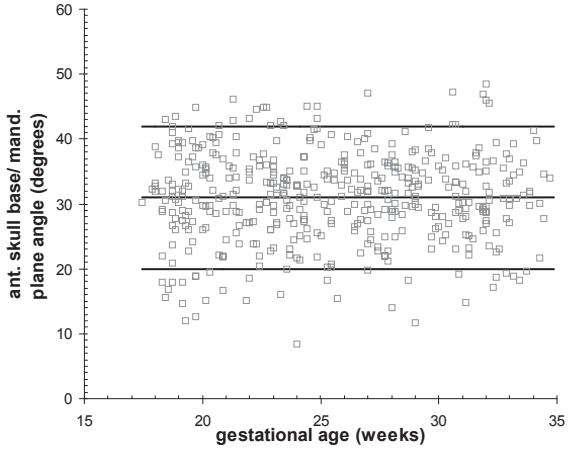


**Figure A11:** Anterior skull base/ mandibular plane angle (degrees) relative to gestational age (weeks). Curves represent fitted mean values with 5th and 95th percentiles.


**Figure A12:** Fetal biparietal distance (mm) relative to gestational age (weeks). Curves represent fitted mean values with 5th and 95th percentiles.

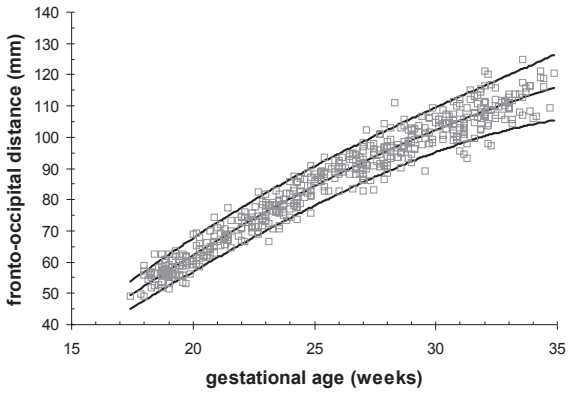


**Figure A13:** Fetal fronto-occipital distance (mm) relative to gestational age (weeks). Curves represent fitted mean values with 5th and 95th percentiles.

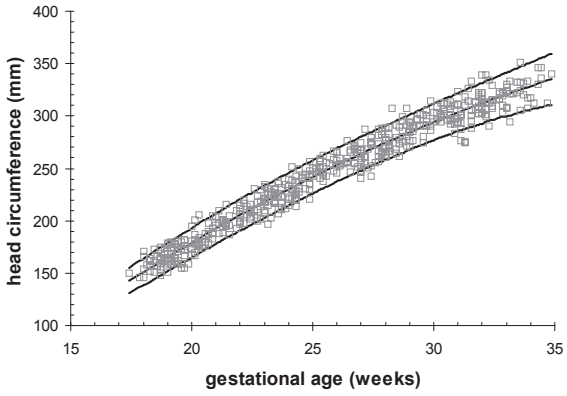


**Figure A14:** Fetal head circumference (mm) relative to gestational age (weeks). Curves represent fitted mean values with 5th and 95th percentiles.

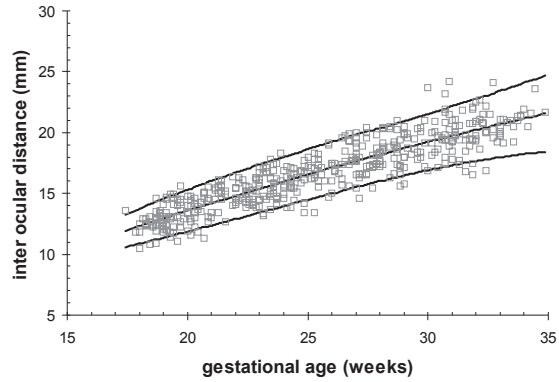


**Figure A15:** Fetal inter ocular distance (mm) relative to gestational age (weeks). Curves represent fitted mean values with 5th and 95th percentiles.

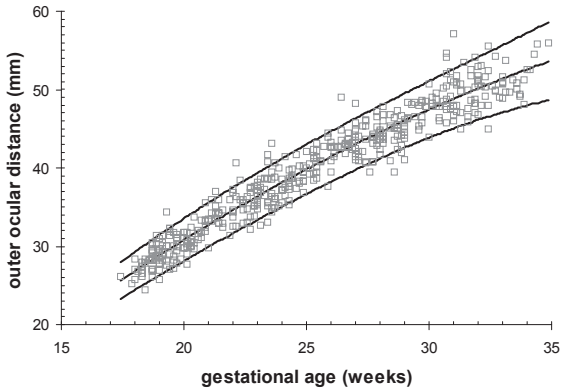


**Figure A16:** Fetal outer ocular distance (mm) relative to gestational age (weeks). Curves represent fitted mean values with 5th and 95th percentiles.

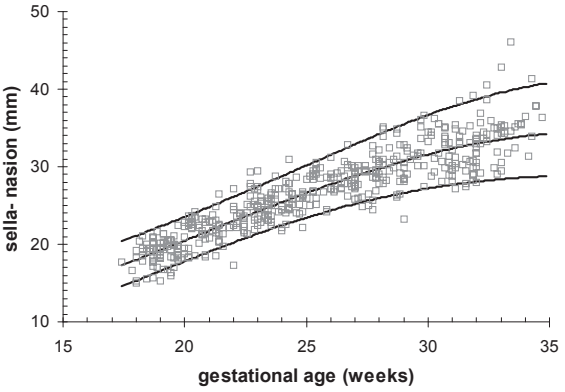


**Figure A17:** Sella- nasion (mm) relative to gestational age (weeks). Curves represent fitted median values with 5th and 95th percentiles.

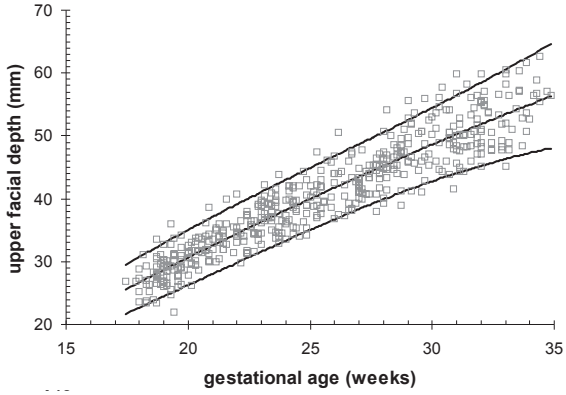


**Figure A18:** Upper facial depth (mm) relative to gestational age (weeks). Curves represent fitted mean values with 5th and 95th percentiles.

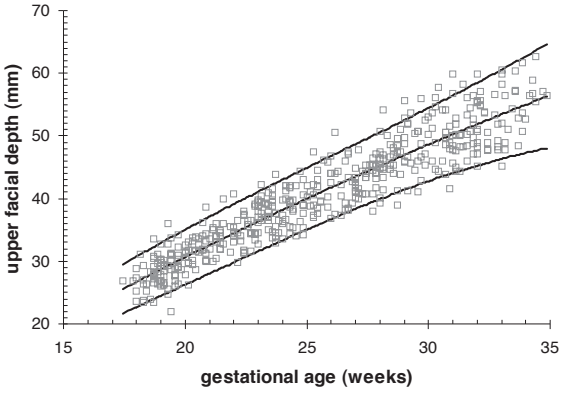


**Figure A19:** Fetal bitragal breadth (mm) relative to gestational age (weeks). Curves represent fitted mean values with 5th and 95th percentiles.

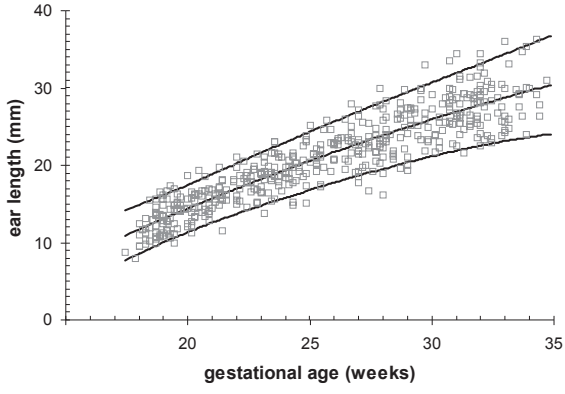


**Figure A20:** Fetal ear length (mm) relative to gestational age (weeks). Curves represent fitted mean values with 5th and 95th percentiles.

## Appendix regression equations

The regression equations (mean/ median) and standard deviation around the curves of craniofacial measurements relative to gestational age minus 20 (x or halfway point):

Figure A1: Skull height
Mean: $31.04 + 2.084x - 0.0544x^2$
Standard deviation: $\sqrt{(8.17-0.106x+0.082x^2-0.0030x^3)}$

Figure A2: Total facial height
Mean: $27.94 + 2.130x - 0.0407x^2$
Standard deviation: $\sqrt{(5.25+0.63x-0.025x^2-0.0014x^3+0.00014x^4)}$

Figure A3: Upper facial height
Mean: $10.62 + 0.916x - 0.0236x^2$
Standard deviation: $\sqrt{(1.83-0.093x+0.052x^2-0.0070x^3+0.00033x^4)}$

Figure A4: Lower facial height
Mean: $17.36 + 1.203x - 0.0164x^2$
Standard deviation: $\sqrt{(4.10+0.58x-0.0029x^2-0.0046x^3+0.00030x^4)}$

Figure A5: Fetal bizygomatic breadth
Mean: $30.27 + 2.145x$
Standard deviation: $\sqrt{(10.61+0.324x+0.0200x^2)}$

Figure A6: Nasal width
Mean: $10.72 + 1.153x - 0.0329x^2$
Standard deviation: $\sqrt{(2.38+0.188x-0.0148x^2-0.00088x^3+0.000081x^4)}$

Figure A7: Palatal length
Mean: $15.07 + 0.763x$
Standard deviation: $\sqrt{(3.69-0.026x+0.024x^2)}$

Figure A8: Bigonial breadth
Mean: $23.16 + 1.392x$
Standard deviation: $\sqrt{(8.42+0.076x+0.0306x^2)}$

Figure A9: Outer palate width
Mean: $20.46+1.585x - 0.0182x^2$
Standard deviation: $\sqrt{(5.58-0.22x+0.0091x^2-0.016x^3+0.00010x^4)}$

Figure A10: Anterior cranial base/ palatal plane angle
Mean: 28.09
Standard deviation: 2.63

Figure A11: Anterior cranial base/ mandibular plane angle
Mean: 31.07
Standard deviation: 2.64

Figure A12: Biparietal distance
Mean: $49.49 + 3.446x - 0.0348x^2$
Standard deviation: $\sqrt{(6.99+0.954x-0.0480x^2-0.00646x^3+0.000619x^4)}$

Figure A13: Fronto-occipital distance
Mean: $62.29 + 4.816x - 0.0818x^2$
Standard deviation: $\sqrt{(10.60+1.29x-0.096x^2-0.0043x^3+0.00094x^4)}$

Figure A14: Head circumference
Mean: $179.07 +13.57x - 0.207x^2$
tandard deviation: $\sqrt{(73.92+6.122x-0.5108x^2-0.01884x^3+0.00470x^4)}$

Figure A15: Inter ocular distance
Mean: $13.564+ 0.622x - 0.0057x^2$
Standard deviation: $\sqrt{(1.11+0.146x-0.011x^2-0.0001x^3+0.000064x^4)}$

Figure A16: Outer ocular distance
Mean: $30.82 + 1.932x - 0.0270x^2$
Standard deviation: $\sqrt{(2.72+0.253x-0.0070x^2-0.0018x^3+0.00021x^4)}$

Figure A17: Sella- nasion
Median: $10^{Y*}$
Standard deviation: $10^{Z‡}$
$*Y= 1.3106+ 0.02664x -0.00078x^2$
$‡Z=\sqrt{(0.0014-0.00016x+0.000026x^2-0.0000008x^3)}$

Figure A18: Upper facial depth
Mean: $30.63 + 1.938x-0.0142x^2$
Standard deviation: $\sqrt{(7.18+0.49x-0.034x^2+0.0004x^3+0.00035x^4)}$

Figure A19: Bitragal breadth
Mean: 49.98 + 2 .754x
Standard deviation: $\sqrt{(18.24-0.211x+0.098x^2)}$

Figure A20: Ear length
Mean: 14.40 + 1.310x –0.0158$x^2$
Standard deviation: $\sqrt{(0.022-0.008x-0.0042x^2+0.0005x^3+0.00002x^4)}$